IMPREGNATION OF ACTIVE PHARMACEUTICAL INGREDIENTS INTO POROUS CARRIERS

by

THAMER A. OMAR

A dissertation submitted to the

School of Graduate Studies

Rutgers, The State University of New Jersey

In partial fulfillment of the requirements

For the degree of

Doctor of Philosophy

Graduate Program in Pharmaceutical Science

Written under the direction of

Fernando J. Muzzio

And approved by

_____

_____

_____

_____

New Brunswick, New Jersey

October, 2019

ABSTRACT OF THE DISSERTATION

Impregnation of Active Pharmaceutical Ingredients into Porous Carriers

By THAMER A. OMAR

Dissertation Directors:

Professor Fernando J. Muzzio

Launching of a new drug into the market consumes significant resources and research effort and it involves a number of complex steps in drug substance and drug product development. The essential component of drug product development is often the optimization of the physical properties of the drug substance. The effect of a drug's physical properties on pharmaceutical development can be seen from the first step to the final step of development process. For instance, choosing the preferred solid-state form of the drug can influence the early steps of drug manufacturing such as the drug-substance isolation method, and it can also alter some properties of the final dosage form such as the stability and dissolution behavior of the finished product. A simple approach to product development is desirable to shorten the required development steps, preferably by excluding some unit operations. Therefore, it is of interest to develop a pharmaceutical

manufacturing method that can simplify drug product development. In this dissertation, the impregnation of drugs into porous carriers is examined as an approach to achieve this aim.

This work implemented the essential tools for successful drug impregnation into porous carriers and specified the requirements for equipment and materials, which are necessary to perform this goal. A set of analytical methods to fully characterize the impregnated products was also studied. Preliminary studies regarding the use of a fluidized bed dryer as an impregnation device were presented to illustrate the applicability of this device. Also, a case study of continuous impregnation using a continuous blender as an efficient device for continuous impregnation was carried out.

The first aim of this dissertation investigated the impregnation of an active pharmaceutical ingredient (API) into a mesoporous carrier (excipient) in a fluidized bed using different transport solvents. Impregnation and drying occurred simultaneously in the fluidized bed, and this method precluded several challenges encountered in other impregnation methods. Our results showed that the method of fluidized bed impregnation yielded a product with high uniformity and overcame several challenges presented by traditional physical blends.

The second aim expanded the use of a fluidized-bed dryer for impregnation of active pharmaceutical ingredients (APIs) to include different porous carriers. Impregnating different porous carriers with the same drug allowed us to answer fundamental questions about impregnation such as drug dissolution and blend uniformity. Since there can be large differences in the prices of porous carriers/excipients, it is also important to investigate how product properties vary with different carriers to allow one to make cost/benefit

decisions in terms of the different carriers. The results demonstrated that a fluidized-bed dryer can be successfully used to impregnate Indomethacin into porous carriers with different pore sizes. The resulting impregnated products displayed a significant improvement in some essential properties such as blend uniformity and drug dissolution, which are necessary to develop and formulate APIs into various pharmaceutical dosage forms.

The third and last aim investigated the development of a new manufacturing method to continuously impregnate APIs into porous carriers using a Glatt GCG-70 blender. This work focused on the characterization of the GCG-70 blender with consideration to the process parameters (flow rate, impeller rotation), porous carrier type (Neusilin or Fujicalin), and tracer amount (low, medium, and high). The characterization of the continuous blender depended on two main strategies. The first strategy was investigation of the flow behavior of the carriers in the blender. This step was accomplished by conducting residence time distribution measurements, material hold up measurements and strain calculations. The second strategy was evaluation of the blend uniformity of the impregnated products using NIR spectroscopy. These two strategies provided a good understanding of the performance of the GCG-70 blender as a piece of equipment for impregnation.

Dedications

This dissertation is dedicated to:

My ***mom*** and the memory of my ***dad***,

My ***brothers*** and ***sisters***,

All my ***friends***,

My ***wife***,

My little princess, ***Mayar***, and

My two heroines, ***Ibrahim*** and ***Yamin***

Acknowledgements

During this work, I have been privileged to have the support and help of many individuals. Firstly, I would like to express my deepest gratitude to my advisor Prof. Fernando Muzzio. Fernando, thank you for your continuous support, inputs and motivation. Without your guidance this work would not be possible. Beside my advisor, I am very grateful to Prof. Benjamin Glasser for his patience, time, encouragement, and improving my writing skills. My sincere thanks also go to the rest of my dissertation committee Prof. Bozena Michniak-Kohn and Prof. Tamara Minko for their time, support and comments on this dissertation.

I would like to thank the National Science Foundation's Engineering Research Center for Structured Organic Particulate Systems (ERC-SOPS) for allowing me to learn a great deal about science and communicate with others in the field. I was fortunate to work with many members of the ERC, who have helped me, encouraged me, and provided valuable inputs and ideas that have improved my research progress. In this respect, I would like to express my sincere gratitude to former and current ERC-SOPs members, Dr. Andrés D. Román-Ospino, Dr. James Scicolone, Dr. Sarang Oka, Dr. Gerardo Callegari, Dr. Savitha Panikar, Dr. Pallavi Pawar , Dr. Yifan Wang, Dr. Douglas Hausner, Dr. Sonia Razavi, Golshid Keyvan, Zhanjie Liu, Tianyi Li, Jingze Li, Qiushi Zhou, Shashwat Gupta, Yi Tao, Hao Chen, and Wei Meng. I would also like to acknowledge Suraj Kumar Katepally and Aman Rastogi for their fine work and help in my laboratory experiments.

I would particularly like to thank my parents, who were always there for me, without your love and encouragement, I could not be in this position today. Finally, to my

beloved wife Hiba, who has been supporting me during all the moments. Your patience, sacrifices, and encouragement have been invaluable.

Table of Contents

List of Tables

List of Figures

Chapter 1 Introduction

1.1 Background

Solid dosage forms such as tablets and capsules are the most common dosage forms among all prescription drugs (1). Solid dosage forms comprise of a mixture of excipients and active pharmaceutical ingredients (API), which are uniformly distributed within the excipients. The degree of uniformity in drug content in the product depends mainly on the material properties of the ingredients and the mixing process. The extent to which the API is homogeneously distributed throughout the excipients during the manufacturing process is mostly a function of the particle size distributions, densities, and particle shapes of all the components. The difference in properties of the APIs and excipients is usually substantial and this can result in a mixture with poor homogeneity. This often influences adversely the drug content uniformity of finished products. Regarding patient safety, intensive regulation efforts have been applied to ensure a product with acceptable content uniformity (2,3). This problem is more critical in pharmaceutical products with low average API content. The amount of API in some dosage forms is lower than 0.1% by weight (4). In these cases, it is very difficult to ensure a uniform distribution of API throughout the excipients. Therefore, ensuring high homogeneity for products with low API concentration is a big challenge in pharmaceutical manufacturing. Tablets and capsules presently represent more than 70% of the total dosage forms made in the whole world (1). Poor uniformity of the blend and poor content uniformity of the final dosage forms can be attributed to several overlapping factors (4–8). Segregation, insufficient mixing, differences in both the particle size distributions and densities of the blend's

components are some of the main factors, which can lead to problems in homogeneity of the blends and final dosage forms. Controlling the particle size of the drug substance is a crucial factor in solving problems with content uniformity. However, the particle size of API is also important to ensure proper drug release. Moreover, the particle sizes of other additives are also important to ensure products with good flowability and high homogeneity. Any difference in particle size and particle size distribution between the drug and excipients can lead to inhomogeneous products (9). Accordingly, to ensure a safe product, the blend homogeneity during the process and the content uniformity of the finished products should be thoroughly studied. This situation is more relevant in products with low API %. Therefore, regulatory guidance has been created to ensure a final product with high content uniformity.

In this context, the Food and Drug Administration (FDA) requires companies to determine the relative standard deviation of (RSD), which is an indicator of product homogeneity, for blend uniformity to be not more than ±6%(10). The content uniformity required by the United State Pharmacopeia (USP) is restricted to an RSD value of 6%. To avoid the risk of producing any out-of-specification batch on a production scale, industry maintains tighter limits such as RSD of 3%. It has been stated by United States FDA that not only the tablets but also the granules used to produce the tablets should meet the content uniformity criteria. These FDA directives have forced industries to pay direct attention to this aspect of the manufacturing process.

Solubility and dissolution behavior are critical properties, which should be thoroughly evaluated before incorporating any drug into final dosage form. These properties have direct influences on drug absorption and ultimately on its bioavailability.

In 1995, Amidon et al (11) proposed The Biopharmaceutical Classification System (BCS). In BCS, drugs were classified according to their solubility, intestinal permeability and dissolution behavior. In this system the drugs were classified into four classes where drugs in class II and IV have low solubility. It has been estimated that 90% of new chemical entities, 40% of the top 200 marketed drugs in the USA, and 33% of drugs in the USP fall in the low solubility class (12–14). Accordingly, huge efforts have been conducted to develop novel formulation approaches in order to improve the solubility and dissolution behavior of drugs.

M. Saffari et al. (9) discussed the improvement of both content uniformity and dissolution behavior of poorly soluble drugs using a new loading method. In this study, porous mannitol was used as a porous carrier and nifedipine and indomethacin were used as model drugs. The results showed that the RSD in all cases was less than 4% RSD. This indicates that the blends were homogeneous. Also, the results presented 80% drug release in all blends within 15 minutes. Similarly, the amorphization extent of Ibuprofen after co-grinding with kaolin (hydrated aluminium silicate) was investigated. The results indicated that Ibuprofen existed mainly in a stable amorphous form after milling with kaolin. Also, the results showed that there was a significant improvement in drug dissolution (15).

Equally, the amenability of using ordered mesoporous silicate SBA-15 to improve the dissolution behavior of poorly soluble drugs was tested. Ten drugs were impregnated into mesoporous silicate SBA-15 using solvent impregnation method. Characterization of impregnated products revealed that all drugs were amorphized inside the porous carriers. All these products presented improvement in their dissolution behaviors. Furthermore,

these impregnated products were stable after storage at 52% relative humidity for 6 months (16).

The effects of different porous carriers on the physical stability and dissolution rate of indomethacin have been studied as well. Indomethacin was amorphized with 6 porous silicates using co-grinding technique at room temperature and 75% relative humidity (RH) in a rolling jar mill. The amorphizing products were physically stable for 3 to 6 months at 40°C/75% RH. Moreover, the results showed that the amorphization time, chemical stability, dissolution, and solubility were largely depended on the physicochemical properties (surface area, crystallinity, presence and absence of metal ions such as Mg2+, Al3+, Ca2+) of the silicates (17).

The effect of ordered mesoporous silica (OMS) on the in vivo bioavailability of itraconazole has been conducted. The oral bioavailability of the product materials was compared to the crystalline itraconazole and the marketed products using dogs and rabbits as animal models. The results pointed out that itraconazole, which was loaded into OMS, presented a significant improvement in all pharmacokinetic parameters comparing with crystalline itraconazole. However, the itraconazole loaded into OMS showed the same oral bioavailability as the marketed sporanox®. These results indicated that loading of itraconazole into OMS can be considered as a promising tool to improve the in vivo bioavailability of poorly bioavailable drugs(18).

In an article entitled “Solubility modulation of bicalutamide using porous silica”, the applicability of using AEROPERL_300 Pharma as porous carrier to improve the dissolution behavior of bicalutamide (BCL) has been studied. Results indicated that there

are significant improvements in the dissolution profiles of the products comparing with neat BCL. This improvement in the dissolution profiles was mainly due to high surface area, increasing hydrophilicity and BCL amorphization (19). So far, the dissolution enhancement of poorly soluble drug Tranilast (TLT) was studied using a solid dispersion technique. Neusilin (NEU) was used in this work as an inorganic porous carrier and it was co-processed with hydrophilic surfactants such as labrasol and labrafil. TLT/NEU/surfactants have been formulated into different formulas and continuously filled into capsules. Physicochemical characterizations revealed that TLT partially amorphized inside the NEU. In addition, inline-NIR showed that TLT and NEU could interact by forming H-bonding, which can improve the dissolution behavior of TLT(20). Additionally, Pardhi, V et al (21) evaluated the improvement in the cytotoxic effect of niclosamide after loading it into mesoporous drug delivery systems. The results pointed out that there is a significant improvement in dissolution behaviors of loaded silica carriers compared to pure drug. However, structural geometry, pore size and microenvironment pH had a noticeable effect on drug dissolution profiles. Approximately 3-fold and 2-fold increasing in the cytotoxic effect of niclosamide loaded Syloid-244 and Sylysia 350 at 1:2 ratios respectively were pointed out comparing to the pure drug.

Likewise, Liu, L et al (22) tested the applicability of using precipitated and non-precipitated silica in improving the solubility of artemether. In addition, the dissolution showed a significant improvement in the dissolution profile of dispersion products. The authors attributed this improvement in the dissolution rate to high surface area of porous carriers, amorphization of drug, and enhancement of wettability. However, Oguchi et al (23) stated that the improvement of drug solubility and dissolution after loading it into

porous carriers is mainly due to amorphization of poorly soluble drugs inside the pores of the porous carrier. micro-pores while ibuprofen was mainly positioned inside the micro-pores in all cases. Moreover, the dissolution studies showed that all products presented fast release profiles. On the other hand, Bahl, et al (25) observed that the improvement in drug dissolution after co-grinding with silicate was not due to amorphization alone. Various polymorphs and a pH change of the medium were observed. These changes were mainly due to the presence of silicic acid and ions (Mg2+ and Al3+) in the dissolution media. Accordingly, they concluded that amorphization alone is not the main cause of the dissolution improvement. Acidity, ions, and silicic acid can be considered as main causes for dissolution improvement. Mellaerts et al (24) studied the physical state of poorly soluble drugs (Itraconazole and Ibuprofen) inside the pores of the ordered mesoporous silica material SBA-15 and examined the mechanism of dissolution improvement using this carrier. The results showed that itraconazole was in mesopore and

Although the loading of drug into porous carrier mainly serves to increase the dissolution rate, some studies showed that using this approach could also control or prolong the release rate of drug dissolution. F. Qu et al.(25) focused on studying the effect of both pore size and morphology of mesoporous silica on drug loading and drug release. They showed that both drug loadings and dissolution profiles depend on the pore size and the morphology of mesoporous carriers. Also, they found that large pore size with spherical morphology resulted in the fastest drug dissolution. In the same way, Verraedt, E. et al (26) demonstrated that amorphous microporous silica (AMS) could be utilized to control the release of the antiseptic chlorhexidine. The results showed that the dissolution behavior of chlorhexidine was very slow and extended for 7 days. This release profile was controlled

by AMS, which has pores less than 1 nm. Particles size and pore diameter of AMS were the main factor controlling the release profile of chlorhexidine.

It has also been confirmed that using porous carriers can improve the stability of drugs. Mallick S, et al (15) conducted a study to investigate the amorphization extent of Ibuprofen after co-grinding with kaolin (hydrated aluminium silicate). Their study indicated that Ibuprofen existed mainly in a stable amorphous form after milling with kaolin, and there was a significant improvement in drug dissolution. In another study, Ibuprofen (API) and mesoporous SBA-15, a submicron porous carrier, were co-sprayed together at different ratios to produce amorphous dispersions. All products showed fast dissolution profiles and were stable under stress conditions (40 ^{o}C and 75% humidity). Furthermore, Bahl and Bogner (27) tested the impacts of indomethacin (IND): Neusilin US2 (NEU) ratio and the humidity level on the amorphization, stability and the mechanism of interaction between IND and NEU. They found that the resulting products were stable at accelerated conditions. R. Laitinen et al.(28) mentioned that amorphized drug products generally need stabilizers. Polymers are mainly used as carriers and stabilizers for these products, but using polymers leads to some problems, such as slow drug release. Therefore, alternative approaches should be developed to overcome these obstacles. The importance of using mesoporous silicon and silica-based carriers to stabilize the amorphous drugs has been thoroughly discussed. A. Krupa et al (29) studied the effect of magnesium aluminometasilicate (Neusilin US2) (NEU) on the stability of ibuprofen (IBU) at elevated temperatures. Results indicated that the presence of NEU stabilizes IBU at high temperature. Correspondingly, Q. Wei et al (30) studied the physical stability of rutin after loading it into AEROPERL_300 Pharma. The resulting materials showed fast dissolution

profiles and stable products. X. Li et al (31) prepared solid dispersions by loading azithromycin (AZI) into Aerosil 200 using ball mill (BM) and hot melt extrusion (HME). The results indicated that HME produced physically stable solid dispersions while BM resulted in products with low physical stability. This is mainly due to the formation of H-bond in BM method while H-bond did not exist in the products of HME. H-bond formation enhances the re-crystallization process and produces physically unstable products.

In addition, Gupta et al (32) found that adsorption of drugs into porous carriers enhances the dissolution and the bulk properties of drugs. In their study, drug was adsorbed into the surface of Neusilin. The resulting products presented faster dissolution profiles with good flowability and acceptable compactibility than the corresponding physical blends. Shah, A. and Serajuddin, A.T.M. (33) demonstrated that the addition of Neusilin US2 (NEU) into solid dispersions of haloperidol enhanced the tabletability, the flowability and the dissolution behaviors of the resulting materials. Similarly, Suhas G. Gumaste et al (34) found that the addition of Neusilin into the preparation of self-emulsifying drug delivery systems (SEDDS) improves the flowability, content uniformity, tabletability and dissolution rates of the producing materials.

1.2 Impregnation

As mentioned previously that loading of drugs into porous carriers has many applications and benefits in the development of pharmaceutical dosage forms. As such, significant efforts have been applied to invent new porous carriers with new applications. Schlack et al (35) compared the physical and powder properties, compressibility, and compactibility of di-calcium phosphate anhydrous (Fujicalin) with directly compressible di-calcium phosphate di-hydrate (DCPD). Fujicalin presented the same or maybe better

flow properties than DCPD. Upon compaction both excipients presented the same deformation mechanism, fragmentation. However, SGDCP produced significantly harder tablets. In another study, the authors evaluated the amenability of using template mesoporous silica (MCM 41) as a carrier for biologically active molecules. Ibuprofen (IBU) was used in this study as a model drug because it is commonly used as an anti-inflammatory drug and is hydrophobic in nature. Furthermore, it has a small molecular size, which allows it to be placed inside very fine pore size of MCM 41. The in vitro release profile was measured using simulated biological fluids (gastric and intestinal) showed a significant improvement in the release of IBU(36). Speybroeck et al (37) discussed the applicability of using ordered mesoporous silicate SBA-15 as a promising carrier to improve the solubility of a group of poorly soluble drugs. All drugs were successfully loaded into SBA-15 and produced stable amorphous products. Thus, it can be concluded that SBA-15 can be successfully used to improve the dissolution behavior of poorly soluble drugs. Also, evaluation of the effects of surface properties, pore volume, surface area, and particle size of mesoporous silicon (thermally oxidized and thermally carbonized) and mesoporous silica (Syloid AL-1 and 244) on the drug loading efficiency and dissolution behaviors of itraconazole (ITZ) has been conducted. The results indicated that the loaded ITZ was in amorphous form, and there was a significant improvement in the dissolution behavior of ITZ. Nevertheless, the mesoporous silica showed stable products after storage under accelerated conditions while silicon products presented drug degradation after storage (38).

The physical and tableting properties of Silica Aerogel®, Neusilin® US2 (magnesium aluminometasilicate), Florite® (calcium silicate) and Aerosil® 200 (colloidal

silica) have been studied as well. Although the tabletability of Neusilin® is independent on the silicate concentration, the tablet's hardness of Florite® is concentration dependent. However, increasing the concentration of Aerosil® and Aerogel® resulted in decreasing their tablets' hardness. All tablets from pure silicates showed sufficient tensile strength except Aerosil®(39).

Consequently, loading of drugs into porous carriers leads to change in many physicochemical properties of drugs. Therefore, it is of interest to examine these changes by using different characterization techniques. For instance, Differential Scanning Calorimetry (DSC), Powder X-ray Diffraction (PXD), and Raman Spectroscopy can be used to confirm the amorphous state of drugs inside the pores of porous carriers. Also, particle size distribution and flow properties can be used to show that the drugs are inside the pores and not at the surfaces of porous carriers. Furthermore, dissolution profiles and droplet penetration can be included to characterize the improvement in the solubility and wettability. Accordingly, various studies have been conducted to confirm these changes.

M. Llusa et al (40) studied the changes in the wettability of product materials using a modified Washburn method. Different physical blends were prepared with various percent of Magnesium stearate and different shear and strain rates. Results showed that an increase in the lubricant's concentration from 0.5% to 2% with increasing shear and strain significantly increased the blend's hydrophobicity. This phenomenon is important because it can lead to over-lubrication during the preparation of pharmaceutical blends. J. Knapik, et al (41) utilized broadband dielectric spectroscopy (BDS), differential scanning calorimetry (DSC), and X-ray diffraction (XRD) to study the molecular mobility and crystallization kinetics of ezetimibe. The results showed that ezetimibe rapidly

recrystallized from amorphous state at temperature (T) below and above its glass transition temperature and the structural relaxation time of amorphous ezetimibe was exactly similar to the recrystallization time ezetimibe from amorphous state. Similarly, the crystallization tendencies of three amorphous drugs, etoricoxib, celecoxib, and rofecoxib were tested using broadband spectroscopy. The results of dielectric broadband spectroscopy and infra-red (IR) indicated that etoricoxib underwent a tautomerization, which was the main reason behind improving its physical stability. In addition, hydrogen bonds between the single isomers might be existed possibly leading to stronger stabilization of etoricoxib (42). In another study, a robust test to characterize the physical stability and investigate the phase separation during the screening studies of drug development was developed. The authors concluded that isothermal calorimetry is an efficient test to study the physical behavior of spray dried dispersions, and orthogonal analytical techniques such as pXRD, ssNMR and FTIR were helpful keys to study the physical stability in more details(43). In another study, the mechanical properties, thermal properties and tableting behavior of amorphous solid dispersions (ASD) has been characterized. The characterization methods included differential scanning calorimetry (DSC) and nano-indentation (44).

1.3 Impregnation Methods

Impregnation has been applied traditionally in catalysis manufacturing. In this process, catalytic species is loaded into porous materials as a solution or a suspension (45,46) . However, it has been reported that this method is also suitable to load porous material with drugs (16,47,48). This method simply consists of mixing the loading solution with the porous carrier. Penetration of the drugs into carrier's pores occurs by capillary action. Then, the resulting product is dried to exclude any solvent.

Different methods have been developed to load the drugs into porous carriers. For instance, C. Charnay et al (36)loaded a drug into a template mesoporous silica (MCM 41) using two different loading approaches and various solvents. The results showed that the solvent has an important effect on the drug loading. The highest loading was obtained using hexane as a solvent while there was no drug loading using DMA. In another work, the properties of amorphous products produced by different preparation methods had been compared. Solid dispersions of Neusilin and Sulindac were produced using both ball milling (BM) and Cryo-milling (CM). The results demonstrated that BM materials presented better physical stability than CM materials at accelerated conditions. Simultaneously, amorphous dispersions of these two components were produced using a scalable hot melt extrusion (HME) process. The results indicated that HME materials showed the same physical properties as milling materials while the dissolution behavior of HME was better than the dissolution behaviors of milling materials (49). Correspondingly, the impacts of carriers and preparation methods on the features of amorphous solid dispersion of itraconazole were explored. The results indicated that Neusilin showed faster amorphization than Veegum, and Calcium Phosphate Dibasic Anhydrous. Furthermore, the solvent-deposition method presented higher dissolution rate than the ball milling method. Consequently, these results suggested that both the type of solid carriers and the preparation method have a clear effect on the drug deposition, amorphization time, physical stability and drug dissolution rate (50). In addition, Azithromycin-Aerosil200 solid dispersions were produced by two methods: ball milling and hot melt extrusion. X-ray diffraction and DSC demonstrate that most of the products were completely amorphous. FT-IR showed that there was a hydrogen bond between the drug and Aerosil-200. The

results also suggested that hot melt extruded products were more stable than ball milled products(31). Maniruzzaman et al (51) developed a one-step loading method using a twin-screw extruder. This researcher also studied the behavior of Mg Al metasilicate (Neusilin) as a mesoporous carrier in hot melt extrusion processing of indomethacin (IND) for the manufacturing of solid dosage form. All extruded products showed that IND existed mainly in amorphous form with fast dissolution behavior and excellent physical stability under accelerated conditions (40 ^{o}C, RH 75%) for 12 months. Also, the impregnation of fenofibrate on mesoporous silica using incipient wetness and supercritical carbon dioxide methods was studied. The results showed that the drug loading efficiency using supercritical impregnation was higher than for the incipient wetness method. Also, supercritical impregnation reduced drug crystallinity more than for the incipient wetness method. From these results, one can conclude that supercritical impregnation is better than incipient wetness impregnation to load Fenofibrate and to reduce its crystallinity (52).

While most of the previous methods hold promise, they also possess some drawbacks and limitations. Co-grinding of drugs with porous carriers needs a long milling time to accomplish amorphization. Hot melt extrusion (HME) mainly depends on the use of polymers and require a melting process to prepare the solid dispersions (SODs). Accordingly, HME could result in drug-polymer interaction, and chemical degradation of the drugs, and in some cases, the chemical degradation of the polymers. Hence, drugs, polymers and other excipients should be carefully selected to produce SODs with good properties. Furthermore, the implementation of supercritical CO2 to load drugs has limitations, which include the restricted solubility of most drugs in the supercritical CO2 and the cost of its application in the large scale. Recently, lipid containing drug products

have been adsorbed into porous carriers to improve some properties. However, this approach mainly results in products with poor flowability and poor compactibility. Therefore, there is a significant need to develop a novel loading method that can bypass all the above drawbacks and limitations mentioned above.

1.4 Fluidized bed impregnation

Recently, Grigorov et al (53) attempted a new method to impregnate drugs into porous carriers. This method involved spraying the drug solution into porous carriers within a fluidized bed (FB). Impregnation and drying occurred simultaneously and the method enabled the practitioner to achieve different drug loadings independent of the drug's solubility. This approach eliminated the need to repeat spraying and drying cycles, unlike the wet impregnation methods. Furthermore, the method displayed a uniform distribution of the API within the carrier, thereby resulting in a product with excellent blend uniformity and a narrow particle size distribution. Moreover, this method is easy to scale-up. Fluidized bed impregnation is a single step process to load drug substances into a carrier and eliminates several operations from the drug substance development routine. In addition, fluid bed impregnation also eliminates unit operations such as blending and granulation from the drug product development process. Fluid bed impregnation is easy to integrate in a manufacturing train, and also lends itself to continuous processing.

1.5 Continuous impregnation

While most other industries such as petrochemicals, catalysts, and food transitioned large fractions of their production processes to continuous manufacturing (CM) procedures decades ago, the pharmaceutical industry still depends predominantly on conventional batch manufacturing processes. This delay in implementing CM to pharmaceutical

processes is due to the rigid regulatory rules to introduce new manufacturing processes. Until recently, this led to a “freeze” of the process development toolbox in pharmaceutical manufacturing (54,55). However, batch manufacturing is not an efficient approach for either manufacturing or development of pharmaceuticals. This manufacturing procedure requires many manufacturing steps and necessitates a complex and risky scale-up studies (56). In recent years, large efforts have been devoted to finding alternative processes that are feasible, acceptable and robust. Continuous processes can be considered as a potential alternative to developing and enhancing the pharmaceutical manufacturing and it has recently got the interest of both industry and regulatory authorities (57–64). As mentioned above, CM were implemented in many industries such as chemicals, food, household, and many others. Many advantages, which mainly include reproducibility, affordability, and robustness, have been reported (56). Accordingly, US FDA has characterized CM as an emerging technology (64–68). Recently, five drugs manufacturing processes depending on CM methods have been approved in the USA by FDA and many others are expected in the coming years (69).

Pharmaceutical companies are potentially seeking to conduct CM process in manufacturing of new and existing products. While approaches to implement CM technology may vary among practitioners, a consensus is rapidly emerging regarding the importance of understanding process dynamics to achieve reliable process performance and ensure acceptable product quality (58,66,70,71). Continuous processes offer many advantages including: less exposure to powders and pharmaceutical products, less handling, and efficient built-in quality control. Also, continuous processes could enable 24 hour automated production line (lights-out operation) and a simple scale-up requirement,

which is easily achieved by elongating the production time with no need to increase the equipment's dimensions as in batch processes (56). Moreover, CM offers better controllability, and lower manufacturing cost by decreased footprint and labor (54). For these and other reasons, CM has been gaining more momentum, and several techniques have been reported for continuous process. As continuous processing offers significant advantages over batch production (automation and a reduction of batch to batch variation, labor cost and processing time), several types of equipment providing a successful continuous process have been reported such as continuously operating mixers, high shear granulators and fluidized bed granulator (72–74). As mentioned early in this section, due to the rigid nature of pharmaceutical regulatory framework, the pharmaceutical industry has remained largely confined to conventional batch manufacturing. However, since the inception of the Process Analytical Technologies initiative (PAT) (75), and more recently, the Quality by Design (QbD) initiative (76), significant efforts in designing new manufacturing strategies are underway. The pharmaceutical industry can currently be considered in the process of undergoing a transition from conventional batch manufacturing production to CM. The market globalization, the reduced lifespan of patents and the overall decreased profitability of newly discovered drug substances are encouraging big pharmaceutical companies to shorten the drug development times with maximum throughput by adopting CM (69). Therefore, CM processes can provide an efficient and promising alternative for achieving these goals (77).CM provides better product quality assurance than batch processes, with less labor cost and development time. Furthermore, process analytical tools (PAT) can be easily implemented for the purposes of in-line process monitoring and quality control (51,78).

Residence Time Distribution (RTD) is a parameter, which is commonly used in many unit operations, such as the continuous manufacturing of chemicals, food, catalyst, and pharmaceuticals. RTD was first used in 1953 by Danckwerts (79) as a tool to describe non-ideal liquid mixing in chemical reactors. RTD is defined as the probability distribution of time that explains the amount of time a mass stays in a unit operation (80). One common method to measure RTD is to input a pulse, a rapid concentration, of material that can easily be detected by an analytical method. This detectable material is referred to as a tracer. RTD curves can be utilized to estimate how material fluctuation will convey through the unit operation or to determine when the impurities or wrong added materials will completely leave the system, or when the ingredients in a given product unit were supplied (81). To clarify the RTD concept, as material enters a continuous blender during steady-state operation, most particles stay in this blender for a time close to a certain mean value, defined as the mean residence time (MRT). However, some particles leave the blender more quickly due to faster movement in the axial direction while other particles reside longer in the blender due to unexpected backward mixing or staying in the dead zone of the blender for a while. Therefore, a group of particles moving in a continuous blender at steady state has a range of residence times, called (RTD) (82).

There are two main typical residence time behaviors: plug flow and continuous stirred tank flow. In plug flow, particles entering the blender as a group leave the blender together also as a group. These particles move at the same speed along the blender axis, so just cross-sectional or axial mixing happens. On the other hand, continuous stirred tank flow suggests that when a group of particles entering the blender some of these particles leave quickly and some particles require a very long time to exit the blender. Therefore,

both axial and radial mixing can be seen in continuous stirred tank flow. The behavior of all blenders in real cases is in between these two typical states. Both plug flow and continuous stirred tank flow will be discussed in more details in Chapter 5.

1.6 Organization of the dissertation

The main aims of the work described in this dissertation is to disclose the use of fluidized bed impregnation techniques to the pharmaceutical industry, and to demonstrate its promising advantages over current manufacturing process for solid dosage forms. Effects of material characteristics, solvent properties, and processing conditions are investigated to explore the applicability of fluidized bed impregnation for a wide range of materials. Also, the effects of these factors on the properties of the resulting products were thoroughly studied. The robustness of the fluidized bed impregnation process, and its applicability for a variety of solvents were tested (Specific Aim I). In this work, we tested the impregnation of drug in a porous carrier using both water and methanol. The results of these two solvents were compared to figure out the effects of these solvents on the properties of impregnated products. The method of FB impregnation is further broadened to include other APIs and excipients to demonstrate the robustness and generality of FB impregnation and also to elaborate the effects of carrier characteristics on resulting products (Specific Aim II). In this aim, we studied the efficacy of three different porous carriers to prevent or reduce the crystallization of a drug. These porous carriers mainly differ in pore sizes and bulk properties. Continuous impregnation of drugs into porous carriers have been addressed as well (Specific Aim III). The effect of process parameters, and properties of porous carriers on the residence time distribution (RTD) was studied. Also, the correlation between RTDs and content uniformity have been established.

The work in this dissertation is accomplished in the three specific aims as follows:

Specific Aim I: Studying the feasibility of using Fluidized Bed to impregnate active pharmaceutical ingredients (APIs) into porous carrier using different solvents (Chapter 3).

Specific Aim II: Evaluating the performance of different porous carriers in fluidized bed dryer and studying the effects of these porous carriers on the properties of impregnated products (Chapter 4).

Specific Aim III: Evaluating and Testing the applicability of continuous impregnation methods and studying factors affecting on RTD (Chapter 5).

Chapter 2 Overview of materials, equipment, processing methods, and analytical techniques

2.1 Introduction

Solid dosage forms mainly include tablets and capsules. The formulation aspects of solid dosage forms design depend on many factors such as drug properties, manufacturing and therapeutic considerations. Examples of drug properties that influence the formulation of tablets and capsules, include physical and chemical properties of drug substances. Manufacturing considerations include for example the cost of manufacturing along a specific method. On the other hand, therapeutic considerations, which influence the design of dosage forms, involve patient age, pharmacokinetic and pharmacodynamics of the drug substance, site of action …, etc. Although most APIs can be produced in tablet or capsule form, the selection of suitable manufacturing unit operations to produce a tablet or a capsule is restricted to API properties. The manufacturing unit operations of a tablet or/and a capsule include blending, extrusion, wet or dry granulation, drying and compaction. Most APIs require a combination of at least two-unit operations to be produced as tablets or capsules. All the above-mentioned unit operations have been thoroughly studied, and a substantial knowledge and experience are available to control successfully the manufacturing of almost any API using these manufacturing unit operations (83,84).

Unfortunately, there is limited information on impregnation as a process for manufacturing of solid dosage forms. Although, there is recent interest in the impregnation process, a huge effort is still needed in order to deeply explore this process.

Most current research has focused on the characterization of impregnated products such as drug dissolution and API physical state; however, testing the robustness of this manufacturing process is still required to be investigated. Accordingly, establishing a regime map of the impregnation methods is necessary to deeply understand how this process could be controlled. Also, most of the current impregnation work is still at bench level while a manufacturing process should be conducted on a larger scale.

Simply, an impregnation process consists of two main steps: (1) Mixing of API solution with a porous host, and (2) Drying the resulting product (48,85). The mixing step could be done in any blender such as a V-blender, a granulator, a high shear mixer, and a fluidized bed device while drying step could be done utilizing oven or fluidized bed dryer. If we can combine both mixing and drying in one step, this will reduce the unit operations, powder handling requirement and cost. These benefits can be obtained utilizing fluidized bed for impregnating API into a porous carrier and then drying the product.

In a fluidized bed, both mixing and drying will happen simultaneously. In order to ensure the success of the impregnation process, the process parameters should be carefully selected. Four possible scenarios can occur during the spraying of an API solution or suspension into a porous carrier including: spray drying, coating, agglomeration, and impregnation. The process parameters that control these scenarios are (1) the spray rate (Rs), of the API solution into the porous host (2) the drying rate (Rd), which is the evaporation rate of the solvent and (3) the impregnation rate (Ri), which is the penetration rate of the API solution into the pores of the carrier. The relative rates of these three parameters determine the process outcomes and as the following:

1) Spray drying: This happens when the Rd is much higher than Rs and Ri. In this case, API solution will be dried before arriving the host particles.

2) Coating: This occurs when the Rd is higher than the Rs and the Rs is higher than Ri. This results in a layer coating of API around the host particles because the penetration of API solution into the pores is slow, so API solution will be dried on the surface of host particles before its penetration into the pores.

3) Agglomeration or granulation: This can be noticed either when Ri < Rd < Rs or Ri > Rs > Rd. In the first case, the spray rate is high; thus, a liquid layer of API solution will exist around the host carrier, which "glues" the particles to each other and results in agglomeration or granulation. In the second situation, the impregnation is high, which allows a high amount of API solution to penetrate the pores and leads to pores saturation. At the same time high Rs with low Rd results in accumulation of API solution at the surface of carriers and leads to (undesirable) granulation.

4) Impregnation: This situation can be seen when Ri > Rd ≥ Rs. Impregnation will be achieved in this case because the penetration of API solution into the pores of porous carrier is high. To avoid saturation of pores and agglomeration of particles, the Rs should be less or equal to Rd, which lead to evaporation of solvent before saturation.

In order to ensure a favorable impregnation mode, these three parameters (Rs, Rd and Ri) should be carefully selected. Ri is mainly related to the properties of porous carriers such as wettability and pore size while Rs and Rd are process properties.

On the other hand, in continuous impregnation work, which is presented in this dissertation, drug was successfully impregnated into porous carrier using a continuous high shear blender. This device is an efficient mixer and it is supplied with a nozzle for spraying of the API solution into the porous carrier. However, there is no ability to dry the resulting products within this device. Therefore, the parameters of interest in continuous impregnation are the pumping rate (Rp) of API solution and the impregnation rate (Ri). There are two possible outcomes from this process:

1. Agglomeration or granulation: Ri < Rp. API solution coats the carrier particles and then attaches these particles together. If the Rp is higher than Ri, then we will have granulation because the API solution is dropped into the porous carrier at a higher rate than the penetration of API solution into the pores of the carrier. Then the API solution fills the pores and eventually oversaturation of carrier's pores occurs. As a result, a layer of API solution will be formed at the carrier's surface, which will result in granulation.

2. Impregnation: Ri > Rp. If the pumping rate is slower than the impregnation rate, then impregnation of API solution into the porous carrier will happen. In order to ensure successful impregnation, the mass or volume of API solution should not exceed the absorption or loading capacity of the porous carrier. For this reason, the pumping rate must be less than the impregnation rate.

Accordingly, to ensure successful impregnation using a continuous blender, the pumping rate and impregnation rate should be controlled to keep a reasonable liquid/solid ratio and to avoid exceeding the loading or absorption capacity of the porous carrier at any

location. As mentioned previously, the impregnation rate is a carrier property while pumping rate is a device parameter (which should be carefully selected).

The most common properties for excipients, APIs and solvents relevant to impregnation are discussed in this chapter. In addition, the general processing conditions, the equipment properties and the relevant characterization methods and analytical techniques that were used in this work, are described below in this chapter. The experimental set up and analytical material characterization methods that are relevant to a specific part of the work have been presented in the individual relevant chapters. Lastly, a brief preview of the data is presented at the end of this chapter to exemplify the applicability of using a fluidized bed and a continuous blender to impregnate a drug into a porous carrier.

2.2 Materials and equipment selection

Three main types of materials have been used in this work: the porous carrier, the API, and the solvent. In order to ensure a successful impregnation process, the materials used in this work were carefully selected.

2.2.1 Porous Carriers

The typical porous carriers for impregnation should have enough internal surface area, good flow properties, narrow particle size distribution, be insoluble in most organic solvent, and be physically stable under impregnation conditions. Impregnation is defined as a process of placing chemicals (including drugs) into the pores of a porous host. Therefore, the internal surface area and the pore size of porous carriers play crucial roles in the impregnation process. High internal surface area provides enough absorption capacity to API solution, which results in a high loading of API into the porous carrier.

Moreover, small pore size ensures a stable amorphization of API inside the pores of the carrier. Impregnation also aims to improve the flow properties of API. Selecting a carrier with excellent flow properties is necessary to ensure good flow properties of the resulting impregnated products. Furthermore, the impregnation process by itself requires an excipient with good flow properties because an efficient mixing step is essential to the success of impregnation. This property is very important especially for fluidized bed impregnation because fluidization characteristics of a powder depends mainly on its flow properties. The typical porous carrier should be in groups A and/or B of Gelart's chart (86). In addition, the particle size distribution of the porous carrier is a critical property in impregnation. The particle size distribution has an impact on blend and content uniformity, which are very important (critical) material and quality attributes used in making release decisions of the resulting dosage form. In order to avoid segregation and poor content uniformity of the pharmaceutical products, the particle size distribution of the porous carrier should be very narrow. Also, because in impregnation, we need to dissolve the API in organic solvents, the porous carrier should be insoluble in such solvents. If the porous carrier is soluble in the organic solvents used in the process, this will destroy the internal structure of these carriers and also result in a granulation. Moreover, the porous carriers should be stable during the impregnation process. The porous carriers are also exposed to attrition, and potentially to high temperature. Thus, they should be stable in these conditions. Preserving the original particle size distribution (PSD) of the carrier is essential to the success of the impregnation process.

2.2.2 API Properties

The API used in impregnation should possess three main properties: it should be stable under relevant experimental conditions, it should be soluble to a significant extent in different types of solvents, and it should be inert. As mentioned previously, the impregnation experiments include some harsh conditions such as high temperature and attrition. The API should be physically and chemically stable to these conditions. For instance, if the API is heat labile, high temperature may melt or decompose it. Also, the API should have a relatively high solubility in organic solvents because a key element of impregnation is dissolving the drug in a solvent and then spraying it into a porous carrier in a liquid form. Finally, the API should be inert when combined with the porous carrier. If there is any possible chemical interaction between the carrier and the API, such an API should be excluded from the impregnation study.

2.3 Equipment requirements

In this section, the properties of equipment, which are required to manufacture and characterize the impregnated products, are discussed. These equipments can be classified into two main classes: equipment for manufacturing the impregnated products and equipment to characterize these products.

To enhance the manufacturing of impregnated products, the most important property that should be available in the impregnation device is providing a good mixing. API content uniformity is very important criterion for all regulatory agencies including FDA. The API should be uniformly distributed in the solid dosage forms. In order to get highly uniform products, the mixing device should provide efficient mixing of the porous carrier and the API solution. Furthermore, the most convenient impregnation devices

should have the capacity of drying the impregnated products. In this case, impregnation and drying happen simultaneously. This enhances the impregnation process with no need for separate drying step. In this case, all the required processes will occur in one device.

In this dissertation, two main devices were used for manufacturing of pharmaceutical impregnated products: Fluidized Bed (Minglatt) Dryer and Continuous Glatt Blender.

2.3.1 Fluidized Bed Dryer

In pharmaceutical manufacturing, Fluidized Bed (FB) devices are used as dryers, coaters, and granulators. FB processors have low shear effect, and high mixing performance with high drying capacity. These properties make FB processors an ideal device for impregnation. Fluidizing a porous carrier using a hot air and spraying API into the carrier produce thoroughly dried and highly homogeneous products. In this case, spraying and, loading/drying happen continuously and simultaneously.

The fluidized bed dryer selected here for the impregnation process is presented in Figure 2-3. It is a lab unit (Miniglatt), and its weight capacity is 500 grams. Monitoring process parameters such as process air pressure, atomizing air, temperature, and atomizing air pressure is simple and accurate.

2.3.2 Glatt continuous powder mixer

In continuous impregnation, we used a modified continuous blender, which is also utilized in dry blending. This blender is supplied with a nozzle for spraying the API solution. Ingredients were mixed and impregnated simultaneously. The loss-in-weight feeder is used to accurately dispense the host particles, which flowed to the continuous

blender. The impregnation step occurs in the continuous blender, after which the powder falls into a transition vibratory feeder where the NIR probe scans the powder bed.

The continuous blender (Glatt GCG-70) applies high shear and achieves excellent mixing performance. Figure 2-2 shows the blender tube. The unit was set up with a one-third forward-alternating-forward blade configuration. The first eight paddles and the last eight paddles all were angled in the forward direction to convey the powder forward through the process. The middle eight blades were angled in an alternating forward and backward direction, creating a zone of back-mixing where most of the blender hold up is located. This blade configuration was fixed throughout all the experiments Figure 2-3 illustrates the blending shaft with the blades.

2.4 Analytical methods

The impregnated products should be fully characterized in order to take a complete idea on both microscopic and macroscopic physical properties. During and after loading of API into porous carriers, significant changes in the physical properties of API could happen. These changes can include alteration in the physical state of API (amorphous or crystal), particle size distribution, flow properties, internal surface area, pore volume, and dissolution rate of API. The characterization studies presented in our work cover most of the above- mentioned possible changes in the impregnated products.

2.4.1 Microscopy

To characterize the morphology of impregnated particles, the efficient scanning electron microscopy (SEM) was used. This device clarifies the presence of any coating, agglomeration, and change in the shape or particle size of the impregnated products. The

aim of the impregnation process is to preserve the original morphology of the porous carrier. All SEM pictures were captured using a Zeiss Sigma FE-scanning electron microscope.

2.4.2 Differential scanning calorimetry (DSC)

DSC is an efficient device to study the physical state of drugs. It can differentiate whether the drug is in a crystal or an amorphous form. Moreover, DSC can determine the crystalline form of the drug. It correlates the heat energy input into the drug to the temperature at which physical changes take place. This can determine the thermal behavior of the drug whether it is endothermic (melting) or exothermic (crystallization). If there is no peak observed in the measurement, it means that the drug is in its amorphous form. Differential scanning calorimetry (DSC) analysis was performed using a differential scanning calorimeter Q1000 by TA Instruments.

2.4.3 Powder X-ray diffraction (p-XRD)

p-XRD is also used with DSC to determine the physical state of the drug. Each crystalline drug has a special X-ray pattern, which is usually characterized by the presence of sharp peaks. If these peaks disappear or become broader, it means that the drug is in amorphous form. p-XRD patterns were obtained using a PANalytical X'pert.

2.4.4 Specific surface area (SSA) and Pore-Size Distribution

The most distinctive property of porous carriers is a high internal specific surface area (SSA). SSA of any material depends mainly on the size or volume of its pores. Any reduction in the pore size and SSA after impregnation of the porous carrier means that the drug is successfully placed inside these pores. Specific surface area (in m^2/g) was

performed using Autosorb1 (Quantachrome Instruments, USA). The specific surface area was determined using 7- point N_2 adsorption by the Brunauer-Emmett-Teller (BET) model (87). The specific surface area was measured across a partial pressure range of 0.05–1 and using seven points. All samples were degassed for at least 18 h at 40 °C before the measurement.

2.4.5 UV-visible spectroscopy

As previously mentioned, one of the main aims of the impregnation process is to improve the blend uniformity of impregnated products. Thus, it was imperative to measure accurately the API amounts in impregnated products. Measuring the actual drug loading of impregnated products is essential to determine the API uniformity within these products. The blend uniformity is an important characteristic of drug products and is closely monitored by regulatory agencies. The API content uniformity was measured by taking ten samples from the impregnated material and determining the API amount in each sample, defined in equation 2-1. Then, from the mean value of these data, calculate the relative standard deviation (RSD) can be calculated.

$$RSD = \frac{s}{C} \qquad 2-1$$

In equation (2-1), **C** is the average concentration of the total samples collected in each experiment and **s** is the estimate of the standard deviation obtained using the sample concentrations.

Low value of RSD (i.e., less than 3%) means high blend uniformity while high value of RSD (higher than 5%) means poor blend uniformity. Blend uniformity of most impregnated products was determined using UV-Visible spectroscopy. In this technique,

the absorbance of UV-light by the sample was measured. Then, the absorbance values can be transformed into amounts (mass) using a previously built calibration curve.

2.4.6 Particle size distribution (PSD)

Measuring PSD of impregnated products is important to explore any change in the PSD before and after impregnation. The main aim of impregnation is to keep the original physical properties of the porous carrier with no change. The presence of agglomeration or particle attrition can be detected by measuring PSD. Therefore, it is of interest to study the PSD of the porous carriers before and after impregnation. Particle-size distributions (PSD) of all materials were measured using a laser diffraction technique (Beckman Coulter LS 13320) as shown in Figure 2-4. The working principle of this device depends on scattering of visible light. It measures scattered light angle and intensity. Then, the associated software translates the resulting data into an estimate of the PSD.

2.4.7 Shear cell testing

The properties of the final dosage form depend greatly on the flow properties of the powder used in its manufacturing. For instance, poor flow properties of the blend lead to high variability in tablet weight, which is very important in case of highly potent APIs because it can affect API content. Therefore, it was critical to evaluate the flow properties of the impregnated products and compare them with the original flow properties of porous carriers before impregnation.

The flow properties of pure NEU and the impregnated product were measured using a FT-4 powder rheometer (Freeman Technology Inc., UK). The procedure includes four steps: conditioning, consolidation, pre-shearing, and shearing. Conditioning was

accomplished by placing the tested powder into a glass cylinder. The powder bed was subjected to a helical rotating blade to produce a homogenous, reproducible state of the powder and eliminate any consolidation history. After that, a vented piston was used to achieve a desired consolidation state. The consolidating powder was pre-sheared to achieve a steady state at maximum shear stress. Then, this normal stress was reduced to a new normal stress and the sample was further sheared to achieve a yield point. The pre-shear procedure was repeated five times at different normal stresses to obtain the yield locus (88). All experiments were performed in triplicate. More details about the procedure can be found in Freeman et al. (89).

2.4.8 Dissolution testing

The main aim of any dosage form designed for systemic treatment is to provide an effective drug concentration in the blood (bioavailability). Drug bioavailability depends on the dissolution rate and the dissolution extent of the drug. The dissolution behavior of the drug is determined by the drug properties, dosage form properties, and the surrounding conditions (such as pH and temperature of the dissolution medium). The dissolution profile can be built by drawing the amount of drug released (%) versus time. In order to accurately study the dissolution behavior, the conditions of this study should mimic the physiological conditions of the body. This can be achieved by studying the dissolution behavior of the pharmaceutical products according to the USP (90) . All dissolution testing reported in this dissertation was performed in a 708-DS, 8-spindle, 8-vessel USP dissolution apparatus type II (paddle), with automated online UV-Vis measurement (Agilent Technologies).

2.4.9 Gravimetric Feeder Studies

For the current study, a single K-Tron KT20 (Coperion K-Tron Pitman Inc., NJ) loss-in-weight feeder configured with a pair of twin coarse-concave screws was used to dispense material at a controlled mass flow rate. The KT20 loss-in-weight feeder consists of three parts: a volumetric feeder, a weighing platform and a gravimetric controller. The controller adjusts the screw speed based on the feedback from the load cell, which records weight change over time of the material in the hopper. The first step was to tare the feeder and calibrate it with a standard weight. Next the powder was loaded into the hopper and feed-factor calibration was performed according the K-Tron protocol, to determine the maximum mass flow (feed factor) for the given material, screw size, and screw configuration. Subsequently, when a set-point is given, the feeder will determine an initial screw speed based on the ratio between the given set point and the feed factor.

2.4.10 Online near infrared (NIR)

An FT-NIR Matrix spectrometer (Bruker Optics Billerica, MA, USA) was utilized for spectral acquisition in this study. The probe was placed approximately 9 cm above the vibratory feeder, which is the necessary distance to obtain clear spectra. Keeping the location at a fixed distance between the NIR device and the powder samples was a crucial step for getting reproducible data, minimizing the sampling errors, and allowing all the points in the sample to have the same probability in the analysis (91). The software OPUS 7.0 from Bruker was used to control the NIR instrument and to construct the calibration models. Figure 2-5 shows the NIR set up used here, which included a vibratory feeder that transports the impregnated products continuously with no interference with the flowability. The calibration spectra were obtained by controlling the amount of API in the flow stream

while recording multiple spectra. This was done at 5 levels of API concentration in order to obtain the intensity of the associated API wavelength peak to the concentration of the API. This set up was utilized for both the calibration and for the actual residence time distribution (RTD) experiments.

Near infra-red (NIR) spectroscopy was utilized to measure residence time distribution (RTD) and monitor relative standard deviation (RSD) of the content. In an RTD experiment, a tracer pulse of a high contrast material is introduced in the system and it is measured as it leaves the system, enabling the determination of residence time, back-mixing, dead zones, and other important phenomena. The use of online real-time measurements was selected over other methods because it has many advantages. For instance, it can provide accurate and precise data while the experimental runs are occurring. It provides instantaneous and clear knowledge of when the tracer pulse starts exiting the system to when have fully exited the blender, which gives an idea about when the next experimental step should be proceeded (92–95). Since NIRs acquisition was fast, did not require any treatment, nor any sample preparation, it was the optimal device to obtain inline data acquisition. Furthermore, NIR spectroscopy was flexible enough to detect the concentration of a tracer in the liquid phase.

2.5 Preliminary impregnation study

Two methods were tested: 1) Fluidized bed impregnation method and 2) Continuous impregnation method. These methods of impregnation were tested with the following goals:

- Confirmation of concept – Assessing some advantages of FB impregnation method

- Extending the application of FB impregnation-Performing impregnation of two APIs on one porous carrier
- Demonstrating the capability of continuous impregnation using Glatt's continuous blender

2.5.1 Fluidized bed impregnation

In this part of our preliminary studies, the capability of a FB dryer to impregnate Griseofulvin (GF) and improve its solubility was demonstrated. Also, the ability of the FB dryer to co-impregnate Chlorpheniramine (CPM) and Ibuprofen (IBU) into a porous carrier was studied. The co-impregnation of two APIs has many advantages, including accuracy of combined dosing, elimination of a blending step, and elimination of segregation issues.

In these experiments, a fluidized bed granulator and dryer, the MiniGlatt, was utilized as an impregnation equipment. The procedure developed for the fluidized bed impregnation consisted of many steps. The mass of NEU loaded (220 gm) ensured that the bottom of the spray nozzle is reached by the fluidized powder bed. This is important to confirm that the nozzle is completely immersed into the fluidized powder bed during the impregnation. This condition is also necessary to prevent spray drying and allow a direct contact of the API solution droplets with solid particles of porous carrier. The impregnation process started by fluidizing NEU. Then, the heater was turned on and the inlet temperature was set at 80 ^{o}C. When the porous carrier temperature approached to about 60 ^{o}C, the pure solvent was sprayed. Once the steady state is achieved (constant product temperature), the spray was switched to API solution. After achieving the desired loading, the spray was switched back to the pure solvent for pre-selected time. This step is necessary to rinse the

pumping tubes and the spraying nozzle. Then, the resulting product was dried using a hot air. After that, the product was unloaded and placed in a tray to collect samples. Two preliminary FB experiments were conducted, and the results are discussed below.

2.5.1.1 Preliminary FB experiment #1

In this study, Griseofulvin (GF) was impregnated into magnesium aluminum silicate (Neusilin US2) using the fluidized bed dryer. GF was selected as a model drug because GF (class II drugs) is practically insoluble in water with challenging physicochemical properties. Substantial efforts have been conducted to improve the solubility of this drug. Some of the methods used, such as micronization, improve dissolution at the expense of worse material properties or more complex manufacturing processes. Therefore, the main aim of this work is to enhance the solubility of GF while also improving some other physicochemical properties such as flow properties using a simple process, FB impregnation.

The impregnation procedure of this experiment was the same as the procedure described in section 2.5.1. Since Griseofulvin has a limited solubility in methanol, the solvent in this experiment was composed of a mixture of methanol and acetone in a 1:1 ratio.

In this study, GF was impregnated in three different concentrations. 1, 5 and 10 %. Furthermore, the PSD, flow properties, and dissolution profile of impregnated products were characterized.

Particle size distribution (PSD) testing was conducted to evaluate any changes due to particle breakage, particle agglomeration, particle coating, and/or spray drying. PSD

measurements of pure and impregnated NEU is presented in Tab 2-1. The results showed that the impregnated products preserved the same PSD as pure Neusilin, which suggests that the drug is impregnated inside the pores of the Neusilin. Also, these results indicated that there is no evidence of spray coating, agglomeration, or fines due to particle attrition.

Dissolution was performed in 1000 ml of DI water at 50 rpm and 37 ^{o}C using the dissolution apparatus type I. Samples were withdrawn at predetermined time intervals (each 3 minutes) for 120 min using a peristaltic pump attached to the dissolution device. The amount of released IBU was determined spectrophotometrically. The Dissolution profiles of pure GF and 1% GF impregnated product were presented in Figure 2-6. The results showed a distinctive improvement in the dissolution behavior of GF after impregnation with NEU. The amount released of GF in pure crystal form was less than 1% in 3 minutes while impregnated product released about 40% of GF in 3 mins. Moreover, the impregnated product needed 36 min to release more than 90% while just 28% of pure GF was dissolved in the same period. This showed that impregnation can be an effective tool to enhance the solubility of practically insoluble drugs such as GF.

2.5.1.2 Preliminary FB experiment #2

The present study discusses the co-impregnation of two drugs, which are the antihistamine Chlorpheniramine maleate (CPM) and the non-steroidal anti-inflammatory drug Ibuprofen (IBU). The co-amorphous CPM-IBU mixture is important for many reasons. First, such composition could give a therapeutic benefit in the treatment of pain, fever, common cold, flu symptoms and allergic conditions. Second, these two drugs show poor compressibility, which means that there are some difficulties in manufacturing them as a solid dosage form. Moreover, IBU belongs to class II drugs according to the BSC,

which indicates that its bioavailability mainly depends on its water solubility. Consequently, converting of this drug into the amorphous form is expected to improve its bioavailability. Also, it has been shown that co-amorphization of two drugs at the same time could improve the physical stability of resulted co-amorphous products. Ultimately, since CPM is a basic drug and IBU is an acidic drug, these two drugs would be good models to show the applicability of co-amorphization for a wide range of drugs with different physicochemical properties.

Accordingly, the main aims of this preliminary case study were:

- To check the amenability of using FB dryer to impregnate two drugs into one porous carrier.
- To study the amorphization of two drugs into one porous carrier.
- To check the distribution of these two drugs in the blend.

In this work, all the experimental conditions were kept the same as for the previously mentioned cases in section 2.5. The two APIs (CPM and IBU) were simultaneously dissolved in the same solvent (Methanol). Target loading was set at 10% CPM and 20% IBU. Then, the solution was sprayed into NEU. After that, the resulting products was dried.

The impregnated product was analyzed by HPLC to determine the drugs contents and the blend uniformity of these two drugs. The best conditions to measure CPM and IBU accurately was optimized. Th mobile phase consisted of ammonium acetate buffer at pH 4 and acetonitrile (45:55). C18 (Agilent Eclipse-XDB) column was used and the injection volume was 20 µl. The results shown (Tab 2-2) indicated that while the target loading

(w/w%) of IBU was 20%, the actual loading was 20.99%; and for CPM while the target loading was 10%, the actual loading was 10.63%. This means that there is no loss of either APIs during the impregnation step and the experiment was run smoothly. Also, blend uniformity was evaluated in this work. Blend uniformity is an important parameter that should be measured to evaluate any pharmaceutical blend. It explains how the API is distributed within the pharmaceutical excipients. Results showed that RSD% of CPM was 1.21 and IBU was 0.89. The RSD% results of CPM and IBU indicated a highly uniform distribution of both APIs within the porous carrier. Generally, it is not an easy task to get a highly uniform blends, especially when working with two drugs. This is mainly due to insufficient mixing of ingredients or due to differences in physical properties such as particle size. Accordingly, complex formulation procedures and multiple unit operations need to be applied to obtain an acceptable blend uniformity. However, using FB dryer (a single unit operation) enables us to get a highly homogenous product of two APIs with no need to change the physical properties of these drugs.

In order to characterize the physical state of IBU and CPM in the co-impregnated product, the patterns of X-ray diffraction (XRD) were established on the pure IBU, pure CPM, and the co-impregnated product (Co-IMP). The XRD patterns of pure CPM and pure IBU showed sharp peaks (crystalline forms of these drugs). However, the disappearance of these peaks in the Co-IMP product demonstrated that these APIs are in amorphous forms. Figure 2-7 shows that the XRD patterns of pure IBU, which has distinctive peaks at 16°, 20°, and 22°, indicates that pure IBU is crystalline substance. Also, XRD patterns of pure CPM, which presents typical peaks at 19°, and 20°, demonstrate that pure CPM is in

crystalline form. However, the XRD pattern of Co-IMP product has no peaks, which means that both CPM and IBU were existed in amorphous forms inside NEU.

2.5.2 Continuous Mixing Process for the Manufacturing of Impregnated products

Continuous manufacturing process has several well-known technical and economic advantages over batch manufacturing. The aim of this preliminary study was to evaluate the feasibility of using a continuous mixing process as a tool to manufacture impregnated product and to examine the performance of porous carriers during this process. Furthermore, the purpose of this work is to investigate the improvement in some physicochemical properties of Ibuprofen (IBU) as an active pharmaceutical ingredient (API). To sum up, the main objectives of this preliminary study are:

1) Exploring the feasibility of using Glatt continuous blender for impregnation
2) Showing the improvement in some drug properties such as content uniformity and dissolution

In this experiment, the Glatt continuous blender (GCG-70) with a granulation shaft was used to impregnate IBU into a porous carrier. This blender was run at two rotation speeds (300 rpm and 600 rpm). IBU solution was prepared by dissolving 100 g of IBU in 1500 g of Methanol. The IBU solution was pumped through two nozzle positions: position 1 (at the 25% position along the axis from the entrance), and position 2 (at the middle point of the blender). Other experimental conditions included: pump rate: 25 ml/min; powder feeding rate: 5kg/h; shaft: granulation shaft (see Figure 2-8) A schematic of the continuous impregnation set up is depicted in Figure 2-9.

The mean residence time (MRT) of the Glatt continuous blender was determined using an independent measurement of the powder hold-up. The impregnated products were analyzed by UV-spectroscopy to measure average loading and blend uniformity of the impregnated IBU. Physicochemical characterization was conducted using a Laser-diffraction, Scanning Electron Microscopy, FT4 (shear cell), Raman spectroscopy, XR-ray diffraction and dissolution behavior.

All the products showed good homogeneity. RSD value less or equal to 4% were observed (see Tab 2-3). Generally, the actual IBU loading was lower than the theoretical value, which was calculated based on the concentration of IBU solution and the feeding rate. This indicates that there was a small loss of the drug during the run of the continuous impregnation step. Experiments using nozzle at position 1 showed better IBU loading than experiments using nozzle at position 2. All the results of measured blend uniformity were less than 4% RSD, which indicates that a uniform blend was obtained.

Blender hold-up was calculated by subtracting the mass exiting the blender to the total mass that flows into the blender, at steady state (See Figure 2-10 a&b). The hold-up measurements can be used to calculate the mean residence time (MRT). MRT is the time spent by a tracer material inside the blender. It can be calculated using equation 2-2:

$$Mean\ Residence\ Time\ (hr) = \frac{hold\text{-}up\ (kg)}{flow\ rate\ \left(\frac{kg}{hr}\right)} \qquad 2-2$$

The calculated MRTs of GCG-70 were 47.17 seconds at 600 rpm and 177.77 seconds at 300 rpm. In these experiments, the feeding rate was kept constant at 5 kg/h while the rotation speed was changed from 300 rpm to 600 rpm. The results showed that the rotation speed affected both the blender hold-up and the MRT. After increasing the

rotation speed from 300 rpm to 600 rpm, the MRT is reduced from 177.77 sec to 47.17 sec. This is due to the decrease in the powder hold-up, and consequently in the value of MRT, as the rotation speed of the blender increases.

The Raman spectroscopy results showed that IBU mainly existed in amorphous state as shown in Figure 2-11. The pure IBU has sharp peaks in the regions between (1200-1800 cm^{-1}) while these peaks disappeared in the IBU impregnated products. The absence of these sharp peaks from impregnated products indicated that the IBU was existed in amorphous form in these products.

Tab 2-4 shows the D_{10}, D_{50}, and D_{90} and Figure 2-12 presented PSD of the pure Fujicalin (FUJ) and 2% IBU-FUJ impregnated product using high shear blender at 600 rpm. Tab 2-4 reveals that impregnation of IBU at 600 rpm had an impact on D10, D50, and D90 as compared with pure FUJ before impregnation. Mixing speed at 600 rpm resulted in a decrease of D_{10} from 63 µm to 32.6 µm, D50 from 131 µm to 111.6 and D_{90} from 180 µm to 146 µm. This suggests that this process was associated with a particle size reduction due to high shear attrition of the carrier by the blender blades. Figure 2-12 supported these results. It is clear that PSD of the impregnated product shifted toward small particle size.

Figure 2-13 displays the results from the shear cell study. The curve depicts the shear stress (Incipient), kPa versus the applied normal stress (Incipient), kPa. The results of this study demonstrated that at the same applied normal stress (Incipient) both pure FUJ and 2% IBU in FUJ product showed approximately the same shear stress (Incipient). Moreover, the cohesive force for pure FUJ was (- 0.276) and for 2% IBU in FUJ product

was (-0.103). Both of these values are very low. This means that both products showed good flow properties with no substantial differences between them.

Also, the results demonstrated a substantial improvement in the dissolution behavior of IBU after impregnation. Ibuprofen is classified as class II drugs (Poorly Soluble-Highly Permeable) according to Biopharmaceutical Classification System (BCS). Thus, any increase in its solubility leads to a significant improvement in its bioavailability. As mentioned in Chapter 1, the impregnation process could lead to a significant improvement in the dissolution rate of poorly soluble drugs. This improvement is due to two main reasons. The first reason is increasing the surface area of the drug by placing it in a carrier with a high surface area, which leads to increase the surface area of the exposed drug into the dissolution medium and eventually results in improving the dissolution behavior. The second reason is the possibility of changing the drug state from crystal to amorphous state. The amorphous form of the drug is more soluble than the crystal form. Thus, placing the drug particle in small pores with a high surface area leads to a clear improvement in the dissolution extent and dissolution rate of poorly soluble drugs. As part of this study, dissolution tests were performed on both pure IBU and impregnated IBU to check the effect of the impregnation process on the dissolution rate and extent of IBU. Dissolution was carried out in 900 ml of DI water at 50 rpm and 37 ^{o}C using the rotating paddle method. Samples were withdrawn at predetermined time intervals (every 3 minutes) for 60 min using a peristaltic pump attached to the dissolution device. The amount of released IBU was quantified spectrophotometrically. The results presented in Figure 2-14 demonstrated that the impregnated product releases about 85% of IBU within less 5 minutes while less than about 10% of pure crystal IBU was released within 5 minutes.

These results suggested that impregnation method could be used as an efficient technique to improve the dissolution rate of a poorly soluble drug.

2.6 Summary of Preliminary Data

API was successfully loaded into a porous carrier using a Glatt FB dryer. This process was simple to run, and it was easy to manipulate its parameters to achieve different results. For instance, a wide range of API loading could be performed by just changing the spray time. Moreover, impregnation and drying happened simultaneously in this process. This makes FB dryer a perfect device for impregnation. Also, the preliminary results showed that there are no fines generated by attrition or spray coating, or agglomeration, which means that the process runs smoothly. However, the processing parameters of the FB dryer such as spray rate, flow rate of drying air, atomizing rate, pumping rate etc., need to be carefully controlled to achieve the desired results.

API was also successfully impregnated into a porous carrier using a continuous Glatt blender containing a granulation shaft, followed by drying using a Miniglatt fluidized bed dryer. The API loading level can be changed by increasing the concentration of API solution or by increasing the pumping rate. Blend uniformity was acceptable (less than 4.5) with all experiments. However, the nozzle position 1 showed less API loss. The RPM has a clear effect on the hold –up and MRT, where 600 rpm showed lower hold-up and shorter MRT than for 300 rpm. However, wet masses were observed during the run of some impregnation experiments, especially with increasing the pumping rate. This might be due to the distance between the granulation shaft (thick) and the wall of the blender, which is relatively small. Any increase in the pump rate leads to a high local liquid to solid ratio. This eventually results in the formation of a wet mass. This problem could be fixed by

adjusting the pump rate of API solution or by increasing the solids feeding rate. However, the degrees of freedom available to solve this problem were limited. Accordingly, the blending shaft was changed from granulation shaft (thick) to a blending shaft (thin). Therefore, in Chapter 5, a blending shaft has been used in the continuous impregnation experiments instead of a granulation shaft.

Both fluidized bed impregnation and continuous impregnation methods will be studied in more detail in the Chapters 3, 4 and 5, respectively.

2.7 Figures

Figure 2-1 Miniglatt Fluidized Bed

Figure 2-2 The continuous blender tube (Glatt GCG-70)

Figure 2-3 The blending shaft of the continuous blender

Figure 2-4 Laser diffraction analyzer (Beckman Coulter LS 13320)

Figure 2-5 Bruker NIR set up

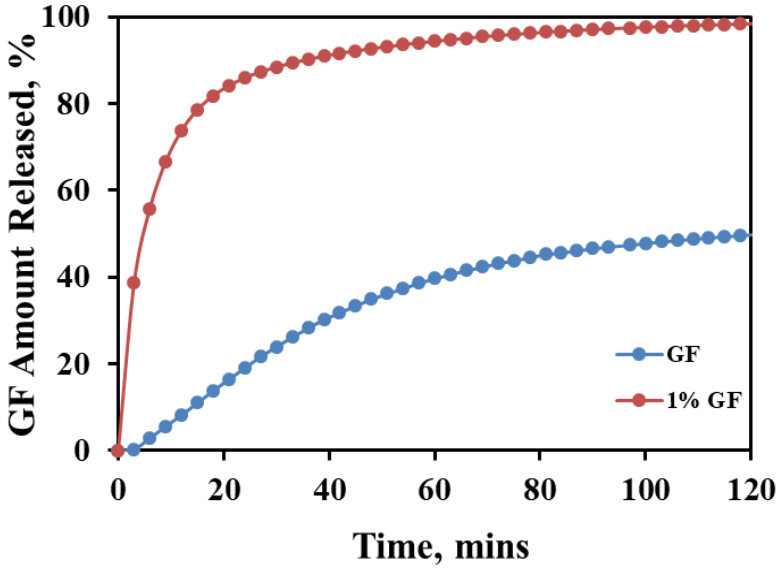

Figure 2-6 Dissolution behavior of Neusilin Impregnated products containing GF in DI Water

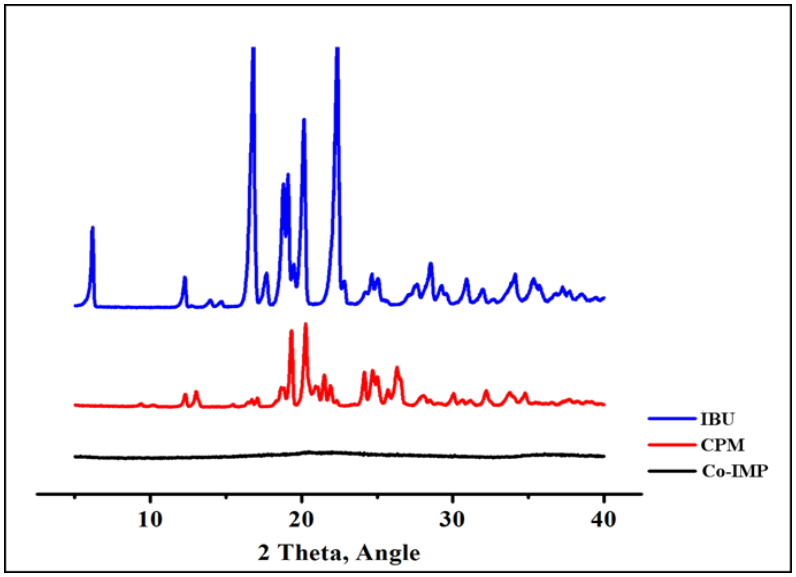

Figure 2-7 PXRD of pure Ibuprofen (IBU), pure Chlorpheniramine (CPM), and a co-impregnated product (Co-IMP)

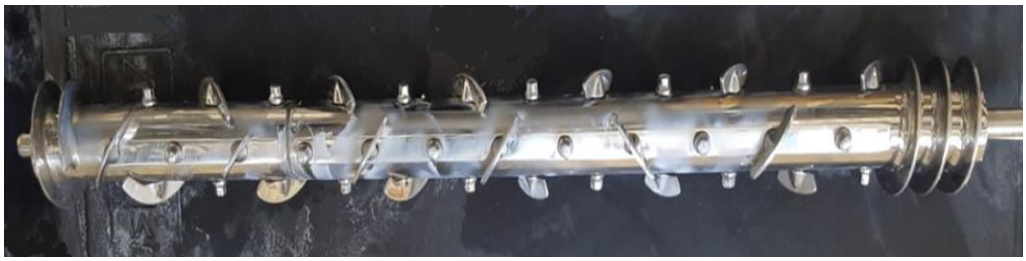

Figure 2-8 Granulation shaft and its blades

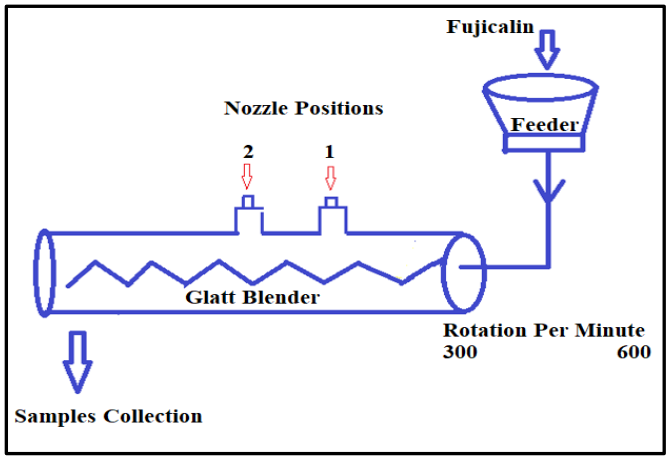

Figure 2-9 Continuous Impregnation Set Up

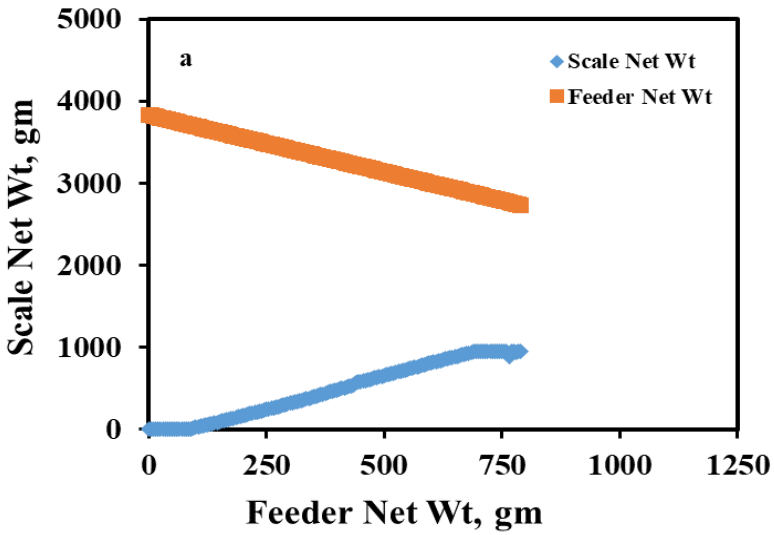

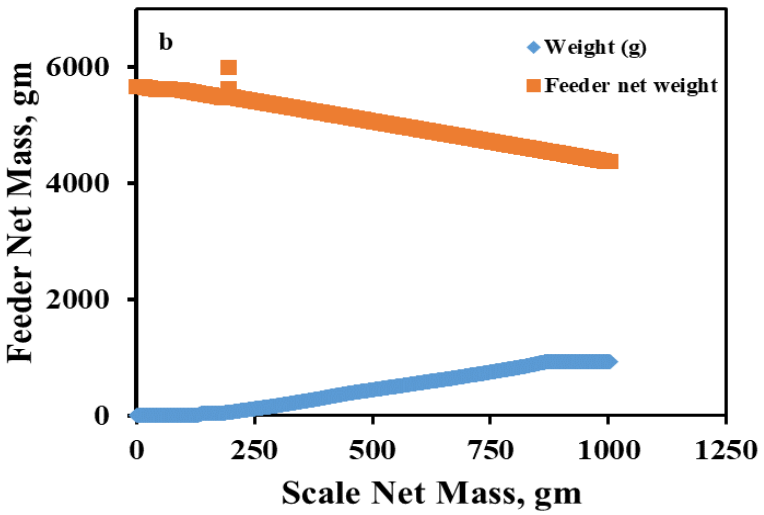

Figure 2-10 Hold Up Measurement of Glatt Blender at (a) 300 rpm and (b) 600 rpm

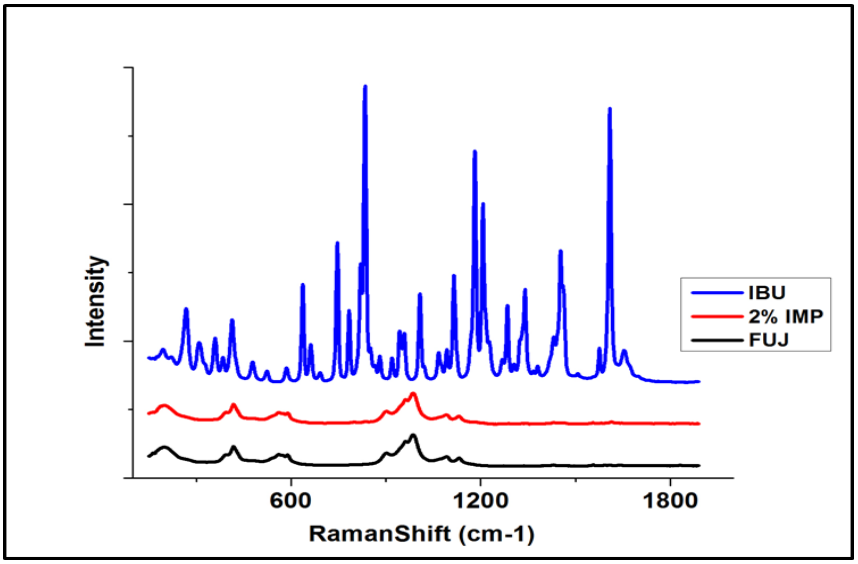

Figure 2-11 Raman Study of Ibuprofen Impregnated Products with FUJ (Continuous Blender)

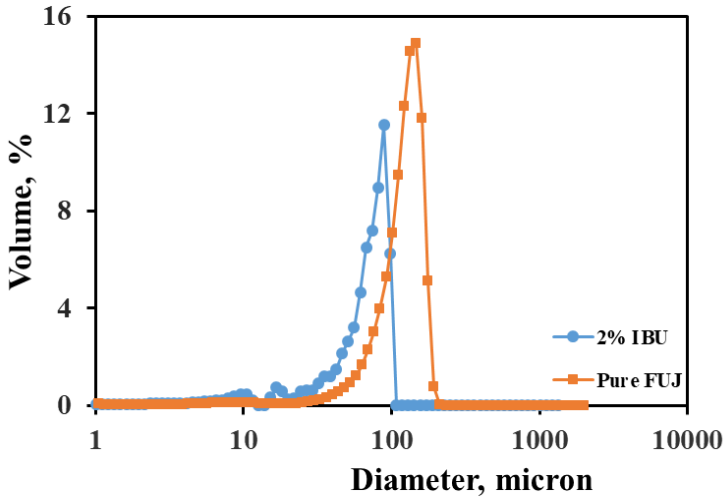

Figure 2-12 Particle Size Distribution of Pure FUJ and 2% IBU impregnated in FUJ

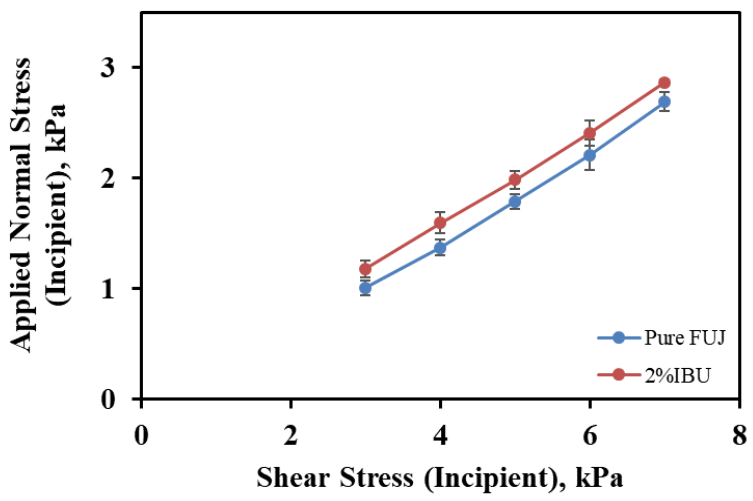

Figure 2-13 Shear cell measurements by FT4 of Pure FUJ and 2% IBU impregnated in FUJ

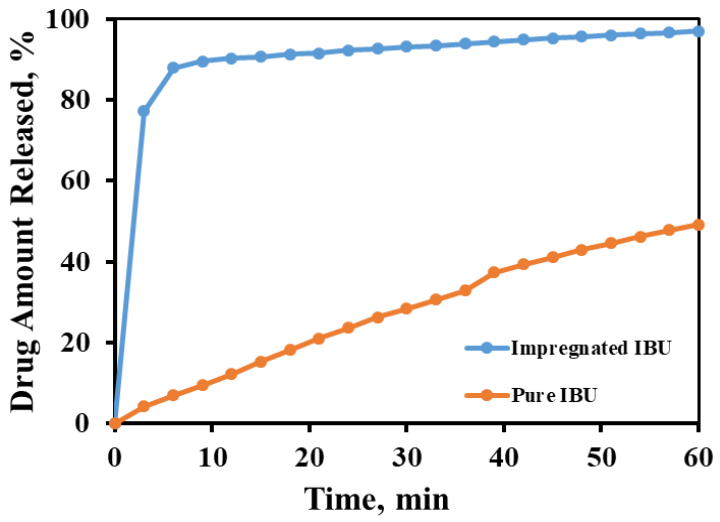

Figure 2-14 Dissolution Behavior of Pure Ibuprofen and Ibuprofen impregnated in FUJ

2.8 Tables

Products, %	D_{10} (µm)	D_{50} (µm)	D_{90} (µm)
Pure NEU	**55.10**	**124**	**205**
Pure GF	**5.11**	**18.95**	**37.64**
1% GF-NEU	**63.77**	**133.7**	**201.9**
5% GF-NEU	**59.34**	**126.45**	**200.15**

Tab 2-1 Particle size of NEU, GF and impregnated products

Sample	Target Loading (w/w%)	Actual Loading (w/w%)	RSD %
CPM	**10**	**10.63**	**1.21**
IBU	**20**	**20.99**	**0.89**

Tab 2-2 The loading and blend uniformity study of co-impregnated product

Nozzle Position	Blender RPM	Target Loading (w/w%)	Loading, %	RSD, %
1	300	2	1.82	3.1
	600		1.81	3.4
2	300		1.49	4.7
	600		1.43	2.3

Tab 2-3 The loading and blend uniformity study of IBU impregnated product using a continuous blender

Products, %	D_{10} (µm)	D_{50} (µm)	D_{90} (µm)
Pure FUJ	63	131	180
2% IBU-FUJ 600rpm	32.63	111.6	146.06

Tab 2-4 Particle size of FUJ, IBU impregnated products using a continuous Glatt blender at 600 rpm

Chapter 3 Manufacturing of Pharmaceuticals by Impregnation of an Active Pharmaceutical Ingredient into a Mesoporous Carrier: Impact of Solvent and Loading

3.1 Introduction

As mentioned in Chapter 1, impregnation is the process of placing chemical substances (such as drugs) inside porous carriers using a solution or a suspension. Recently, there has been an increasing interest in the use of mesoporous carriers (MC) in drug delivery (24,96) because of their amenable physical properties such as a narrow particle size distribution, high surface area, good flow properties, and small pore sizes with narrow distribution (52). The high surface area of these carriers allows them to absorb several compounds, including poorly flowing materials such as oily drugs. Since these compounds are completely embedded within the porous carriers, the physical properties of the impregnated products are almost identical to the carrier, thereby facilitating their handling and further processing (97,98). Moreover, the drug within the pores of the MC mainly exists in an amorphous form, which is known to improve its dissolution (99). Very small pore sizes of the MC, for example Neusilin US2, result in confining of the drug, which limits the drug's mobility and inhibits the drug's recrystallization inside these pores (41,99). Accordingly, impregnation of drugs into a MC can improve some crucial properties of the drugs such as its dissolution behavior (100). In contrast, other pharmaceutical manufacturing processes used to improve drug properties, involve many challenges in terms of processing steps, and controlling product quality (101,102). The production of drug-carrier complexes that are independent of the physical properties of the active ingredient, along with its dissolution behavior, makes them useful amenable for

development of solid oral dose product. Thus, one aim of this work is preserving the physical and chemical properties of the composite, which is considered as a benefit in terms of the drug properties. Also, MCs can be used to reduce the drug's adverse effects. For example, oxybenzone, which is used in sunscreen preparations, was successfully loaded into a MC (MCM-41) to reduce its side effects (103). A thorough discussion about the new applications of mesoporous silicon dioxide and silicates in drug product development can be found in Qian and Borgner (104).

Lastly, impregnation eliminates the need for several intermediate processing steps, in both the drug substance and the drug product development routines. Drug substance and drug product development are intertwined processes, where drug product development completely depends on properties of the drug substance. Drug product development, irrespective of the manufacturing route, is sensitive to change in the properties of the drug substance. Thus, enabling superior control of the drug substance attributes is beneficial for a successful drug product development. The monitoring and control of physicochemical properties of the drug substance is not a simple task and involves many unit operations. In general, it begins with choosing the state of the drug substance –crystalline or amorphous. This is followed by working to achieve the desired physical properties. Crystalline drug substances are relatively stable and pure and are preferentially used in manufacturing of solid dosage form over the amorphous form of drug substances. However, achieving the desired properties of the crystalline drug substance is challenging and involves manipulating the crystallization process variables, and controlling the filtration and drying process steps (105). Amorphous form of drugs, albeit being good alternatives, are usually physically unstable. It is also difficult to control their physical properties during drug

substance and drug product development. As previously mentioned, using MCs improves the physical stability of amorphous drug substances (41,99) and facilitates control over some of the essential drug substance attributes such as particle size, flow properties, and dissolution behavior.

Consequently, several loading methods have been developed for incorporating crystalline drugs into MC. Loading drugs into these carriers can be done by co-milling (99), melt adsorption using hot-melt extrusion (106), spontaneous evaporation and sublimation (107,108), co-spray drying (109), and wet impregnation (16,18). However, several of the previous techniques exhibit drawbacks and manufacturing challenges. For instance, both co-milling and hot melt extrusion may lead to a change in the physical structure of the drug due to elevation of the drug's temperature above its glass transition temperature. In addition, some drugs show polymorphism at high temperatures, which can lead to loss of the drug's stability and therapeutic effects. Furthermore, co-grinding can also change the morphology of both the drug and the carrier (15,99) resulting in products with poor flowability and poor compactability. The spontaneous evaporation and sublimation method were also found to be challenging from a process configuration and scale-up perspective. For instance, it is difficult to control process parameters, ensure product quality, and achieve amenable scale up of a porous dispersion, which was prepared using flash evaporation (110). On the other hand, wet impregnation has been found to be comparatively successful. It can be achieved using several different approaches. The most routine approach involves dissolving the drug in a suitable solvent and mixing this solution with a porous carrier, followed by filtering of the resultant impregnated product (18,48,111) One drawback of this method is the difficulty in achieving an accurate desired

drug load, and the large equilibration and filtration cycle times. Wet impregnation can also be performed by a method called ‘incipient wet impregnation’, which includes mixing the drug solution with the porous carrier followed by evaporating the organic solvent from the mixture. The mixing and drying are usually repeated more than once (36) However, like standard wet impregnation, this method is slow and often results in non-homogeneous loading of the carrier.

Recently, Grigorov et al (53) attempted a new method to impregnate drugs into porous carriers. This method involves spraying the drug solution into porous carriers within a fluidized bed (FB). Impregnation and drying occur simultaneously, and this method enables the user to achieve different drug loadings independent of the drug’s solubility.

While Grigorov et al (53,100) examined the impregnation of Acetaminophen (APAP) in Dibasic Calcium Phosphate and Fenofibrate in Neusilin, they used a single solvent (methanol) to impregnate selected drugs in a single carrier material. It is of interest to look at the same drug in a different carrier and look at the same drug with different solvents to examine the effect of solvents. In this work, the impregnation of APAP in Neusilin using both water and methanol were examined. The results of these two solvents to determine what effects these solvents will have on the properties of impregnated products and their dissolution behaviors were compared as well. In addition, our results for APAP in Neusilin can be compared to previous work for APAP in methanol impregnated in Dibasic Calcium Phosphate. Thus, this work aims to test the robustness of the fluidized bed impregnation process, and its applicability for a variety of solvents. Impregnation of Acetaminophen (APAP) into a magnesium/aluminum metasilicate (Neusilin ^{R} US2 (NEU)) has been studied in a Mini-Glatt spray fluidized bed dryer/granulator. Different APAP

loadings have been investigated and the physical properties of the impregnated product have been thoroughly characterized.

3.2 Methods

3.2.1 Experimental Set-up and Impregnation Procedure

Based on the preliminary experiments, the procedure applied for the fluidized bed impregnation experiments using a Mini-Glatt consisted of the following steps:

1) Load fluidized-bed dryer with NEU (about 220 g) until the top spray nozzle is reached. Thus, during fluidization, the nozzle is located within the bed to reduce spray drying.

2) Run the fluidized-bed dryer to a stable fluidization profile and adjust the inlet gas temperature to 80 ^{o}C.

3) Begin spraying the pure solvent (methanol or water). Spraying only pure solvent at the beginning is necessary to reach a steady state temperature of the product.

4) After achieving a steady state (constant product temperature), start spraying the APAP solution. The APAP solution is prepared by dissolving a desired quantity of APAP, based on the drug load, in pure Methanol or DI water. It is preferable for the API concentration in the solvent to be as low as possible; adding a large amount of drug in a short time this may lead to poor blend uniformity. At the same time, if the API concentration is extremely low, then the operation will take a long time. Therefore, we chose API concentrations that allows completion of the experiment within a few hours and leads to low RSD values.

5) Once the desired quantity of API is sprayed in solution form, we spray pure solvent for 20 min. Spraying pure solvent after spraying the drug solution is essential to dissolve any APAP at the surface of NEU and impregnate it.

6) Dry the impregnated product until the product temperature reaches 50°C.

7) Cool down the product and discharge.

The resulting impregnated product was placed in a tray. Ten samples were extracted from different random locations in the tray. These samples were stored inside glass vials and used for the blend uniformity study. APAP was impregnated into NEU for four different loadings (w/w), namely, 0.1, 1, 9, and 24 % using methanol as a solvent, while it was impregnated using water at three different concentrations: 0.1, 1, and 5%. Details of the experimental conditions and the process parameters are presented in Tab 3-1. All experimental conditions were kept constant except the APAP solution concentration, which was changed according to the target loading in the same amount of time.

3.2.2 Analytical Methods

The analytical methods were employed in order to characterize the impregnated product and the pure carrier. These methods were done using the same conditions, which are prescribed in Chapter 2, including:

- SEM and Particle Size Distribution
- Shear Cell Tests (88,89)
- Specific Surface Area (SSA) and Pore Volume Distribution (87)
- X-Ray Powder Diffraction
- Raman Spectroscopy

- Differential Scanning Calorimetry (DSC)
- Dissolution Behavior
- Drug loading and Blend Uniformity

Drug loading was measured using UV/Visible spectroscopy (Varian Cary 50 Bio, Agilent Technologies, USA). As mentioned previously, ten samples were extracted from each experiment to get a representative RSD value. 400 mg from each sample was placed in 100 ml conical flasks; and methanol was added until the 100 ml mark. This dispersion was sonicated for 40 minutes and left overnight at room temperature to ensure a complete extraction of APAP from NEU. Samples were then withdrawn from each flask using a millipore (0.45 µm) syringe filter. The UV readings at λ=247.5nm were acquired and analyzed to quantify the amount of APAP in each sample. In order to quantify the measured absorbance, a calibration curve was built by acquiring the UV absorbance of five different concentrations of APAP in methanol.

Consequently, the APAP loading of each sample, the mean, the standard deviation and the % relative standard deviation (% RSD) along with the confidence intervals (C.I.) of the measurements for each batch were computed using equation 3-1 (112):

$$\nu \in \left(\sqrt{\frac{(n-1)\,V^2}{(\chi/\mu)^2{}_{1-\alpha/2,n-1}}}, \sqrt{\frac{(n-1)\,V^2}{(\chi/\mu)^2{}_{\alpha/2,n-1}}}\right. \qquad \textit{3-1}$$

Where: $\boldsymbol{\nu}$ is the confidence interval; $\boldsymbol{V}$ is the expected value of the RSD measurement; $\boldsymbol{n-1}$ is the degree of freedom; $(\boldsymbol{\chi/\mu})^{\boldsymbol{2}}$ is Chi-on-Mu-square, which is a statistical value, that can be obtained from a table for different significance levels and degrees of freedom.

Raman spectra were acquired using a RAMANRXN1™ (PhAT System™) from Kaiser Optical Systems, Inc., MI, USA. Before starting sample measurements, the device

was calibrated using Cyclohexane as a standard. Measurements were performed under the following conditions: laser wavelength at 785 nm; spectral coverage from 150 to 1875 cm^{-1}, exposure time at 30 s; laser power of sample at 400 mW. Raman spectra were acquired for both impregnated and physical mixtures of 5%, 9%, and 24% APAP in NEU. 5%, 9%, and 24% physical blends (w/w) of APAP and NEU were prepared using a Lab-RAM mixer (Resodyn™ Acoustic Mixers, Inc., USA) at 60% intensity for 3 min vibration time.

3.3 Results and Discussion

3.3.1 Particle Size distribution (PSD) and SEM

The particle size distribution (PSD) of the pure carrier and the impregnated product is shown in Tab 3-2 and Figure 3-1. It can be observed that the PSD of the pure NEU is almost identical to that of the impregnated product. The preservation of the particle size distribution of the carrier and the absence of fines confirm the feasibility of impregnating drug into porous carriers using a fluidized bed.

The absence of fines, indicated by no significant change in the D_{10} (see Tab 3- 2), is also indicative of a gentle process, without major attrition of the carrier particles (53,99).The creation of excessive fines during processing, and their subsequent presence in a formulation are generally undesirable. Presence of excessive fines in a formulation can lead to poor flow and dusting. What is also observed is that the mean particle size of the impregnated product lies between 128.3-136.3 µm. This makes them suitable for most oral solid dose unit operations. These products are also similar in particle size to a large number of the common pharmaceutical excipients. So, these impregnated products are compatible to mix with most pharmaceutical excipients, which are used in manufacturing of solid

dosage forms. For instance, the mean particle size of lactose monohydrate -SuperTab® 11SD and microcrystalline cellulose-Avicel pH102 are 116 and 124 µm, respectively. This makes them amenable to physical homogenization with excipients, and alleviates segregation risk (2). Furthermore, particle agglomeration or aggregation of the impregnated product was not observed. The D_{90} of the impregnated product is approximately the same as the D_{90} of the pure NEU.

SEM pictures of the pure and impregnated NEU are shown in Figure 3-2. As can be seen in this Figure, the impregnated products possess a spherical morphology, which is essential for good flow properties. SEM pictures of the impregnated product indicate that the morphological properties of the impregnated product are similar to pure NEU. The process of loading and drying of the drug particles within the carrier does not result in any discernable change in the external morphology of the carrier particles. There is no evidence of granulation, agglomeration or coating of the carrier particles during the impregnation process.

The pure carrier is spherical in shape and the preservation of this sphericity is crucial for maintaining good flow properties of the carrier particles. The preservation of the particle size and morphology of the impregnated product by this method is a significant advantage over other impregnation processes such as co-grinding or milling of drugs with porous carriers (15,52,99), where strong attrition may lead to significant changes in surface morphology and particle size distribution.

3.3.2 Shear Cell Tests

NEU US2 has good flow properties and compactibility, which are important in manufacturing of solid dosage forms, especially tablets. Flow properties of pharmaceutical solid powders are crucial requirements to successfully formulate them into final dosage forms. The flow properties of different impregnated products compared to pure NEU are shown in Figure 3-3.

This Figure is a plot of the measured shear stress vs. the applied normal stress. The resultant yield loci of the impregnated product are compared with pure NEU. The flow properties of the impregnated product are highly comparable to the flow properties of pure NEU. The data also suggests that the API has been successfully impregnated inside the NEU. If there is any APAP at the surface of NEU, this will result in a discernible change in the flow properties of the product mixture due to the largely poor flow properties of APAP as compared to NEU. However, our results showed a negligible effect of APAP impregnation on the flow properties of the final products. This suggests that there is no APAP at the surface of the impregnated products and the APAP has been placed inside the pores of the NEU. The result is in agreement with previous work on impregnation of API into porous carriers (53). The preservation of the flow properties of the pure NEU even after impregnation is an important advantage of this method, over other impregnation techniques.

3.3.3 Specific Surface Area (SSA) and Pore Volume

The BET surface area and pore volume of pure and impregnated NEU are presented in Tab 3-3 and Figure 3-4. The surface area of NEU, which is determined using the BET method, was significantly reduced after being loaded with APAP. The free surface area of

NEU before APAP loading was 390.4 (m^2/g) while it was 264.5 (m^2/g) and 226.8 (m^2/g) after loading with 5% and 24% APAP, respectively. This indicates that the surface area of 5% APAP loading represents about 67.8% of that of the pure NEU while the surface area of 24% APAP loading equals to 58.1% of the pure NEU**.** Results also revealed that the pore volume of pure NEU (1.742 cc/g) was higher before being loaded with 5% APAP (1.308 cc/g) and 24%APAP (1.091 cc/g), as expected.

These results indicated the impregnation of the drug particles within the carrier rather than external deposition. This study employs reduction in pore volume as an indicator of impregnation rather than reduction in pore size. This is because NEU has a very small pore size, around 5 nm, and these pores are irregular in shape. This makes it challenging to accurately quantify the reduction in pore size. Moreover, Greg et al. (113) concluded that from the shape of BET curve, one can estimate the pore shape of porous carriers. This means that porous carriers with different pore shapes result in different BET behaviors. According to these findings, the pore shape of NEU is slit type. Slit- type pores do not have regular dimensions. Therefore, it is better to depend on pore volume and not pore size in this study.

3.3.4 Loading and Blend Uniformity

Tab 3-4 shows the results of loadings and blend uniformity for all impregnation experiments. The APAP loadings of all experiments are very close to their target loadings. This indicates that FB impregnation is successfully able to load APAP into NEU, with little APAP loss.

FB impregnation produces a blend with high uniformity (53) and the results in this study confirmed that (see Tab 3- 4). The blend uniformity in this study was calculated as a relative standard deviation (%RSD). All impregnation experiments showed a high blend uniformity with an RSD value of less than 5%. Achieving satisfactory blend uniformity can be challenging, especially for formulations with low API content. Using FB impregnation, satisfactory blend uniformity was achieved even for API loads as low as 0.1% and 1%. These results are in agreement with previous studies (53,88).

3.3.5 Physical State of APAP loaded into NEU

To study the state of APAP in the impregnated product, X-Ray diffraction of pure APAP, pure NEU, 5% APAP impregnated in NEU using DI water as a solvent, and 24% APAP impregnated in NEU using methanol as a solvent were conducted. The results are shown in Figure 3-5.

The diffraction pattern of pure APAP presented a complete crystalline state while NEU US2 pattern showed a complete amorphous form. The crystalline form of APAP was confirmed by the appearance of several sharp peaks with high intensity: 11.97°, 13.64°, 15.37°, 16.54°, 18.03°, 18.78°, 20.25°, 23.32°, 24.20°, and 26.35° at 2 Theta (θ) diffraction angle. Pure NEU showed a broad halo pattern, which confirms its amorphous structure. The diffraction pattern of 5% APAP in NEU resemble the pattern of pure NEU US2. These results thus indicate that APAP is converted into its amorphous state after being impregnated. The pattern of 24% APAP in NEU showed some small peaks with very low intensity: 26°, 24°, 23°, 18°, and 14° at 2 θ diffraction angle. Nevertheless, this pattern did not show any clear sign of APAP crystallinity. In general, the observed results of the XRD study revealed that APAP exists mainly as an amorphous form in NEU.

Similar findings were obtained from the Raman study which is presented in Figure 3-6.

In the Raman scattering study, the spectra from 200 cm^{-1} to 1800 cm^{-1} were acquired for all samples. For APAP, many sharp peaks were observed in the regions of 790-900 cm^{-1} and 1200-1660 cm^{-1}. These regions were further elaborated into 797, 858, 1236, 1324, 1560, 1611, and 1649 cm^{-1}, which represent CNC ring stretching, ring breathing, C–C ring stretching, amide III, amide II, ring stretching, and amide I modes, respectively (114–116) However, pure NEU showed no peaks. 5% and 9% APAP in NEU have spectral pattern which resembles pure NEU (see Figure 3-6a and Figure 3-6b). On the other hand, the spectra of 24% APAP in NEU, as shown in Figure 3- 6c, revealed that there are very reduced peaks observed in the 790-900 cm^{-1} and 1200-1660 cm^{-1} regions. This difference in Raman spectra between 5%, 9% & 24% APAP in NEU might indicate that there are a few crystals of APAP at the surface of NEU or within the NEU particles. In order to clarify these results, a physical mixture of 5%, 9%, and 24% APAP in NEU were prepared by using a Lab-ram mixer. Raman spectra of APAP and NEU physical blends were acquired. Raman data of 24% APAP in NEU showed some crystallinity while other characterization tests did not show such behavior. Figure 3- 6a and 3-6 b showed that 5% and 9% physical mixtures of APAP in NEU have relatively sharp peaks in the 790-900 cm^{-1} and 1200-1660 cm^{-1} regions while impregnated products at the same concentrations do not show any significant peaks in these regions. On the other hand, Figure 3-6c demonstrated the differences in spectra of 24% impregnated NEU and the physical mixture. The physical mixture showed more intensified peaks at the same previously mentioned wave number regions. Also, peaks intensities of the physical blends are dependent on the % of APAP

while the impregnated products did not show such behavior. Although, the peak intensity of impregnated products was significantly lower than that of the physical mixtures, the results indicate that for 24% APAP in NEU crystalline APAP could exist in the product. At the same time the impregnation reduced the content of APAP in the crystalline form.

DSC is an efficient technique to study the state of solids. Appearance of phase transitions help to recognize glassy from crystalline while disappearance of phase transitions means molecular dispersion (no peaks) of drugs within carriers. DSC curves are shown in Figure 3-7 for pure and 5% and 24% of APAP impregnated in NEU. The DSC study of 1% APAP in NEU has not been conducted because we would not expect that the presence of tiny amounts of crystalline drugs in samples (10 mg) containing 1% APAP in NEU could be detected by DSC. From Figure 3-7 it can be seen, that pure APAP has a strong endothermic peak at 170 ^{o}C, which characterizes the melting point of crystalline APAP, while, pure NEU does not show any peak, which indicates its amorphous state. No peaks were also observed for 5% and 24% of APAP in NEU. The DSC curves resemble to a large extent that of pure NEU. The DSC results of impregnated products do not show any peaks (exothermic or/and endothermic) in cooling data (not shown) and heating data. The DSC results indicated that the drug is molecularly dispersed (no peaks in the DSC) in the NEU as has been explained by Mellaerts et al. (48). For a molecular dispersion, the solid is in amorphous form, in which the intermolecular forces are broken down and the molecules are separately distributed within the carrier nano-pores. Thus, the formation of ordered structure and re-crystallization are prevented by the confining effect of the pores. The results, which are in agreement with XRD and Raman spectroscopy, further support the argument of amorphization of APAP during FB impregnation.

3.3.6 Drug Dissolution Behavior

The dissolution behavior of impregnated products was compared with the dissolution behavior of pure APAP using different dissolution media. Figure 3-8 shows the dissolution profiles of pure APAP and impregnated products in DI water.

The results indicate that there is no significant difference among the dissolution profiles of the samples in this dissolution medium. Impregnation of API into a mesoporous carrier is expected to increase the dissolution rate of this API (100,117) due to its amorphization during the process. However, in this study, the effect of impregnation on the dissolution behavior of the impregnated product is not discernible. APAP has a high solubility in the dissolution medium (DI water) making the profiles indistinguishable from pure APAP (see Figure 3-8). However, the dissolution of impregnated APAP was enhanced in HCl, pH 1.2 media as shown in Figure 3-9. Samples for Figure 3-8 were tested over 100 min while samples for Figure 3-9 were tested over 50 min because the dissolution rates of APAP in impregnated products using 0.1 N HCl as a dissolution medium was faster than the dissolution rates of APAP in impregnated products using DI water as a dissolution medium.

APAP does not show a pH dependent solubility between a pH of 1.2 and 8.0 (118). However, our results showed different dissolution behaviors of APAP in impregnated products using 0.1 N HCl and DI water as dissolution media. This is mainly due to the fact that the improvement in the dissolution profiles of drug after loading it into silicate is not only due to amorphization. The release of silicic acid and ions (Mg^{2+} and Al^{3+}) from NEU into the dissolution medium significantly improves the dissolution rate of drugs. The release extent of these products is more in 0.1 N HCl than other dissolution medium (119).

In addition, the impregnated products in all dissolution media showed a constant rate in the late stage of dissolution, at which the change in the rate of dissolution tends to zero. This behavior might suggest that an interaction could exist between APAP molecules and the NEU (silanol group) in the impregnated products. A further study is needed to explore this interaction in more detail.

3.4 Conclusions

In this study, a highly porous carrier (NEU) was successfully impregnated with Acetaminophen in a fluidized bed. The resulting product was fully characterized, and the results demonstrated that these products have properties amenable for manufacturing as solid dosage forms. The impregnated product showed excellent blend uniformity, good flow properties, and a narrow particle size distribution. In addition, the results indicated that the different evaporation profiles of the solvents do not affect the morphology or loading efficiency of APAP in NEU. Furthermore, the results showed that the blend uniformity did not depend on the drug loading or solvent type. The results also demonstrated that the APAP was present in the pores of the carrier mainly in its amorphous form. This was concluded from Raman spectroscopy, X-ray diffraction measurements, and DSC studies. Drug amorphization was observed because APAP is placed inside very fine pores (about 5 nm), which confined its dimensional growth, and prevented its recrystallization. This would be expected to improve APAP dissolution behavior in media where crystalline APAP shows poor solubility.

The use of a fluidized bed to impregnate APAP into porous carriers eliminates many unit operations in both drug and dosage form development. Application of fluidized bed impregnation in pharmaceutical manufacturing is a promising tool to decrease both

downstream and upstream development efforts, which are necessary to adjust the properties of both drugs and dosage forms. However, additional work must be performed to study the effect of process parameters of the fluid bed operation on the properties of impregnated products. In addition, the conclusions of this work are based on one carrier and one drug substance and further work should be carried out to investigate the generality of our results. Future work should investigate the feasibility of the method for other active ingredients and porous carriers. Moreover, we expect that co-impregnation of API and polymer would potentially alter the properties of the resulting materials and could control their release profiles. Future work should examine co-impregnation of API and polymer as a way to further control properties of the drug product.

3.5 Figures

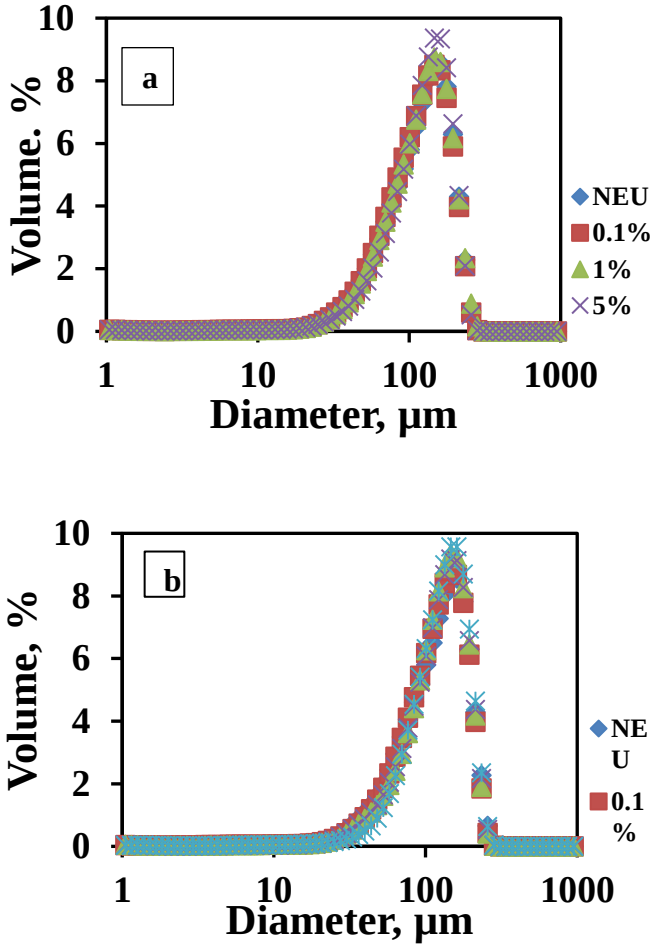

Figure 3-1 Particle size distribution comparison for (a) pure Neusilin (NEU) and impregnated products using DI water as a solvent, and (b) pure NEU and impregnated products using methanol as a solvent. The PSD of pure NEU and the impregnated is comparable in both cases

(a)

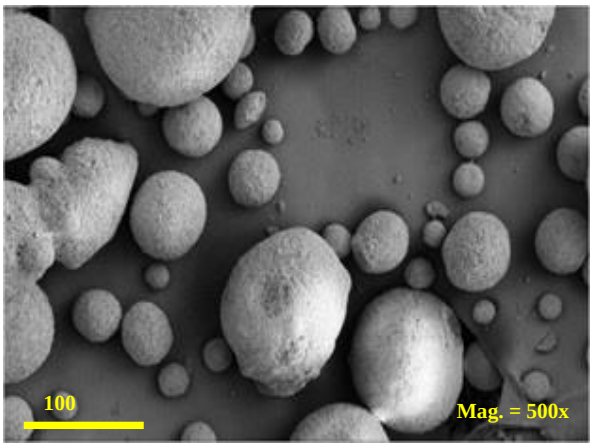

(b)

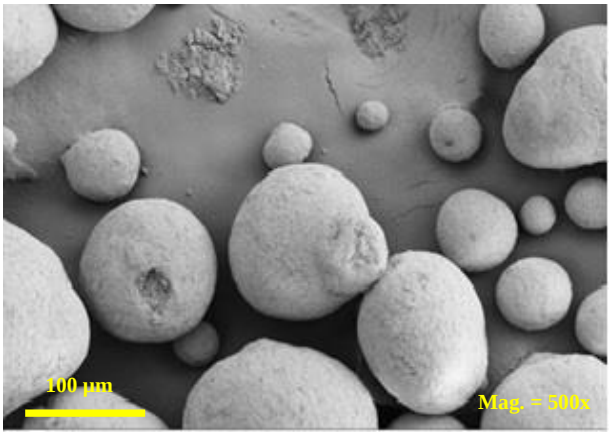

Figure 3-2 Scanning Electron Microscope (SEM) Pictures at magnification 500x of (a) Pure NEU (b) 9% APAP impregnated into NEU. The results indicated that there are no morphological changes after impregnation

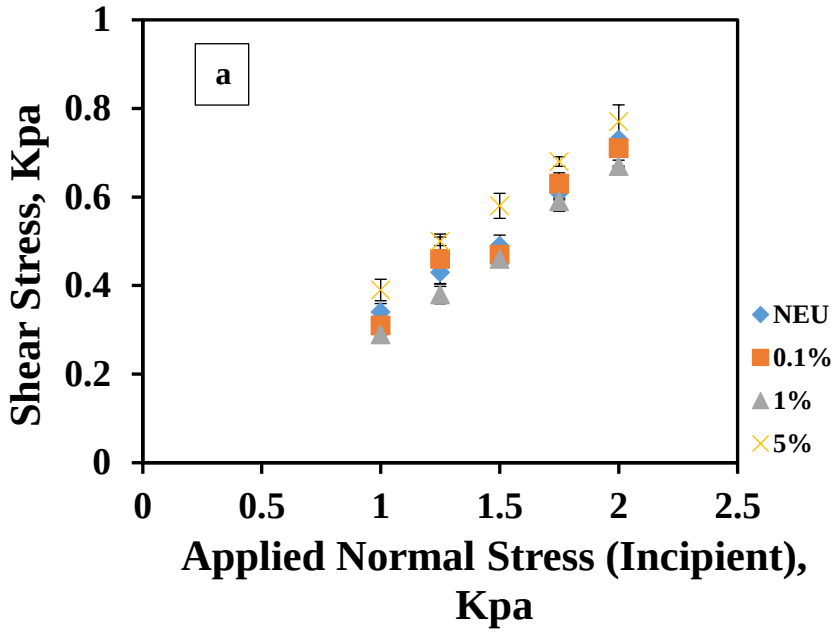

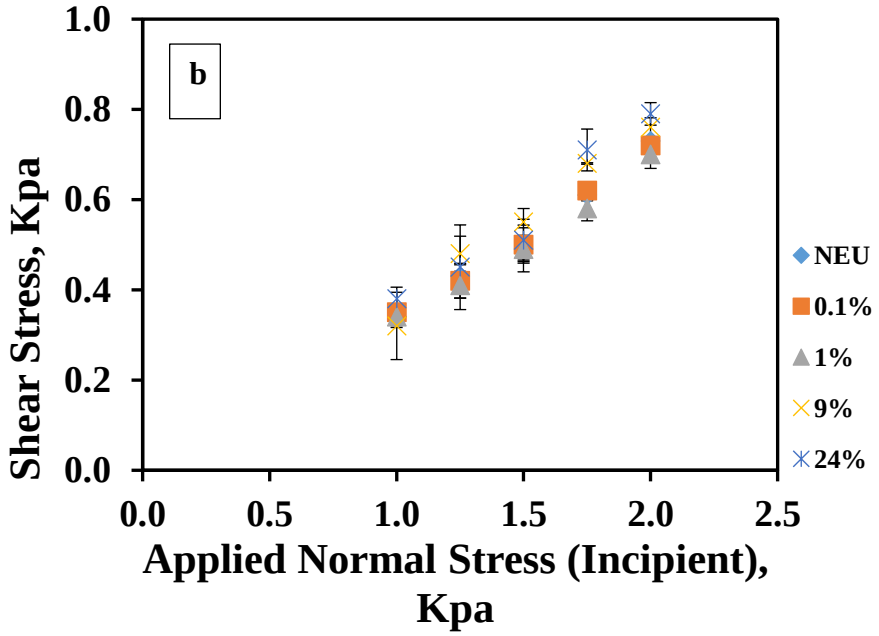

Figure 3-3 FT4 Measurement of (a) pure Neusilin (NEU) and impregnated products using DI water as a solvent and (b) using methanol as a solvent. The good flow properties of the pure carrier are preserved even after impregnation

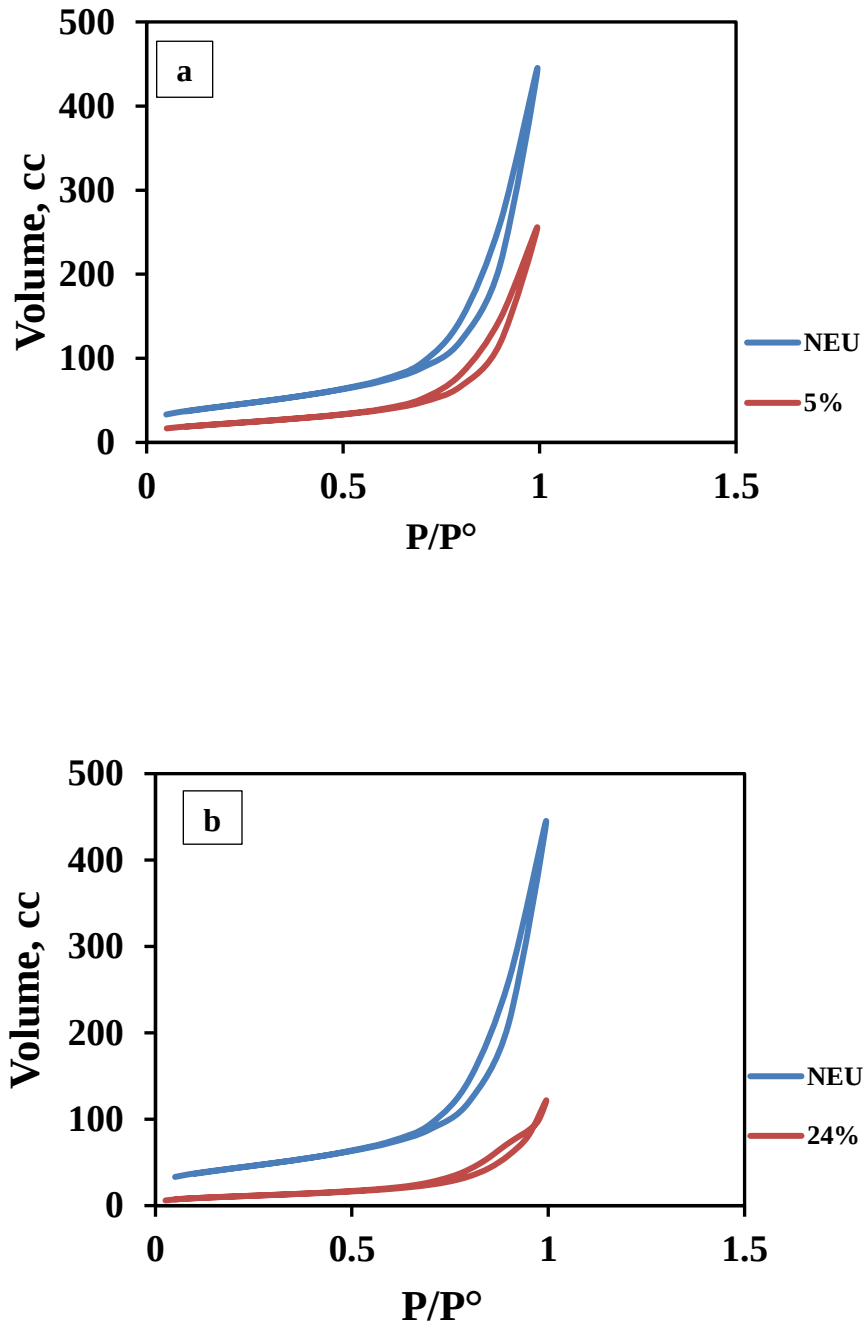

Figure 3-4 BET curves for (a) pure Neusilin (NEU) and 5% APAP impregnated and (b) pure NEU and 24% IMP. There is a clear reduction in surface area after impregnation and it depends on APAP loading

(a)

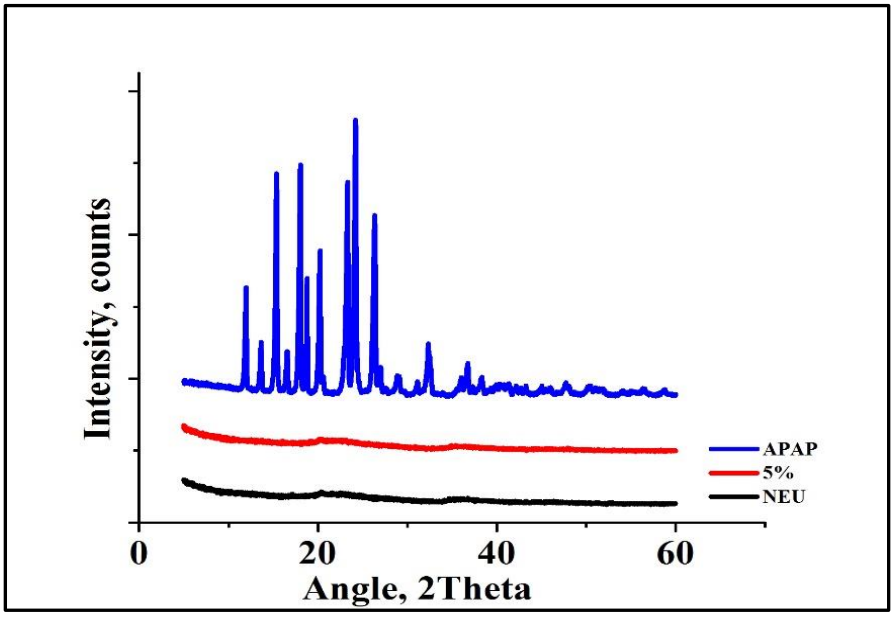

(b)

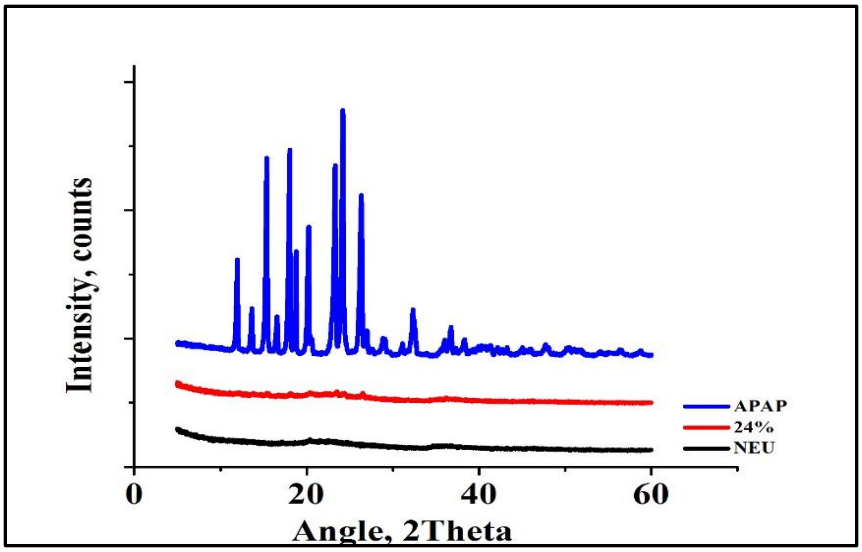

Figure 3-5 PXRD of (a) Pure APAP, Pure Neusilin (NEU), and 5%APAP impregnated, and (b) Pure APAP, Pure NEU, and 24%APAP impregnated (IMP). The APAP in impregnated products presented an amorphous pattern

(a)

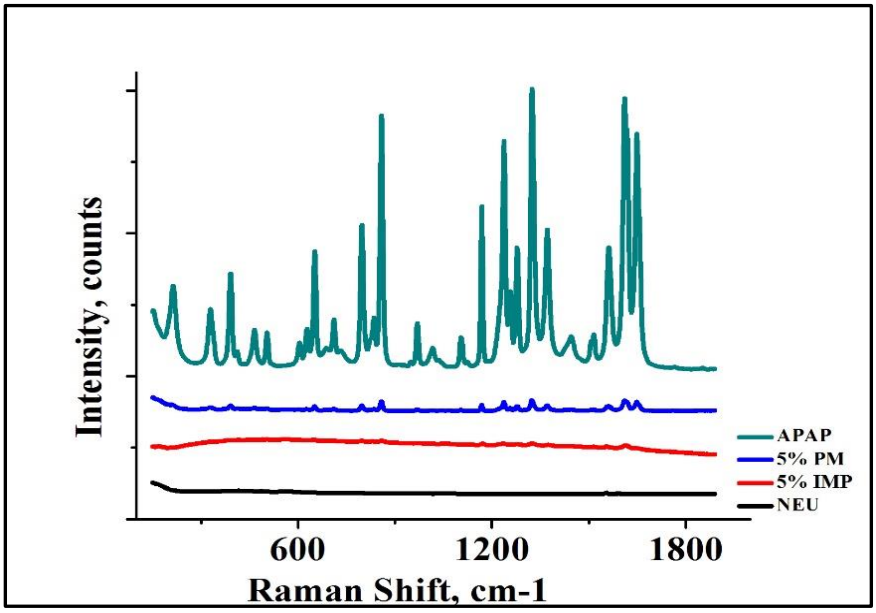
Intensity, counts
600
1200
1800
Raman Shift, cm-1
APAP
5% PM
5% IMP
NEU

(b)

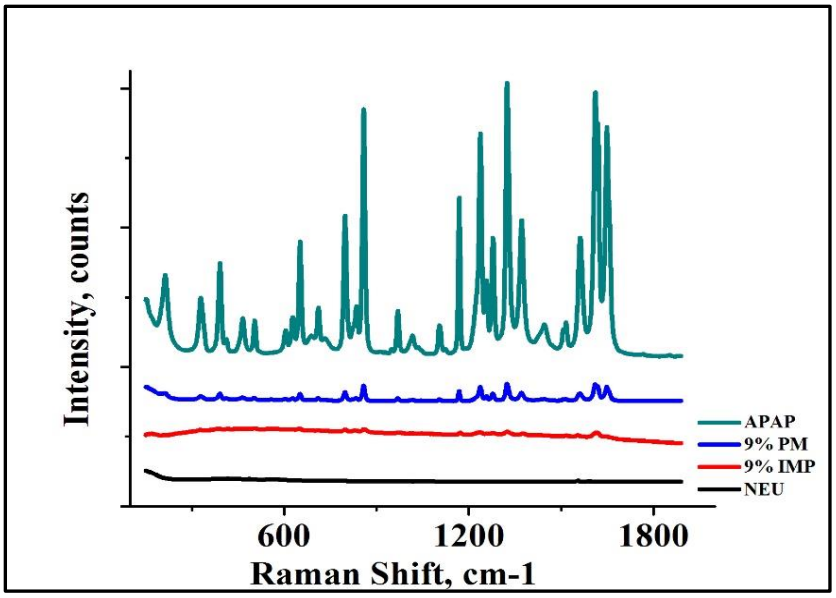
Intensity, counts
600
1200
1800
Raman Shift, cm-1
APAP
9% PM
9% IMP
NEU

(c)

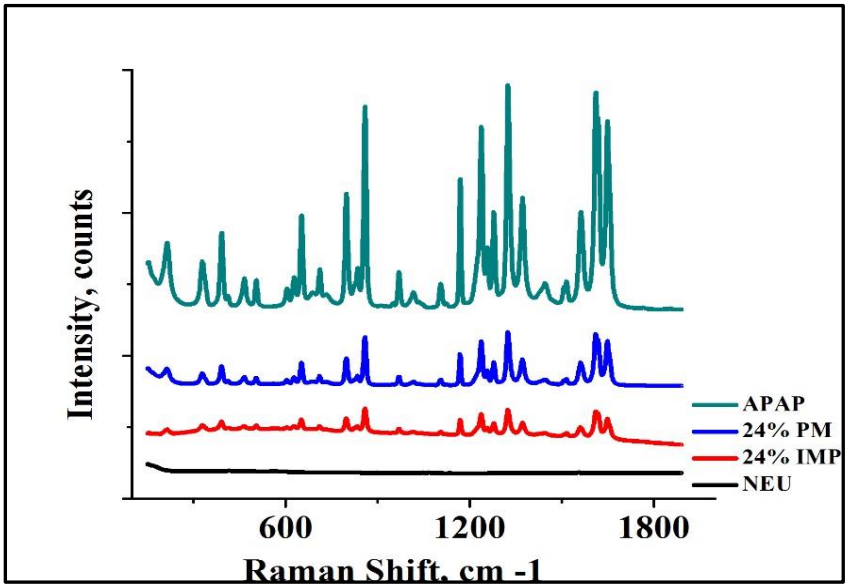

Figure 3-6 Raman spectra of (a) Pure APAP, Pure Neusilin (NEU), 5% impregnated APAP (IMP), and 5%APAP Physical Mixture (PM) (b) Pure APAP, Pure NEU, 9% impregnated APAP (IMP), and 9% APAP Physical Mixture (PM). (c) Pure APAP, Pure NEU, 24% impregnated APAP (IMP), and 24%APAP Physical Mixture (PM). The results showed that APAP existed in amorphous form in impregnated products.

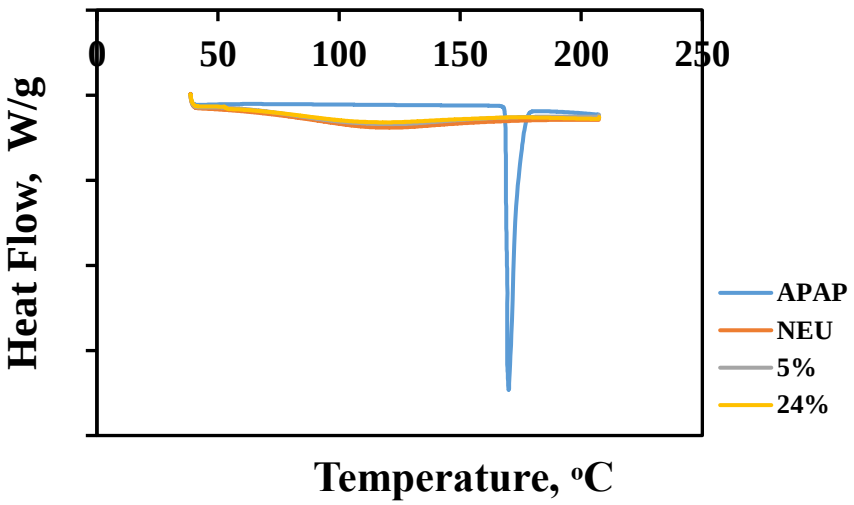

Figure 3-7 Differential Scanning Calorimetry Study of APAP, Neusilin (NEU), and 5% and 24% impregnated products. Pure APAP melted at 170 ̊C while NEU and impregnated products did not show any melting point

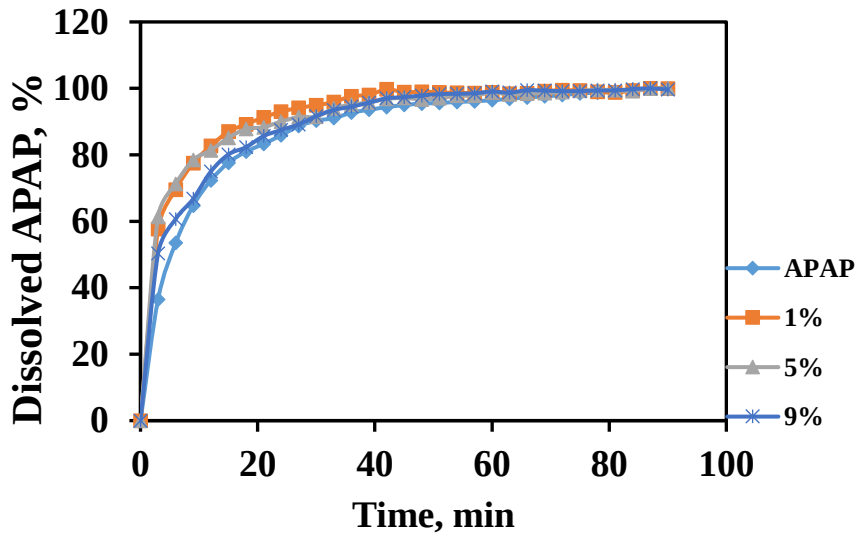

Figure 3-8 Dissolution behavior of pure APAP and the impregnated product using DI water as a dissolution medium. 1% and 5% were prepared using DI water and 9% was prepared using methanol. No discernible differences are observed between the dissolution profiles

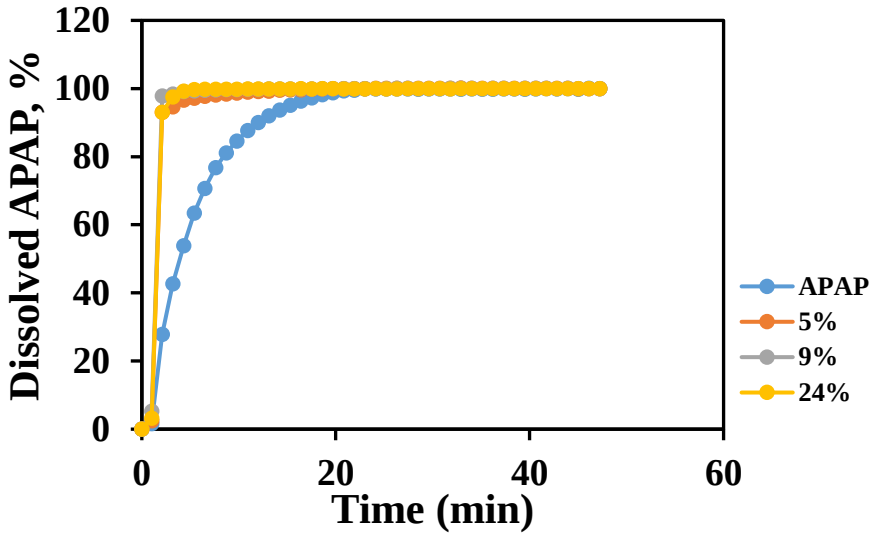

Figure 3-9 Dissolution behavior of pure APAP and impregnated products using 0.1 N HCl as a dissolution medium. 5% product was prepared using Dl water, and 9% and 24% were prepared using methanol. There is a clear difference between the dissolution profiles of pure APAP and impregnated products

3.6 Tables

Products	Pump rate (ml/min)	Inlet gas pressure (bar)	Atomization pressure (bar)	Inlet gas temp. (°C)	Spray Time of APAP (min)
Impregnated	**4**	**0.1**	**0.2**	**80**	**162.5**

Tab 3-1 Conditions for all fluidized bed impregnation experiments

Products, %	Solvent	Mean (µm)	Median (µm)	S.D.	D_{10} (µm)	D_{90} (µm)
Pure NEU		**129.1**	**128.4**	**56.72**	**55.10**	**205.6**
0.1	**DI water**	**127.6**	**126.0**	**55.21**	**55.94**	**202.6**
1		**130.7**	**129.3**	**55.78**	**59.01**	**205.9**
5		**132.6**	**133.0**	**54.2**	**61.45**	**204.6**
0.1	**Methanol**	**128.3**	**127.7**	**54.61**	**57.66**	**201.7**
1		**131.7**	**131.9**	**53.54**	**60.78**	**203**
9		**132.3**	**132.2**	**54.26**	**61.01**	**204.9**
24		**136.3**	**135.5**	**52.66**	**69.44**	**206.8**

Tab 3-2 Particle size of Neusilin and impregnated products. The results indicated that particle size of pure Neusilin is preserved after impregnation

Target Loading	Surface Area (m^2/g)	Total Pore Volume (cc/g)
Pure Neusilin	**390.4**	**1.742**
5%	**264.5**	**1.308**
24%	**226.8**	**1.091**

Tab 3-3 BET studies for Pure Neusilin and Impregnated products. Pore volume and surface area were reduced after impregnation

Target APAP%	Solvent	Average	RSD	C.I.
0.1%	**DI water**	**0.10**	**2.23**	**1.45 - 4.15**
1%		**0.93**	**1.76**	**1.15 - 3.28**
5%		**5.14**	**2.40**	**1.57 – 4.47**
0.1%	**Methanol**	**0.11**	**4.27**	**2.76 – 7.94**
1%		**1.05**	**3.02**	**1.97 – 5.62**
9%		**8.21**	**4.43**	**2.88 – 8.24**
24%		**24.28**	**2.68**	**1.74 – 4.98**

Tab 3-4 Blend Uniformity of Impregnated products. All impregnated products showed good blend uniformity

Chapter 4 Fluidized Bed Impregnation of Active Pharmaceutical Ingredients: Effect of Porous Carrier

4.1 Introduction

This chapter extends the application of fluidized bed dryer for impregnating a different API on various porous carriers and explores their abilities for enhancing dissolution profiles of poorly soluble drug substances. The API under study is Indomethacin (IMN), a well-known non-steroidal anti-inflammatory drugs (NSAIDs). The porous carriers under investigation are:

1) Magnesium aluminum metasilicate (Neusilin®, US2) (NEU) with a 5 nm pore size
2) Granulated silicon dioxide (Aeroperl®300) (AER) with a 30 nm pore size
3) Calcium phosphate dibasic (Fujicallin®) (FUJ) with a 73.5 nm pore size.

Poor drug solubility leads to numerous challenges in drug development, including formulation and storage. The solubility and dissolution behavior of a hydrophobic drug in an aqueous medium can be particularly challenging and various strategies to improve solubility and dissolution have been applied. Often, the solubility and dissolution rate of a drug are the rate-limiting step for oral bioavailability (120) and, different approaches have been applied to increase the aqueous solubility and the oral bioavailability of these drugs (121), such as size reduction, drug amorphization, spray drying (122) , complex formation with cyclodextrin (123), and hot-melt extrusion (HME) (124) . Another common approach is increasing the surface area between the drug and the dissolution medium and it has been verified that increasing the surface area of poorly soluble drugs is an effective tool to

improve dissolution rate of the drug (125). In this context, different approaches have been performed which include milling to fine particles (126–128), emulsification (126), and spray drying of the suspension to produce fine particles (127). Drug amorphization is also considered as a promising strategy to improve a drug's solubility. The amorphous state has a greater free energy, which leads to a greater solubility and higher rate of dissolution, than the crystalline state. However, the high surface energy of the amorphous state is associated with physical and chemical stability problems. Stabilizing the amorphous state usually involves the addition of polymers that are often expensive and can lead to toxicity problems. Therefore, it is of interest to develop techniques which can increase the surface area of the drug, amorphize and stabilize it. A technique that can potentially achieve all these goals is the loading drugs into porous carriers. In particular, loading drugs into mesoporous and nanoporous materials has gained significant attention in the pharmaceutical industry (129). It is estimated that 40% of new drugs have low aqueous solubility, so creation and stabilization of amorphous drugs has recently acquired extensive attention (129–131). A silicate mesoporous carrier has recently been used for adjusting drug release rate, targeting drugs, and producing and isolating metastable polymorphs of drugs (25,132–136). Silicate mesoporous carriers display outstanding properties such as: stable, large surface area, small pore size with narrow distribution, and reproducible surface properties. Moreover, both small and large drug molecules were successfully loaded into the pores using an impregnation technique and the release profile from these products showed diffusion-controlled behavior (96). A distinctive property of the technique of amorphization of drugs by placing the drugs in small pores, is that the small pores provide good physical stability of the drug by inhibiting or suppressing re-crystallization of the

drug substance (129,135,136). According to International Union of Pure and Applied Chemistry (IUPAC) notation (137), the porous carriers can be classified depending on their pore sizes into micro porous for pore size below 2 nm, mesoporous for 2-50 nm, and macro porous for pore sizes larger than 50 nm. A crystal can only be produced and grown if a critical nucleation size is achieved (104) . Accordingly, the nucleation and crystal growth of drug molecules can be inhibited when these molecules are confined in small pores, so the drug/porous carrier systems exist in an inherently disordered state (138,139) and the resulting amorphous form shows a greater solubility and bioavailability than the crystalline form (140). Therefore, the utilization of inorganic excipients as drug carriers to enhance the dissolution behaviors of poorly soluble drugs is a promising technique, which can provide benefits for drug and dosage form development (141).

Properties of the porous carrier can affect the drug loading, dissolution behavior, and stability. The most noticeable features are the pore size, the total pore volume and the surface properties including the surface area. Efforts have been made to investigate the effects of some factors such as pore size, surface properties, and physical properties on the dissolution of drugs from these carriers (135,136). Zhang et al (142) pointed out that the total pore volume and pore size are two important factors to determine the maximum drug loading capacities. Exceeding the loading capacity of the carrier results in loading of extra amount of drugs in the form of a crystal layer on the outside of the carrier particles, which reduces the drug release rate from the pores. Further, Izquierdo-Barba et al (143) compared the release profiles of erythromycin and ibuprofen loaded in the same carrier. They found that erythromycin, which has larger molecular size than ibuprofen, showed a slower release rate than ibuprofen from the same pore size. This difference in the release profile was

clearer as the pore size was reduced. Accordingly, they recommended that the pore size should be at least three times larger than the drug molecule diameter in order to have increased rates of drug release (144). Larger pore sizes lead to an increase in crystal formation as the nano-confinement properties are lost. Therefore, the release rate will be relatively slower due to crystallization.

As mentioned earlier in this chapter, the pore size of mesoporous carriers is very small, thus, nucleation and crystal growth are prevented due to insufficient space for crystallization (126). Although larger pore sizes allow crystallization to occur more readily than smaller ones, kinetic retardation of crystallization can also be noticed (127). Moreover, chemical stability can be improved by interaction between the drug and carrier. In most cases, this interaction involves hydrogen bonding which prevents chemical degradation (145). Despite research efforts in the area of porous carriers, many questions remain considering the effect of putting the same drug into different porous carriers with different physicochemical properties. Impregnating different porous carriers with the same drug allows us to answer questions about drug dissolution, blend uniformity, and other fundamental questions about impregnation. Since there can be large differences in the prices of porous carriers/excipients, it is also important to investigate how product properties vary with different carriers to allow one to make cost/benefit decisions in terms of the different carriers.

In this work, the efficacy of three porous carriers (Aeroperl 300, Fujicalin, and Neusilin US2), in terms of the impregnation of indomethacin (IMN), was studied. IMN was loaded into these three different carriers using a fluidized bed and the crystallization of IMN in the different carriers was investigated. As has been reported in previous work

(146), fluidized bed has successfully been used to load acetaminophen (APAP) into NEU, but it is of interest to also investigate the generality of fluidized bed for impregnation of porous carriers by examining a different drug. Since IMN is poorly soluble and is a highly crystallized drug, it can be considered as a good candidate for this study. Accordingly, it is a challenging task to implement a practical strategy, which ensures amorphization and stabilization of IMN at the same time. Also, it is important to look at the effects of different pore sizes of various carriers on the physical properties of IMN. Thus, the host systems, which were selected in this study, have pore sizes in three different ranges. The average pore size of FUJ is 73.5 nm, the average pore size of AER is 30 nm, and the average pore size of NEU is 5 nm. In order to accomplish this study, the product materials were characterized using scanning electron microscopy (SEM), laser diffraction, BET-surface area, and Raman Spectroscopy. Furthermore, to investigate the surface properties of products before and after impregnation, a droplet penetration method was applied. The *in vitro* release profiles were also studied using a dissolution apparatus.

4.2 Materials and Methods

4.2.1 Materials

Neusilin® US2 (NEU) and Fujicalin (FUJ) were purchased from Fuji Health Science Inc, (Burlington, NJ USA). Aeroperil 300 pharma (AER) was purchased from Evonik (Germany). Methanol, B&J Brand® Multipurpose Grade (purity above 99%), was obtained from VWR International. Indomethacin was obtained from Sigma-Aldrich (USA).

4.2.2 Experimental Procedure

All the experiments were done using the already existed procedure in Chapter 2. IMN was impregnated into the porous carriers NEU and AER at three different concentrations, namely, 5, 9, and 13% by mass whereas it was impregnated on FUJ at 1, 3, and 5% by mass. We can explain why different concentrations were used for FUJ from the other two carriers as the following: one of important requirement to get a successful impregnation is to charge fluidized bed dryer with the porous carrier until the top spray nozzle is reached. During fluidization, the nozzle needs to be located within the powder bed in order to eliminate spray drying. To achieve this goal, the fluidized bed was charged with these three carriers separately. The required masses in gram, which are needed to reach the nozzle in each case, were: 220 gm of NEU; 300 gm of AER; 500 gm of FUJ. The differences in the required masses in each case due to the differences in the bulk densities among these carriers. The measured bulk densities of these carriers using FT4 were 0.18 g/ml for NEU, 0.248 g/ml for AER, and 0.521 g/ml for FUJ. In this work, IMN loaded into carrier as mass by mass using methanol as a transport solvent. IMN has relatively limited solubility in methanol and it is easily re-crystallized when its concentration level in methanol reaches the saturation. Therefore, in case of NEU and AER, higher IMN loading concentration can be achieved comparing with FUJ using the same concentration of IMN solution in methanol. To sum up, the differences in the IMN loading concentrations between FUJ and other porous carrier are due to higher bulk density of FUJ comparing with AER and NEU and limited solubility of IMN in methanol.

4.2.3 Analytical Methods

All the analytical methods in this work were done depending on the already elaborated analytical methods in Chapter 2. The following analytical methods were applied in order to characterize the impregnated product and the pure carrier:

1. SEM and Particle Size Distribution (PSD)
2. Shear Cell Tests
3. Specific Surface Area (SSA) and Pore Volume Distribution
4. Raman Spectroscopy
5. Drug loading and Blend Uniformity
6. Droplet Penetration Study
7. Dissolution Behavior

Drug loading was measured using HPLC (Agilent Technologies, USA). The quantification method using HPLC included the following: a) column - ZORBAX Eclipse XDB-C18 (4.6 × 150 mm); b) mobile phase: Acetonitrile: Water (HPLC grade) 1:1; flow rate-1ml/min; Injection volume-20 µL; UV detection-320nm. As mentioned previously, ten samples were extracted for each experiment. Then, 200 mg from each sample was placed in 50 ml conical flasks; and the mobile phase was added to the flasks. This dispersion was sonicated for 40 min and left overnight at room temperature to ensure a complete extraction of IMN from the porous carriers. Samples were then withdrawn from the supernatant of each flask using a Millipore (0.45 µm) syringe filter and put in HPLC vials for analysis. For determining the amount of API, six standard solutions of IMN in the mobile phase were prepared with concentrations below and above that of the analyzed samples. From these standard solutions, calibration curves were built up and used in all

calculations. Injection volume for each sample was 20 µL. Consequently, the IMN loading of each sample, the mean, the standard deviation, and % relative standard deviation (% RSD) along with the confidence intervals of the measurements for each batch were determined.

The flow properties of the pure porous carriers and the impregnated products were measured using a FT-4 (Freemen Technology, Wayne, PA, USA) powder rheometer. The normal applied stress was 3KPa in case of NEU and AER and 9KPa in case of FUJ. We used different normal stresses in this study because FUJ has higher bulk density than NEU and AER. Thus, it needs higher normal stresses than NEU and AER to get accurate and reproducible shear cell results. The pre-shear procedure was repeated 3 times at different normal stresses to obtain the yield locus (88). More details about the procedure can be found in Freeman et al (89).

Droplet penetration (147) was measured by placing powder beds in a cylindrical container with 25 mm diameter and 20 mm height. Droplet penetration gives a measure of the wettability of powders. The experimental set up is shown in Figure 4-1. The FT4 Powder Rheometer was utilized to prepare these powder beds by conditioning and compressing them. Then, a scraping step was necessary to flatten and smooth the surface of these beds. In order to determine the contact angle of water with the powders in this study, silicon oil (Cannon Instrument Co.), which can completely wet the materials, was used as a reference liquid, and deionized water, as a test liquid. A manual syringe was used to generate the droplets at a constant height, which is at 5mm from the powder bed surface. A CCD camera (AVT Gige camera) was utilized to record the penetration of the droplets using the StreamPix6 video recorder. The frame rate of the camera was 150 frames/second

and the exposure time was 0.3 milliseconds. All the recorded videos were interpreted using ImageJ (NIH) by removing the background and converting the pictures into binary images as shown in Figure 4-2. Then, the droplet volume was counted by assuming the shape of the droplet is axisymmetric. It was observed that the contact area between the drop and the powder bed remains constant during most of the penetration process. The initial volume as well as the contact radius was measured in each experiment and then the hemispherical volume (α=1), $V_1 = (2/3).\ \pi r_c^3$ was used to make the penetration volume non-dimensional. The time was made non-dimensional using the characteristic time given by the equation 4-1 (147),

$$t_c = \frac{r_c}{v_c} = \frac{\varepsilon r_c}{u_c} = \frac{\mu \varepsilon r_c^{\ 2}}{k p_c} \qquad 4\text{-}1$$

The non-dimensional penetration curves are independent of the initial volume and contact radius of the drops. Once the dimensionless penetration times (and contact radii) were measured for both fluids, water (T) and silicone (R), and using the fact that the contact angle of silicone oil is 0°, the contact angle of water was calculated using equation 4-2,

$$\cos(\theta_T) = \frac{\tau_\alpha|_R}{\tau_\alpha|_T}\frac{\mu_T}{\mu_R}\left(\frac{r_c|_T}{r_c|_R}\right)^2\frac{\gamma_R}{\gamma_T} \qquad 4\text{-}2$$

where, $\mathbf{r_c}$ is the contact radius; $\mathbf{p_c}$ is the capillary pressure inside of the powder bed; $\boldsymbol{\mu}$ is the viscosity; $\boldsymbol{\epsilon}$ is the porosity; **k** is the permeability; $\boldsymbol{\theta_T}$ is the contact angle of the test liquid; $\boldsymbol{\tau_\alpha}$ is the penetration time of a fluid of volume fraction α of the hemispherical volume, $\boldsymbol{\gamma}$ is the surface tension. Pure drug (IMN) is totally non wetting and as can be seen in Figure 4-2 the carriers (AER, NEU, FUJ) are hydrophilic; moreover, it can be seen that

the impregnated carriers are still hydrophilic and there is not much change in the wetting properties between pure carrier and the impregnated product.

The dissolution behavior of IMN from the impregnated product was tested using a 708-DS, 8-spindle, 8-vessel USP dissolution apparatus type II (paddle), with automated online UV-Vis measurement (Agilent Technologies). Dissolution tests were conducted on pure IMN and the impregnated products. The experimental conditions were set up as follows: dissolution medium - water: phosphate buffer (1:4); agitation speed – 50 rpm; UV detection – ʎ = 320 nm; temperature – 37°C. A calibration curve was constructed (Abs= 17.345*conc. – 0.0022, R^2 = 0.9999) by measuring the UV absorbance for five different concentrations of IMN in the dissolution media to quantify the measured absorbance.

4.3 Results and Discussion

4.3.1 Particle Size Distribution (PSD) and SEM

The PSD of the pure carriers and the impregnated products are shown and Figure 4-3 and the corresponding D_{10}, D_{50} and D_{90} are shown in Tab 4-1. From this Tab, it is a clear that D_{10}, D_{50} and D_{90} of the pure porous carriers and their impregnated products analogues are same. This indicated that loading of IMN into NEU, AER, and FUJ were successfully accomplished with no fines or agglomeration during the experiment. Excluding fines from solid pharmaceutical products is necessary to ensure good flow properties. Also, it is very important to reduce the dust formation during the manufacturing, especially if we have very potent drugs. Moreover, fines could influence the distribution of drugs within the pharmaceutical excipients during the mixing or granulation process. Sarang *et al* (148) conducted a study to investigate the causes of drug content non-

uniformity in granules, which were prepared by wet granulation using a high shear mixer. They pointed out that the active pharmaceutical ingredient was concentrated in fine granules more than large granules. Therefore, fine granules were super potent, which leads to non-homogeneity of drug content. On the other hand, agglomeration of particles during the impregnation process results in segregation of the impregnated products into granules and/or particles with different particle sizes, which is considered as a failure mode for impregnation process. Furthermore, all the impregnated products presented the same PSDs as that of their corresponding porous carriers. These results support the hypothesis of placing the IMN inside the pores of porous carriers and not forming a monolayer at the surface of the carriers.

SEM images (Figure 4-4) revealed that the impregnated products have the same morphological profiles as that of pure porous carriers. This indicates that fluidized bed impregnation process runs smoothly with no aggressive attrition or agglomeration of the impregnated materials. Preserving the same morphology as the pure carriers means keeping the same original flow properties as the pure carriers, which could be confirmed later by flow properties.

4.3.2 Specific surface area and pore size distribution

Three different porous carriers were selected for this study: NEU, AER, and FUJ. NEU US2 is an amorphous silica product. It consists of fluffy and highly light granules of magnesium aluminometasilicate. In addition, Fuji's company develops NEU US2 to make it neutral that is different from traditional magnesium aluminium silicates whose pH is basic. Its pore diameter is about 5 nm with 390.4 (cm^3/g) specific surface area. AER (300

Pharma) is a granulated colloidal silicon with 30 nm pore diameter and 236 (cm^3/g) surface area while FUJ is a spherical granulated product of dibasic calcium phosphate dehydrate (DCPD) with 73.5 nm pore diameter and 28.7 cm^3/g surface area. An important question could be asked during this study is: where is IMN placed exactly, inside the pores or forming a monolayer at the surface of porous carriers? To address this question, we first need to know the size of IMN molecule and the surface area of each carrier. Moreover, we need to do some important tests to measure the specific surface area and pore volumes of each carriers before and after impregnation. Bahl, D. *et al* (17) calculated the ratio of drug over porous carriers, which is required to form a monolayer coverage inside the pores. This could be done using the size of one drug molecule. The size of one IMN molecule is 4.27 Å * 8.97 Å * 12.66 Å. Using these measurements, the quantity of IMN, which is necessary to form a monolayer on the surface of porous carriers can be calculated. Depending on the lowest and highest dimensions of rectangle bearing the IMN molecules, the ratio of IMN amount per 1g porous carrier, which is critical to form monolayer on the surface of porous carriers, can be calculated. From Tab 4-2, the specific surface area of each carrier was measured using BET-nitrogen adsorption method. The measured surface area of NEU was 390 m^2/g, so 0.21-0.61g IMN would supply a monolayer coverage on 1gm NEU. This equals to a ratio of IMN: NEU of (1:5-1:1.5) w/w. In the same manner, the ratio (w/w) of IMN over porous carriers required for monolayer coverage was calculated to be (1:6-1:2) for AER (surface area, 336 m^2/g). According to these measurements, only high loadings (13% IMN in NEU or AER) are close or above monolayer coverage while low loading percent are below monolayer coverage. In this situation, IMN placed on the surface of porous carriers and not inside the pores. However, this study showed different results from

above calculations and conclusions. The reduction in surface area and pore volume after impregnation can be seen in the Table 4-2 and Figure 4-5. The surface area of pure NEU was 390 m^2/g, and the pore volume was 1.74 cc/g. After impregnation with 13% IMN, the surface area of the impregnated product became 264 m^2/g and the pore volume was 1.3 cc/g. Similarly, the surface area of AER was 336 m^2/g before impregnation, and it became 136 m^2/g after impregnation with 13% IMN. The pore volume of AER was 2.2 cc/g before impregnation, and it became 1.6 cc/g after impregnation. In addition, the surface area of pure FUJ was 28.7 m^2/g, and the pore volume was 0.224 cc/g. After impregnation with 5% IMN, both the surface area and the pore volume of impregnated product was slightly reduced to 26.174 m^2/g and 1.3 cc/g, respectively. These data indicated that the IMN was placed inside the pores of porous carriers due to these significant changes in both the surface area and pore volume of the porous carrier. The reduction in the surface area and pore volume of porous carriers after IMN loading means that this drug occupies a significant part of pores. These results come in agreement with other studies such as Raman spectroscopy, flow properties and dissolution studies. Thus, it is a clear that IMN was placed inside the pores and not at the surface of porous carriers. 4.3.3 Drug loading and Blend uniformity

The blend uniformity of all impregnated product was calculated. The results showed that the content uniformity of IMN in the impregnated products were discovered to be uniformly distributed. All the %RSD values were found less than 5 and all the % content values were close to the target loadings. Therefore, there is no loss in drugs during the loading process. Tab 4-3 demonstrates the details of drug loadings and blend uniformity values.

4.3.3 Flow properties measurement

Powder Flow properties play a distinctive role in manufacturing of solid dosage forms. All impregnated products showed (Figure 4-6) comparable flow behaviors to the pure carriers, which have very good flow properties. Nevertheless, 5% IMN in FUJ presented a little change in its flow behavior comparing with pure FUJ, which might be due to the presence of IMN at the surface of carrier and not inside the pores. This observation needs more characterization to prove the reason behind this difference in the flow properties.

4.3.4 Raman Spectroscopy

Raman spectroscopy studies were done to investigate the physical state of IMN in the impregnated products. The Raman spectra of IMN impregnated products in NEU, AER, and FUJ were illustrated in Figure 4-7a, 4-7b, and 4-7c, respectively. The results showed that IMN exists mainly in amorphous form in all porous carriers. The Raman data of pure IMN presented several distinct peaks showing the crystalline nature of IMN. NEU and AER porous carriers are amorphous and do not develop any peaks, however, FUJ showed some sharp peaks, which indicated a partial crystallinity of this carrier. The high intensity signals of IMN was significantly reduced in the Raman spectra of impregnated products. Physical mixtures of IMN and porous carriers in different ratios presented intense peaks compared to impregnated products using the same components at the same ratios. While the intensity of sharp peaks of IMN is gradually decreasing from neat IMN to physical mixtures, these peaks mostly disappear from all impregnated products indicating a full amorphization state of IMN. This is mainly due to the presence of IMN in a crystalline

state in the physical mixtures. In the case of impregnated products, these products do not show any intense peaks pointing out a complete amorphous state of IMN inside the pores of these porous carriers. Nevertheless, FUJ impregnated products presented some intense peaks indicating a partial amorphization.

4.3.5 *In vitro* dissolution studies

The *in vitro* dissolution profiles of pure IMN and impregnated products of IMN in NEU, AER, and FUJI are shown in Figures 4-8, 4-9 and 4-10, respectively. IMN is practically insoluble in water (149). All impregnated products presented higher dissolution rate and extent than pure IMN. Dissolution behavior enhancement of impregnated products was noticed in the following rank IMN in NEU products > IMN in AER products > IMN in FUJ products > pure IMN. In general, the dissolution behavior of IMN from impregnated products was significantly improved compared to neat IMN. The dissolution rate improvement of IMN from porous carriers is mainly due to the alteration of drug state from crystalline to amorphous state. Amorphous form of drugs is highly energetic, and its thermodynamic barrier of dissolution is low, so it is easily dissolved. This high free energy acts as a driving force for initiating the solubility, so amorphous form is more soluble than that of its crystalline analogue (150). These data came in agreement with Raman spectroscopy. Also, the improvement in the dissolution profiles of impregnated products, comparing with neat crystalline IMN, is mainly due to increase of IMN wettability by placing it inside the pores of porous carriers. IMN is completely hydrophobic in nature. Inclusion of IMN inside the pores of hydrophilic porous carriers makes the outer surface of IMN hydrophilic, so it enhances its wettability. Moreover, the large surface area of

porous carriers significantly improves the dissolution behavior. Nevertheless, silicate porous carriers (NEU and AER) showed better dissolution profile of IMN comparing with FUJ. This faster rate and higher extent of dissolution of silica impregnated products are mainly due to high surface area of silica products comparing with FUJ. Furthermore, silica products possess finer pores than FUJ. Very small pores completely amorphize the drugs because there is not enough space to partially recrystallize while large pore size may lead to partial recrystallization of the drugs. The porous silica facilitates IMN to release in the dissolution medium in the form of very fine particles, which noticeably improve the dissolution rate. Furthermore, the presence of silanol groups in silica products significantly improves the dissolution rate of drugs in the dissolution medium(119). Moreover, Figure 4-8 showed that 1% IMN in FUJ presented less improvement in the dissolution profile than 3% and 5% IMN in FUJ. As discussed previously, each drug has a minimum amount, which is necessary to form a monolayer coverage low ratio of IMN: porous carrier results in placing the drug at the carrier's surface. This critical value depends on both the dimensions of drug molecule and the surface area of carrier. Therefore, at low IMN loading i.e 1% IMN in FUJ, IMN forms monolayer coverage at the surface more. The presence of IMN at the surface might results in easily recrystallization of IMN, which leads to reduction in the solubility and dissolution rate of this product material compared to higher loading of IMN in FUJ.

4.3.6 Wettability of impregnated products

The improvement in the dissolution profile of IMN after impregnation with porous carriers was further explored using droplet penetration method. Tab 4-4 shows the

calculated contact angle of pure IMN, pure porous carriers, and impregnated products depending on droplet penetration. IMN was completely hydrophobic. We were unable to measure its contact angle because of no droplet penetration. The water drop stayed intact at the surface of IMN powder bed. This is an indicator of its poor solubility and very slow dissolution rate. On the other hand, all porous carriers showed good hydrophilicity as indicated by their acceptable contact angles. The contact angles of NEU, AER, and FUJ were 53.4°, 78.0°, and 37.8°, respectively. After impregnation, 5% IMN in NEU, AER and FUJ presented 69.0°, 79.9° and 81.4° contact angles respectively. From these results, we can conclude that loading of IMN into NEU, AER and FUJ leads to mild increase in the contact angle i.e. a slight increase in hydrophobicity, but impregnated products can still be considered as hydrophilic materials. Comparing the contact angle of IMN with impregnated products revealed that impregnation significantly improved the wettability of IMN. Consequently, the dissolution rate of IMN was noticeably enhanced after impregnation. These results come in agreement with the results of dissolution studies. For more details, see Figure 4-11.

4.4 Conclusions

In this work, three different porous carriers were successfully impregnated with IMN using a fluidized bed dryer. The impregnated products were entirely evaluated, and the results revealed that these products generally possess valuable characteristics, which are necessary for manufacturing of solid dosage forms. The resulting products presented a good blend uniformity, agreeable particle size distribution. However, NEU and AER impregnated products showed better flow properties than FUJ impregnated products. Also,

the results indicated that the blend uniformity did not depend on the drug load or carrier type. The Raman spectroscopy showed that IMN is mainly amorphized inside the pores of the porous carriers. The amount of small crystals percent could be pointed out in IMN-FUJ products. Although the dissolution profiles of all the impregnated products were better than pure crystal IMN, IMN-NEU and IMN-AER impregnated products presented faster dissolution rate than IMN-FUJ impregnated products. The differences in impregnated products properties are mainly relied on the differences in the pore size of these products. NEU and AER have smaller pore size and larger surface area than FUJ.

In our previous work, acetaminophen was impregnated into NEU (146) while in this study IMN was impregnated into NEU, AER, and FUJ. Accordingly, this study confirms the generality and feasibility of using fluidized bed process to impregnate different active pharmaceutical ingredients into different porous carriers. This is very important in pharmaceutical industry because different excipients and varieties of drugs should be prepared as solid dosage forms. However, additional work may be required to investigate the amenability of this method for co-impregnation of two drugs into one porous carrier.

4.5 Figures

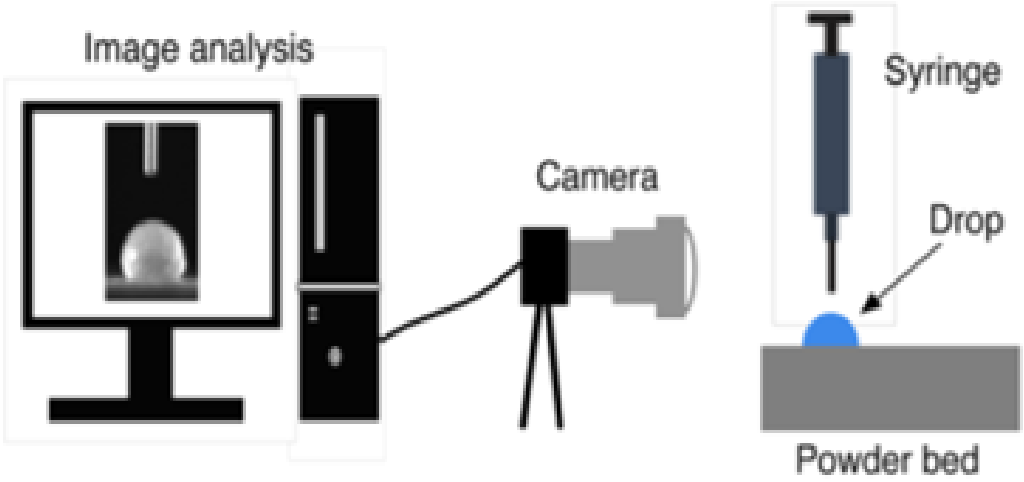

Figure 4-1 Diagram of the droplet penetration setup

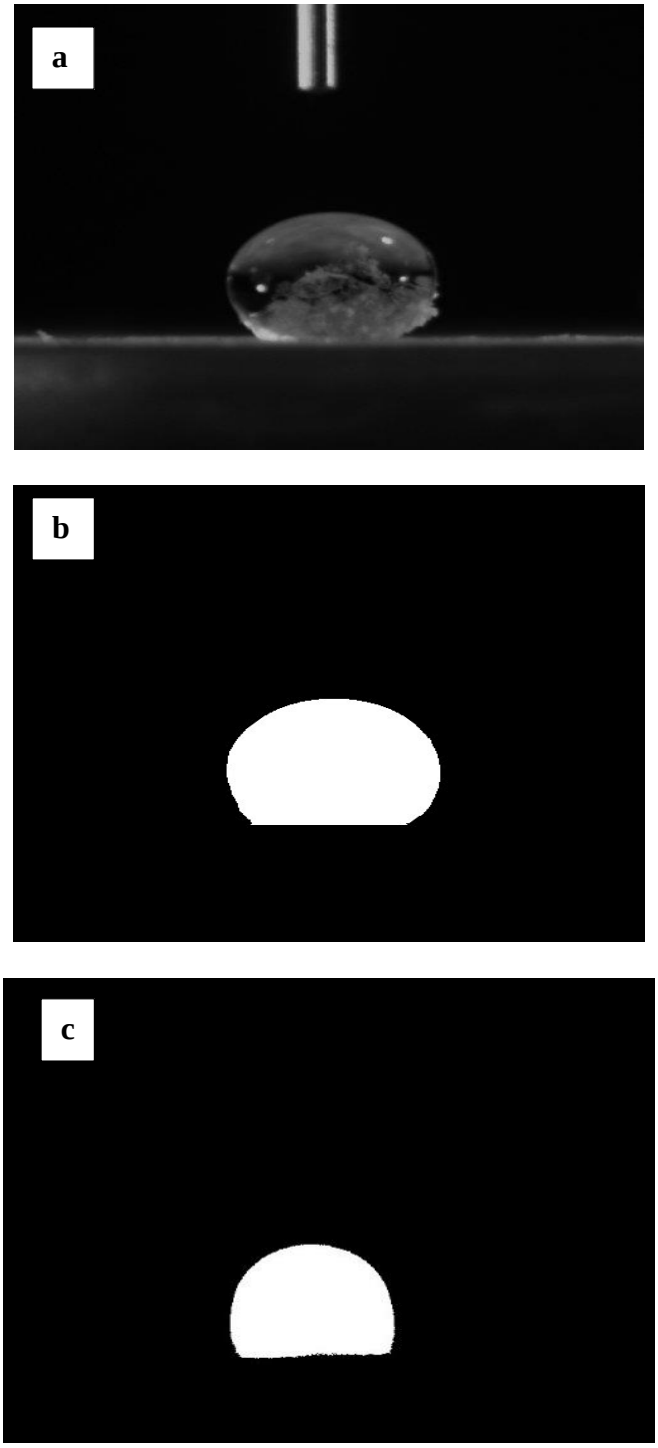
a
b
c

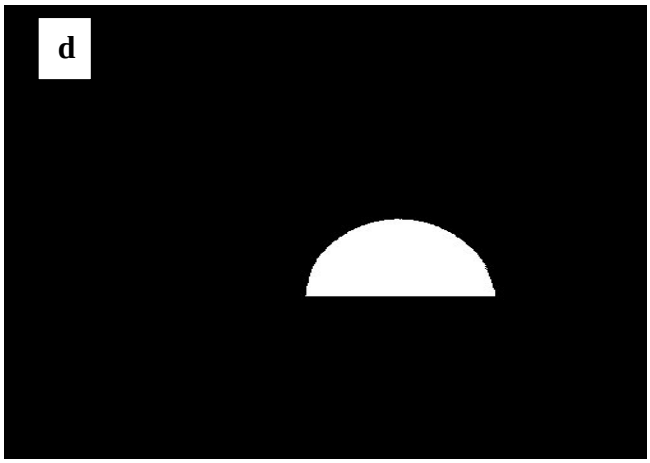
d

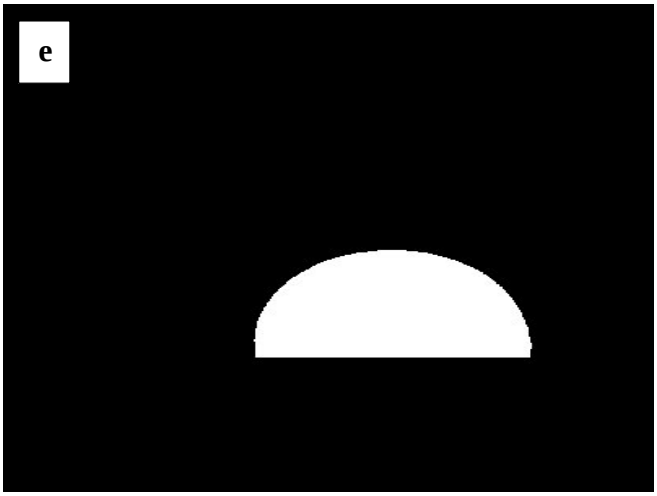
e

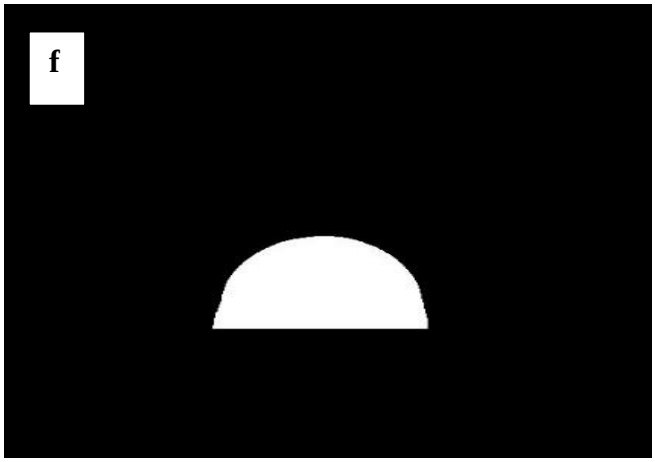
f

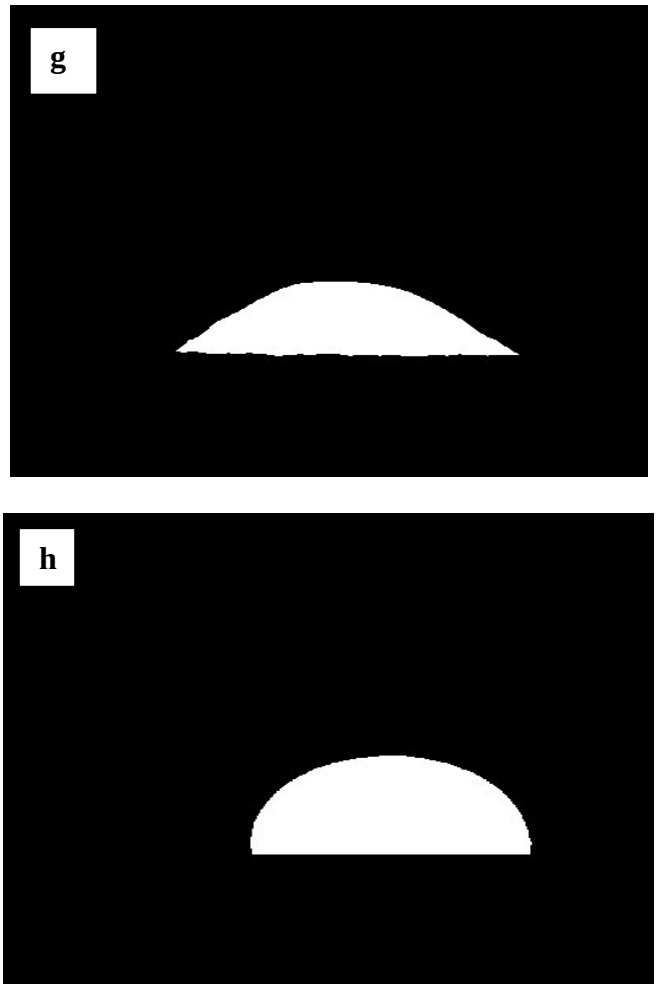

Figure 4-2 (a) & (b) Pictures of droplets before and after excluding the background and binarizing the image respective for pure IMN (c) pure AER, (d) 5% IMN in AER, (e) pure NEU, (f) 5% IMN in NEU, (g) pure FUJ and (h) 5% IMN in FUJ. As it can be seen in the pictures, pure drug (IMN) is totally non wetting. The drug is made hydrophilic by impregnation and it can be seen that there is not much change in the wetting properties between pure carrier and the impregnated product

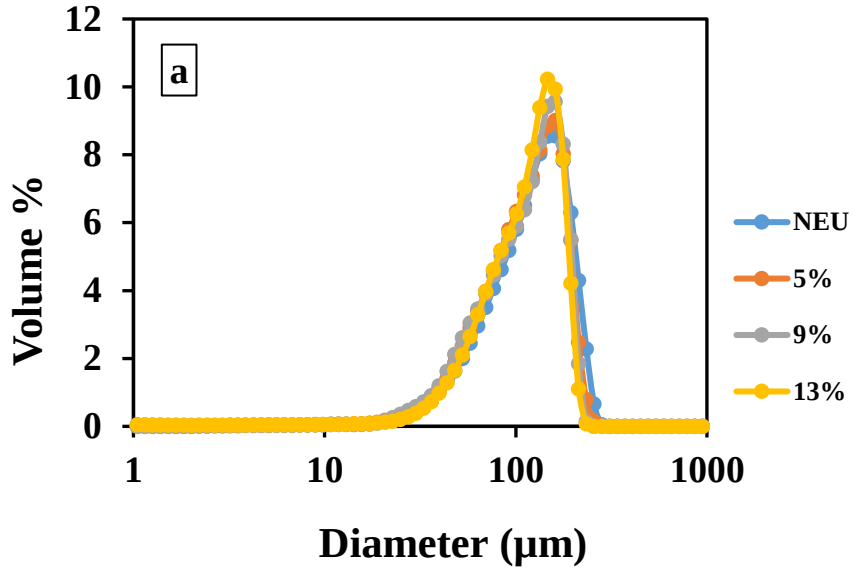
a
Volume %
Diameter (µm)
NEU
5%
9%
13%

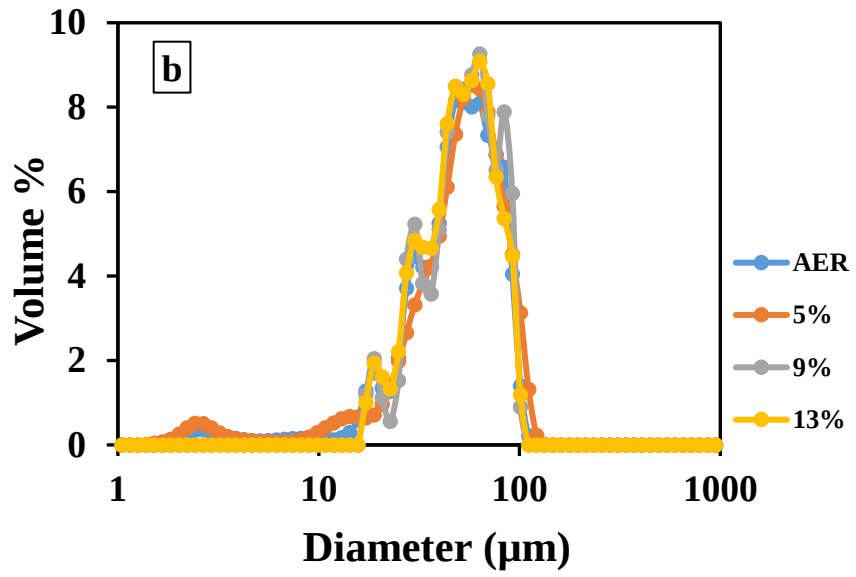
b
Volume %
Diameter (µm)
AER
5%
9%
13%

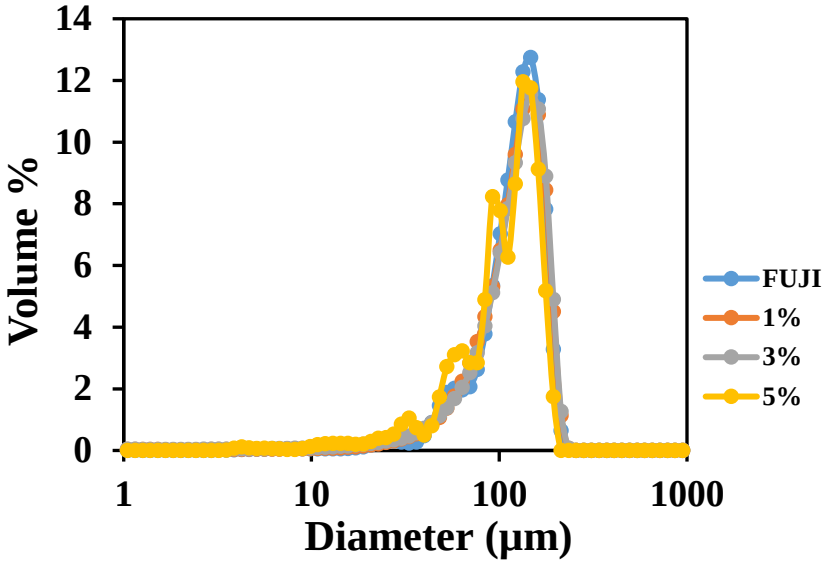

Figure 4-3 Particle size distribution comparison for (a) pure Neusilin (NEU) and impregnated products using, (b) pure Aeroperl (AER) and impregnated products, and (c) pure Fujicalin (FUJ). The PSDs of pure porous carriers and the impregnated products are comparable in all cases

(a)

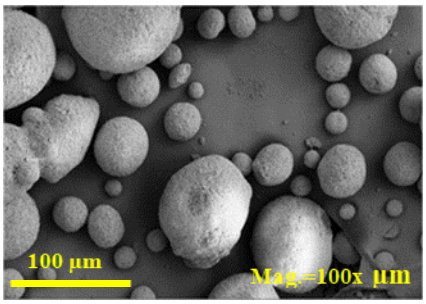

(b)

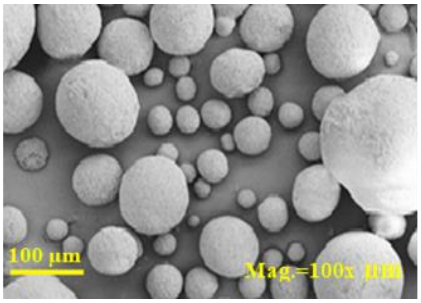

(c)

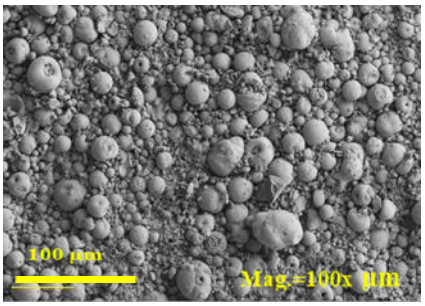

(d)

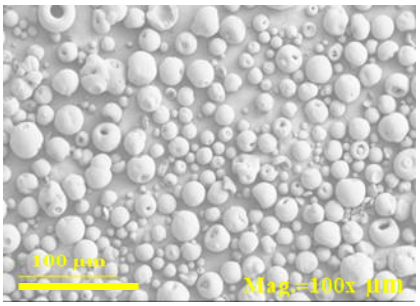

(e)

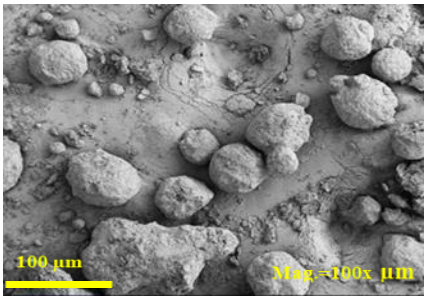

(f)

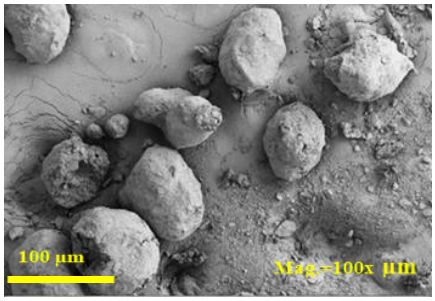

Figure 4-4 Scanning Electron Microscope (SEM) Pictures at magnification 100x of a & b- Pure Neusilin (NEU) and NEU impregnated products, c & d- Pure Aeroperl 300(AER) and AER impregnated products, and e & f- Pure Fujicalin (FUJ) and FUJ impregnated products. The pictures revealed that there are no morphological changes after impregnation

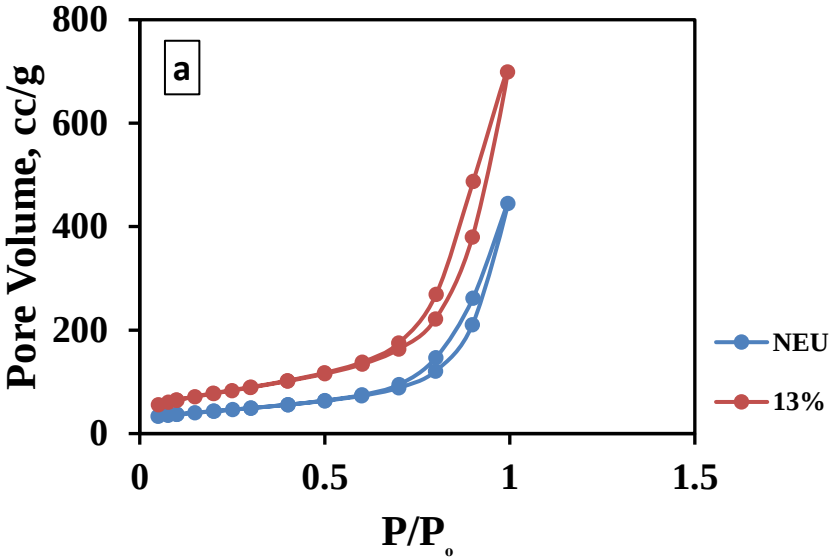

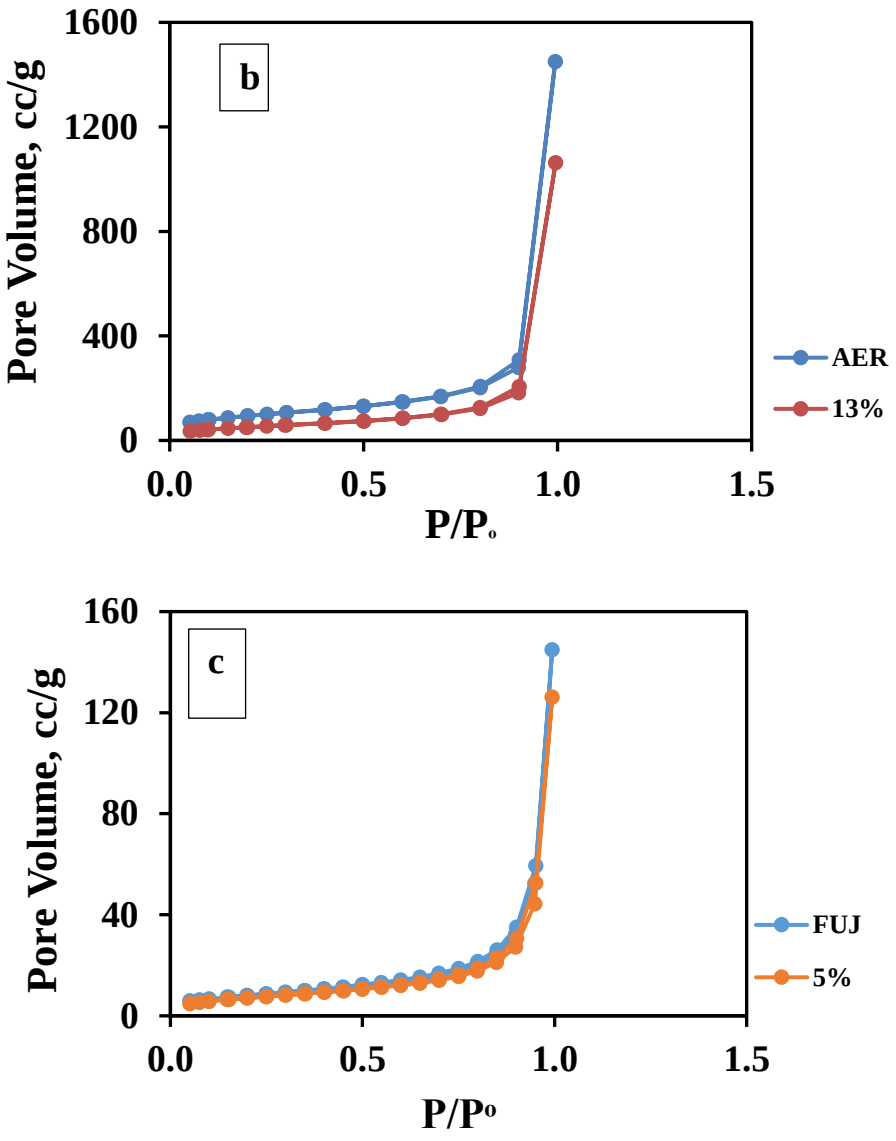

Figure 4-5 BET curves for (a) pure Neusilin (NEU) and 13% impregnated, (b) pure Aeroperl (AER) and 13% impregnated, and (c) pure Fujicalin (FUJ) and 5% impregnated. There is a noticeable decrease in surface area and pore volume after impregnation

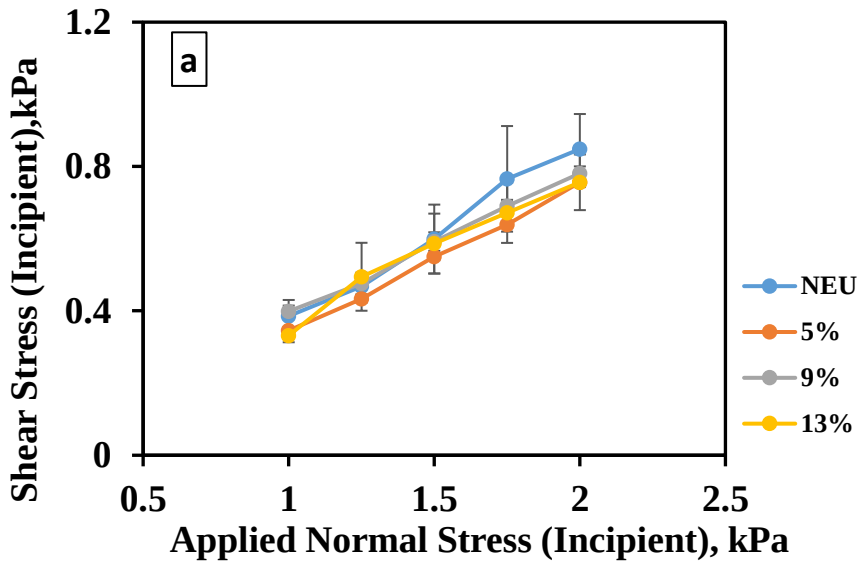
a
1.2
0.8
0.4
0
0.5
1
1.5
2
2.5
Shear Stress (Incipient),kPa
Applied Normal Stress (Incipient), kPa
NEU
5%
9%
13%

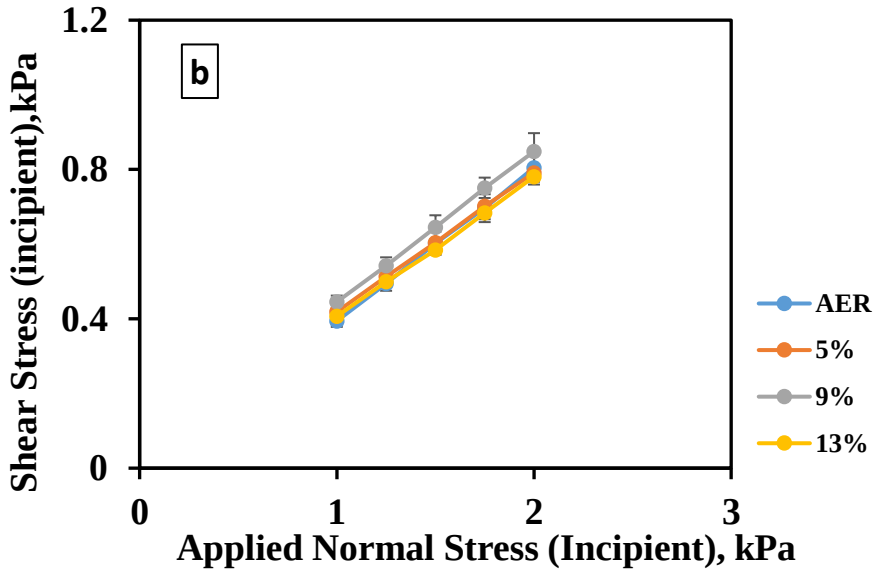
b
1.2
0.8
0.4
0
0
1
2
3
Shear Stress (incipient),kPa
Applied Normal Stress (Incipient), kPa
AER
5%
9%
13%

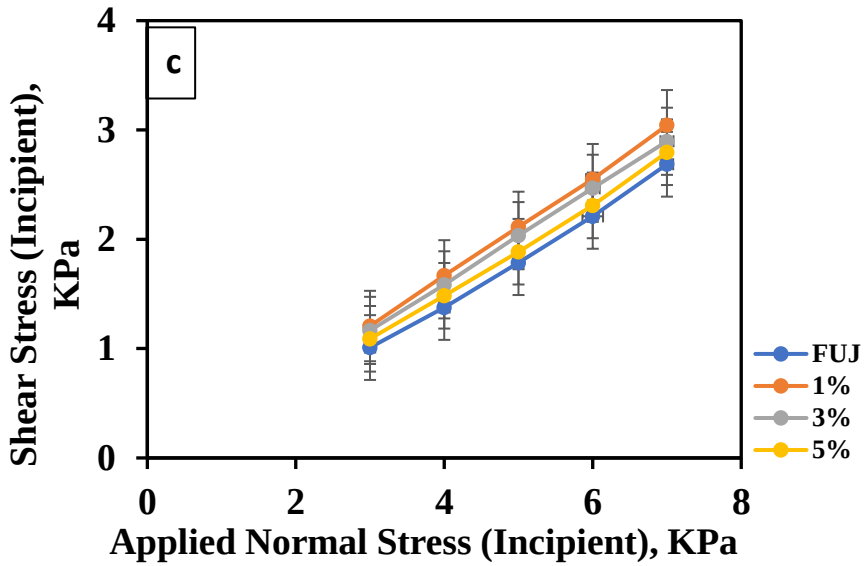

Figure 4-6 FT4 Measurement of (a) pure Neusilin (NEU) and impregnated products, (b) pure Aeroperl (AER) and impregnated products, and (3) pure Fujicalin (FUJ) and impregnated products. The good flow properties of the pure carrier are maintained after impregnation

(a)

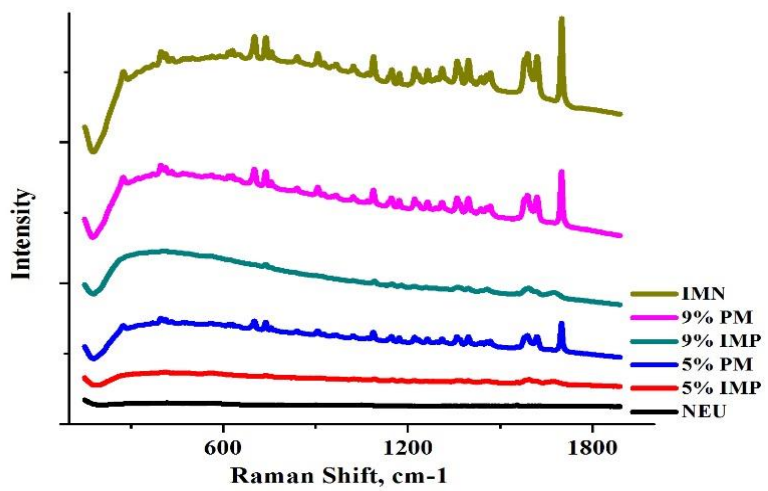

(b)

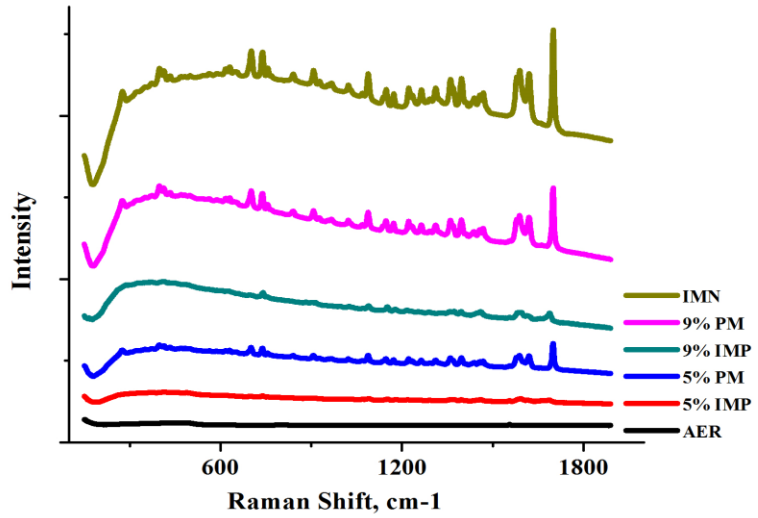

(c)

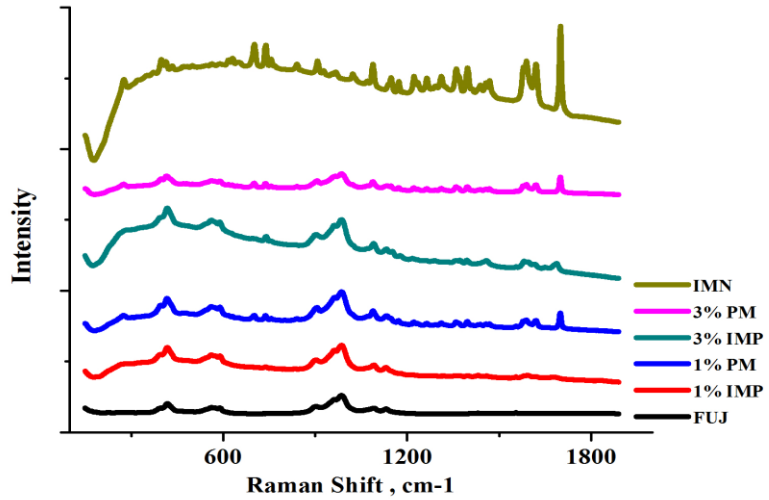

Figure 4-7 Raman spectra of (a) Pure IMN, Pure Neusilin (NEU), 5% & 9% impregnated IMN (IMP), and 5% & 9% IMN Physical Mixture (PM), (b) Pure IMN, Pure Aeroperl (AER), 5% & 9% impregnated IMN (IMP), and 5% &9% IMN Physical Mixture (PM), and (c) Pure IMN, Pure FUJ, 1% &3% impregnated IMN (IMP), and 1% & 3% IMN Physical Mixture (PM). The results presented that there is a clear reduction in the crystallinity of IMN after impregnation

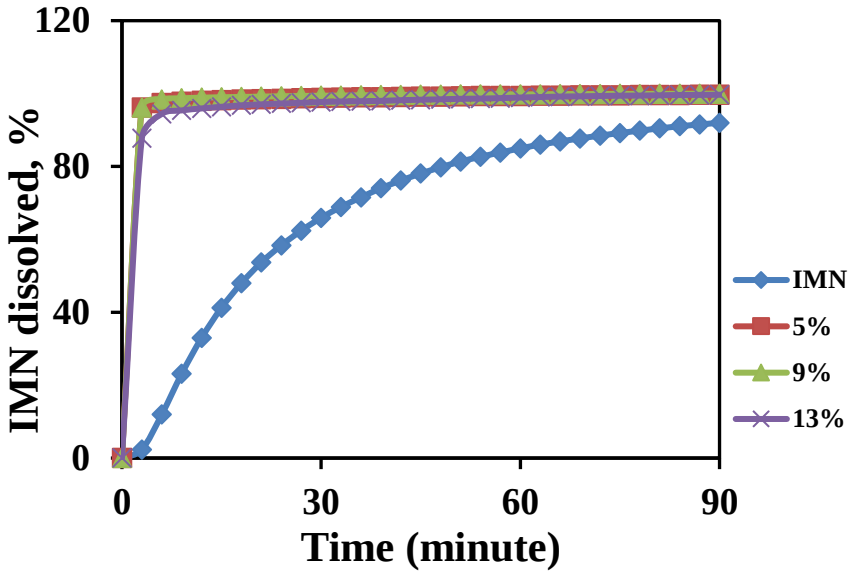

Figure 4-8 Dissolution behavior study of Pure Indomethacin (IMN) and impregnated Neusilin (NEU) to various levels. There is a significant improvement in the dissolution behavior of IMN after impregnation

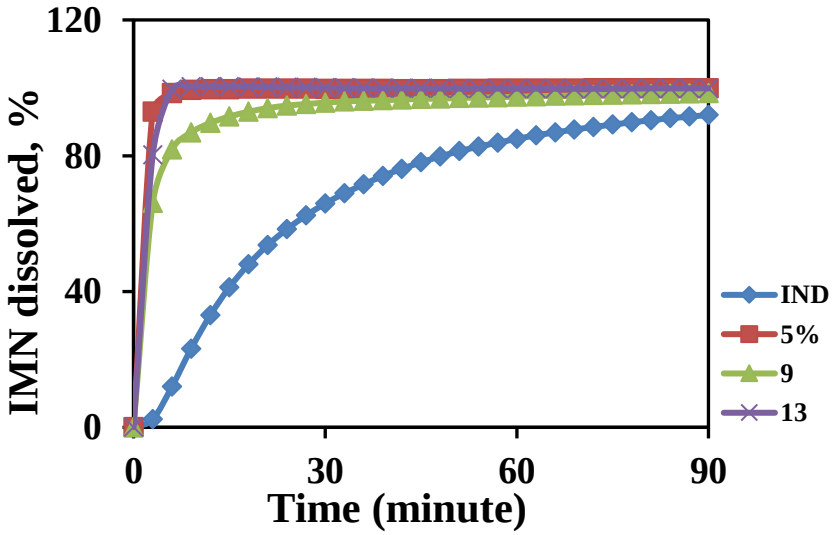

Figure 4-9 Dissolution behavior study of Pure Indomethacin (IMN) and impregnated Aeroperl (AER) to various levels. Most impregnated products showed higher dissolution rates than pure IMN

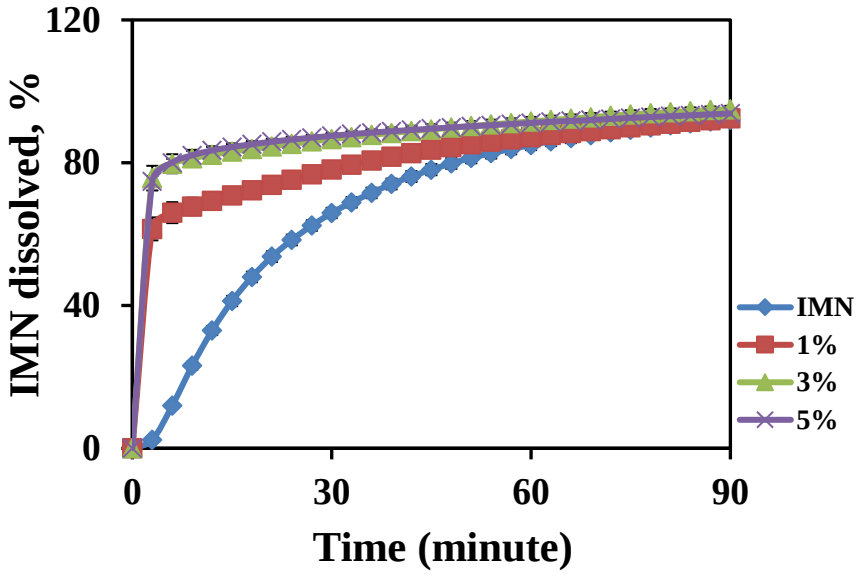

Figure 4-10 Dissolution behavior study of Pure Indomethacin (IMN) and impregnated Fujicalin (FUJ) various levels. The dissolution rates of impregnated products are generally higher than pure IMN

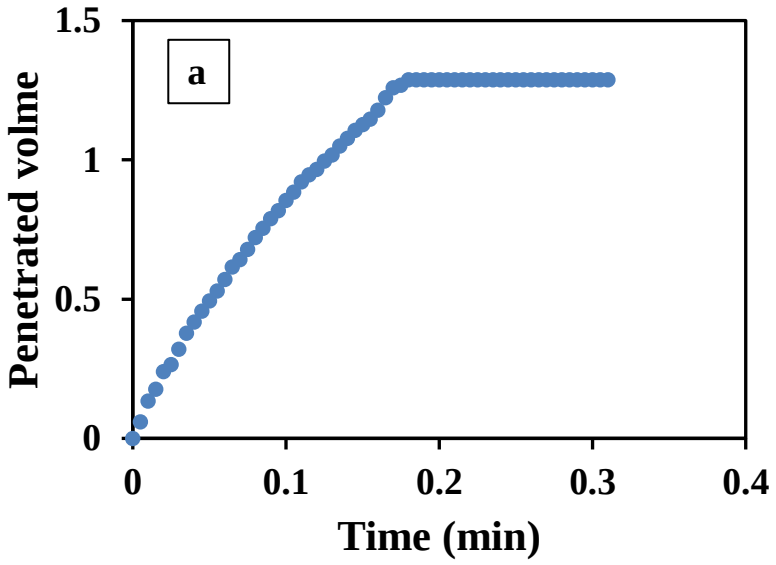

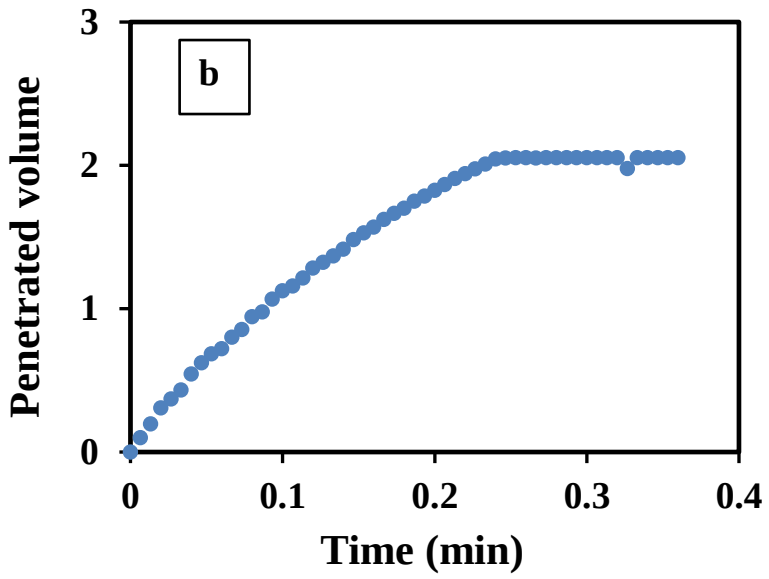
b
Penetrated volume
3
2
1
0
0
0.1
0.2
0.3
0.4
Time (min)

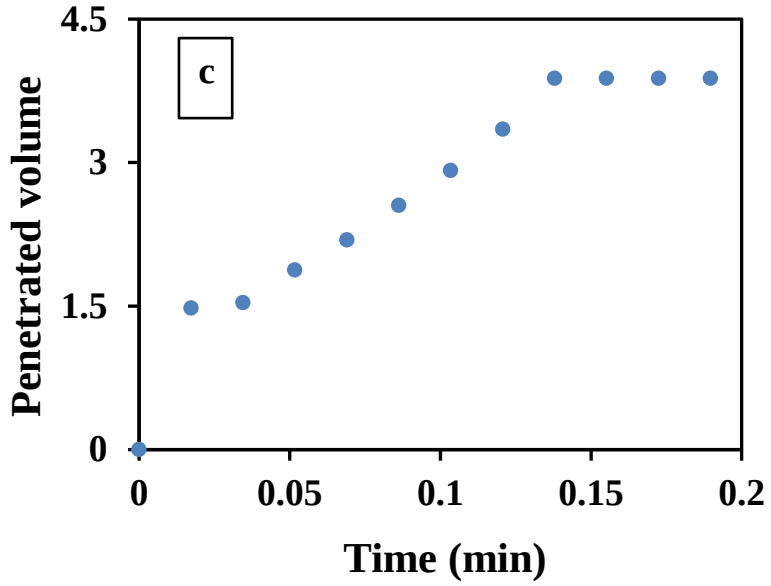
c
Penetrated volume
4.5
3
1.5
0
0
0.05
0.1
0.15
0.2
Time (min)

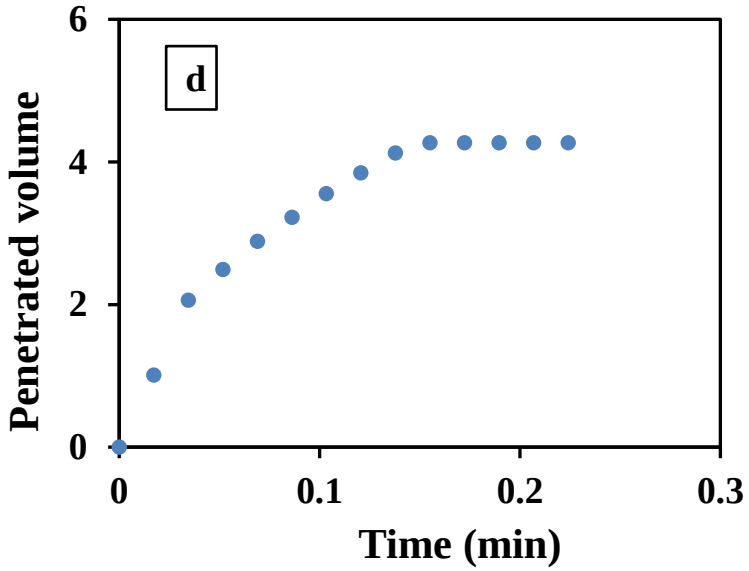
d
Penetrated volume
6
4
2
0
0
0.1
0.2
0.3
Time (min)

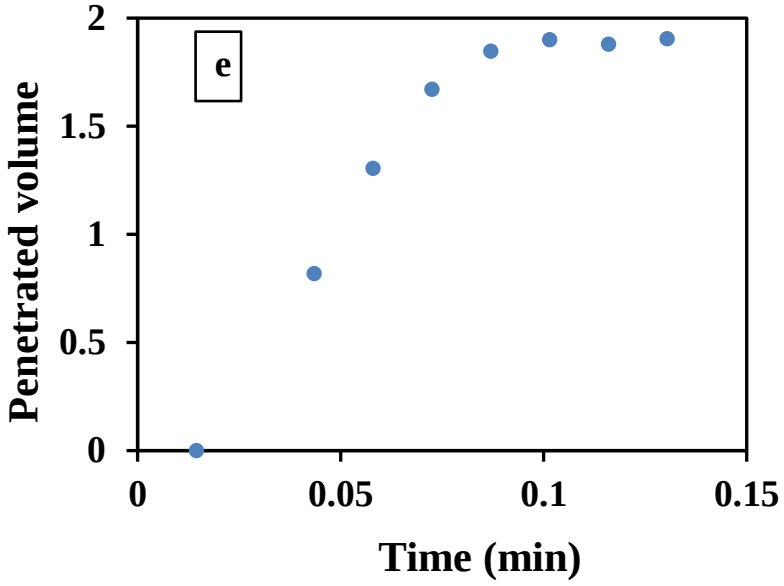
e
Penetrated volume
2
1.5
1
0.5
0
0
0.05
0.1
0.15
Time (min)

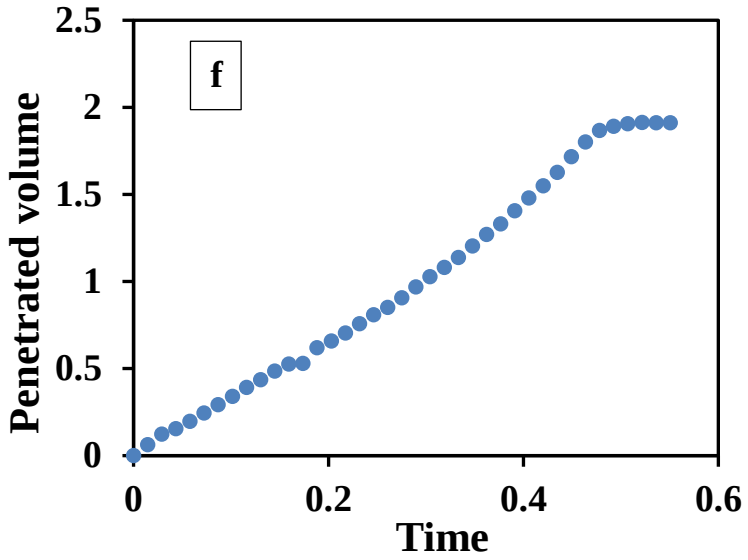

Figure 4-11 Non-dimensional penetrated volume as a function of time for (a) pure AER, (b) 5% IMN in AER, (c) pure NEU, (d) 5% IMN in NEU, (e) pure FUJ and (f) 5% IMN in FUJ

4.6 Tables

Carrier	Impregnated Products	D_{10}	D_{50}	D_{90}
NEU	Pure	41	124	206
	5%	56	121	192
	9%	53	122	188
	13%	56	123	183
AER	Pure	23	52	86
	5%	23	55	90
	9%	28	55	88
	13%	27	51	95
FUJ	Pure	64	131	180
	1%	63	130	185
	3%	62	131	184
	5%	63	130	188

Tab 4-1 Particle size measurement of pure porous carriers and impregnated products. All sizes are in microns

Carrier	Impregnated Products	Surface Area (m^2/g)	Total Pore Volume (cc/g)
NEU	Pure	390.4	1.742
	13%	264.5	1.308
AER	Pure	336.925	2.244
	13%	186.079	1.645
FUJ	Pure	28.708	2.242e-01
	5%	26.174	1.952e-01

Tab 4-2 Surface area and pore volume of pure carriers and impregnated products

Carrier	Impregnated Products	%Loading	%RSD
NEU	5%	4.80	1.2
	9%	9.59	0.73
	13%	11.89	3.22
AER	5%	4.67	2.64
	9%	9.28	3.65
	13%	13.07	4.36
FUJ	1%	0.87	3.92
	3%	2.80	4.80
	5%	4.42	3.83

Tab 4-3 Loading and Blend Uniformity of impregnated products.

Carrier	Product	Contact of Angle (θ)
IMN	Pure	No Penetration (N. P.)
NEU	Pure	53.4
	5%	69
AER	Pure	78.0
	5%	79.9
FUJ	Pure	37.8
	5%	81.4

Tab 4-4 Contact Angles of pure Indomethacin, porous carriers, and impregnated products

Chapter 5 Continuous Impregnation of APIs into porous carriers using a Glatt Blender CGC-70

5.1 Introduction

As mentioned previously in Chapter 1, the pharmaceutical industry primarily has still used the traditional batch manufacturing system; however, a few companies have been modernizing to continuous manufacturing, which has recently shown many advantages to batch, becoming an emerging technology in pharmaceutical industries. Traditional batch manufacturing needs long time from formulation to manufacturing development and it is a material-consuming process. On the other hand, continuous manufacturing has many benefits, including relatively low cost, small equipment size, flexible production volumes, and no need for scale up. Thus, the US FDA is encouraging the companies to adopt continuous manufacturing processes.

Work presented in Chapter 3 and 4 were performed using batch manufacturing equipment where a pre-determined batch-size of impregnated products was produced each run. With the new interest in continuous manufacturing, this chapter will focus on the development of a continuous impregnation process. In order to get a successful continuous impregnation process, the window for impregnation is much shorter than for the batch process. In the batch process, there is a set amount of material and solution that needs to be sprayed over time. In the continuous process, the powder constantly moves through the system; therefore, the solution addition rate needs to be adjusted to the material flow rate to reach a desired output ratio of API impregnated in the porous material. That is why in a continuous impregnation process, it is important to adjust the spray rate according to the

mean residence time and flow rate of powder from the feeder. Also, it is important to determine the maximum allowed spray rate in this process to avoid agglomeration. This step depends highly on the properties of the porous carrier and the throughput of the material. Furthermore, it is of interest to study the effect of process parameters on the properties of the impregnated products. All these steps are necessary to determine the applicability of the proposed continuous impregnation method. In order to test the feasibility of continuous impregnation using a Glatt GCG-70, some preliminary studies were conducted, and the results were discussed in Chapter 2.

In this chapter, a new manufacturing method to continuously impregnate API into porous carriers was investigated. Since the process is constantly in a steady state motion, RTD measurements were thoroughly discussed, and results presented in this chapter. RTD experimentation has been used in pharmaceutical manufacturing to examine the blender performance (151,152) and to characterize the behavior of materials with different properties as they move through the continuous process (153,154). The continuous Glatt blender (GCG-70) was used to impregnate IBU into two porous carriers: Neusilin US2 (NEU) and Fujicalin (FUJ). The blade configurations of the blender shaft were arranged in order to move powder forward, upon entering the blender, to the middle third of blades, which were arranged in alternating angle pattern. The alternating pattern would create a region of hold-up in material, which is a better region to spray the solution to allow for the solution to be dispensed across the material. The regional mixing rate in conjunction with the time the powder remains inside the blender decides the efficiency of GCG-70 as an impregnation equipment. The final third of the blades was directed forward to continue the material flow. The hold up, where the impregnation occurred, was dependent on material

properties, throughput, blender RPM, and blade configuration. Since the configuration was kept constant, the remaining parameters were investigated. When optimizing the process, some period of residence time of the host carrier was desired. If the measured residence time is too fast, that would mean the material does not reside in the blender long enough to allow for the solution to disperse within the flowing powder system; therefore, the unit operation is not efficient to produce enough mixing, and the homogeneity of the resulting products will be very low (155). This means that the efficiency of continuous impregnation process is determined by the balance between two sub-process: a radial flow (batch process) and an axial flow. Hence, the first step in the development and enhancement of any continuous manufacturing process was to examine the RTD and evaluate the effects of different process parameters.

Accordingly, this chapter concentrates on the characterization of the GCG-70 blender with consideration to the process parameters (flow rate, impeller rotation), host type (NEU or FUJ), and tracer amount (low, medium, and high). The characterization of the continuous blender depends on two main strategies. The first strategy was the investigation of the flow behavior of host carriers in the blender. This step was accomplished by conducting RTD, material hold up measurement and strain calculations. The second strategy is evaluating the blend uniformity of the impregnated products using NIR spectroscopy. These two strategies provide a good understanding of the performance of GCG-70 blender as an impregnation equipment.

5.2 Materials and Methods

5.2.1 Materials

Two host carriers were used in these studies, dibasic calcium phosphate (Fujicalin) and magnesium aluminometasilicate (Neusilin US2) were obtained from Fuji Chemical Industries Co., Ltd. (Japan). The API used in these investigations were Ibuprofen 70 (BMS). Ibuprofen was the API used for impregnation and liquid phase tracer in RTD studies. Analytical grade methanol was used as the transport solution, to dissolve the Ibuprofen, and pump it into the devices.

5.2.2 Processing and Online Testing Equipment

The continuous impregnation process consisted of multiple unit operations and online testing equipment including a loss-in-weight (LIW) feeder, a continuous blender, a near infrared (NIR) spectroscopy instrument, a peristaltic pump, and a vibratory feeder. The first operation involved the LIW feeder, which is used to dispense accurately the host particles. From the feeder, the particles flowed into the continuous blender, where the ingredients underwent tumbling. The impregnation step occurred in the continuous blender, after which, the powder fell into a transitional vibratory feeder to control the bed height. Above the vibratory feeder, the NIR probe was placed to obtain the spectral scans. This set up is shown in Figure 5-1. In this work, we utilized the Glatt continuous powder blender (GCG-70), a single K-Tron K-CL-SFS KT20 (Coperion K-Tron Pitman Inc., NJ) feeder for manufacturing of impregnated products. A FT-NIR Matrix (Bruker Optics Billerica, MA, USA) was used for spectral acquisition to study RTD and RSD of impregnated products. The description of these equipments was provided in Chapter 2.

5.2.3 Experimental Set-up

These experiments started with feeding the porous carrier through the LIW feeder into the blender, where the impregnation step occurred immediately once the material reached the nozzle position inside the blender. A peristaltic pump was used to deliver the drug solution through a Tygon® tubing connected to the 0.1 mm diameter nozzle. Figure 5-2 shows a schematic illustration of experimental set-up

Next, the impregnated products were collected from the blender and were dried using a Miniglatt fluidized bed to exclude any residual solvent. The temperature of inlet air was 80 ^{o}C. The air flow pressure was between 0.10-0.15 bar. Once dried, particle size was characterized using a Beckman-Coulter LS 13-320, with a Tornado module for dry powder, to determine if particle size was affected by the process.

5.2.4 Characterization of the Blender by Residence Time Distribution, Hold-up, Strain, and Content Uniformity

5.2.4.1 RTD measurement

Residence time distribution in the blender was calculated to determine the RTD of the API in the liquid phase. The API (Ibuprofen) was used as the tracer as it had a clear and distinguishable NIR peak. To calculate the RTD of tracers in liquid phase (Ibuprofen in Methanol)), the continuous process was first allowed to reach steady state by monitoring the exit flow rate of the system. This was done by allowing the porous carriers (FUJ or NEU) to be fed in the blender for 10-15 min. Once steady state was achieved, the tracer was added, and the time of the pulse was noted. These experiments were performed at 150 and 300 rpm and using 3 kg/hr flow rate. The amounts of tracer were selected such that the

concentration of the tracer at the exit of the mixer would be above the detection limits of NIR method. The Ibuprofen (IBU) solution, used as the liquid form tracer, was prepared by dissolving IBU into methanol to obtain a 20% w/w IBU in methanol solution. The solution was then added into the system using a peristaltic pump at 3 different rpm (25, 60, and 90). The pump was run for 1 minute for each condition. NIR spectra were subsequently acquired at constant time intervals from the outlet of the mixer. These spectra were analyzed to determine the concentration of tracers over time. Thus, a dataset of concentration vs. time was collected. Using this data, the residence time distribution function (E (t)), the mean residence time (τ), the mean centered variance (σ), and skewness were calculated. As mentioned in previous work (56,69), these parameters illustrate axial mixing in a continuous flow system. Mathematical equations for each of these terms are described below, equations (5-1), (5-2), and (5-3).

Residence time distribution *(E(t))* is defined by the equation:

$$\mathrm{E}\ (\mathrm{t}) = \frac{\mathrm{c}\ (\mathrm{t})}{\int_0^\infty \mathrm{c}(\mathrm{t})\mathrm{dt}} \qquad 5-1$$

Where *t* is time, *c (t)* is the tracer concentration as a function of time

Mean residence time *(τ)(MRT)* is defined by the equation:

$$\tau = \int_0^\infty \mathrm{tE}(\mathrm{t})\mathrm{dt} \qquad 5-2$$

Lastly, the mean centered variance (σ_τ^2) (MCV) is defined by the equation:

$$\sigma_\tau^2 = \frac{\int_0^\infty (\mathrm{t}-\tau)^2 \mathrm{E}(\mathrm{t})\mathrm{dt}}{\tau^2} \qquad 5-3$$

The RTD, mean residence time (MRT), mean centered variance (MCV), and skewness were used in this study to estimate the flow behavior and the distribution of drug in the continuous mixer. The RTD was the distribution of material as it passed through the system at steady state, while MRT was the mean time that a particle remains inside the blender (156). The MCV was the variance (square of the standard deviation) normalized by the square of the mean value of the distribution. Standard deviation and MCV are qualitatively similar since both were a measure of the width of the RTD. For a CSTR (Continuously Stirred Tank Reactor), where it is often described as a perfectly mixed stirred tank, the MCV would be equal to one. For a perfect PFR (Plug Flow Reactor), which is often described as a perfectly unmixed system, the MCV would be equal to zero. Flow behavior of real cases without dead zones should fall in-between those two extremes. Thus, a higher value of MCV would indicate better mixing, while a lower value for MCV describes poor mixing conditions. Another important parameter that should be calculated is skewness. The skewness equals to the cubic of standard deviation normalized by the cubic of the mean value of the distribution. The skewness is used to investigate the degree of back mixing and the degree of asymmetry in the RTD curve. Its value could be positive or negative depending on the presence or absence of back-mixing.

Several models have been stablished to describe the RTD in the continuous unit operations. Although these models were primarily developed for liquid unit operations, most of them can be applied for powder flow in unit operations. The examples presented in this study were based on “stirred-tanks-in-series” model. This model presents a mixer as a set of equally sized continuously stirred tank reactors (CSRTs) placed in series (Figure

5-3). While the CSRT model assumes that each mixing unit has perfect back-mixing, placing CSRTs in series results in a realistic mixing model (54).

The Tank-In-Series model, a one parameter model, was used to describe the blender (54,157–161). The tracer concentration versus time of the RTD of the system was fitted with the Tank-In-Series model, equation 5-4, to calculate the number of ideal tanks (CSTRs), n, in series.

$$E(t) = \frac{t^{n-}}{(n-1)!\tau_i^n}\, e^{-t/\tau_i} \qquad 5-4$$

The number of tanks, n, represents the behavior of the mixing system as shown in Figure 5-4, if the value was small, from a broad peak, the system behaves closer to an ideal CSTR, or two CSTRs in series. If the n value obtained was a larger number (sharper peak), it would mean that the system behaves more similarly to an ideal plug flow reactor PFR. ‘0 n-value’ is also inversely proportional to the variance or the ‘spread’ of the RTD plot (54,56,82).

5.2.4.2 Blender Hold-up and Strain measurement

Blender hold-up was defined as the semi-constant mass of powder that resides in the continuous blender during steady state operation. The hold-up is commonly calculated by subtracting the mass exiting the blender to the total mass that flows into the blender, at steady state. The total mass exiting the blender was collected in a vessel on an Ohaus Adventurer catch scale, while the total mass entering into the system was calculated from the total mass the LIW feeder deposits during the run. The hold-up is commonly dependent on the blender impeller speed, the total mass flow rate, and impeller blade configuration(156). After the system was started, powder accumulates in the blender,

creating the hold-up. Small pulses of powder can exit the blender at this time; however, at steady state, the mass flow rate exiting the blender is approximately constant. When the mass flow exiting the blender was identified to be at a constant flow rate, steady state was assumed. This procedure was conducted for both NEU and FUJ at 150 rpm and 300 rpm. The whole line completely cleaned between the experiments to prevent contamination between carriers.

The hold-up measurements can be used to calculate the bulk residence time, or what has also been sometimes called the space-time, which is the average amount of time required by the incoming material as it combines with the blender holdup before eventually exiting the system(156). MRT in this case can be calculated using equation (5-5):

$$Mean\ Residence\ Time\ (hr) = \frac{hold\text{-}up\ (kg)}{flow\ rate\ \left(\frac{kg}{hr}\right)} \qquad 5-5$$

The rotating impeller is the main source of energy in the continuous mixer. This energy is spent in the powder convective transport, friction forces between the powder bed and the impeller, and the mean strain(56). It is crucial to know the number of blades passes because it has an essential effect on the RTD and the rotation rate. With the knowledge of MRT, the average time a particle spends in the system has been identified. Calculating the average time, a particle remains in the system, and knowing the RPM of the blender, the total number of blades passes the average particle experiences was calculated using equation (5-6).

$$Number\ of\ blade\ passes = Blender\ RPM * \left(MRT\ (hr) * 60\ \left(\frac{min}{hr}\right)\right) \qquad 5-6$$

Accordingly, powder hold-up in the mixer is important because it specifies the average residence time, and thus the total average strain experienced by the powder as it travels through the mixer.

5.2.4.3 RSD measurement

To evaluate the quality of mixing (mixing performance) over time, the relative standard deviation of the API content in the impregnated product was computed. Once the powder flow reached a steady state, the drug solution was constantly pumped into the blender and allowed to reach the steady state. When the steady state was achieved by observing constant NIR readings, 100 spectra were collected over the course of the run. The average API concentration was calculated along with the standard deviation. The RSD was then calculated as the ratio of the standard deviation over the average. The target was to obtain an RSD below 5%.

5.3 Results and Discussion

5.3.1 Residence time distribution and metrics

As mentioned previously, determining the RTD of the blender is an essential step to understand the characteristics of the blender. The RTD enhances the understanding of the flow behaviour of the material imparted by the blender. RTD knowledge can help to predict how the blender can filter any noise coming from upstream units, by characterizing the RTD versus process parameters.This means that the RTD can help to build up a robust feed-forward (downstream) and feed-back (upstream) control systems.The control system would monitor the quality control of pharmaceutical products throughout the continuous line .

The RTD's probability distribution function (PDF) was calculated using the tracer concentration obtained from the NIR study and the equations mentioned in Section 5.2. The tracer concentrations were transferred to a standard scale i.e. into the E (t) distribution. This transformation step is necessary to make obvious and representable comparison between RTD tests at different conditions. The RTD curves for all tracer suggested that there are clear differences between the maximum E (t) value among these curves. The maximum PDF value (peak) was 0.5 s^{-1} in which 90 ml of IBU solution was added as a tracer and NEU was used as a carrier at 3 Kg/h and the lowest minimum PDF (peak) was 0.07 s^{-1} in which 60 ml of IBU solution was added as a tracer and FUJ was used as a carrier at 3 Kg/h. Moreover, all tracer curves, which presented in this study displayed two major characteristics. First, a delay time was observed in all the tracer curves. Delay time is the time between tracer addition and the increase in the E (t) in response to increase the tracer concentration. This property is related to the minimum amount of time required for

powders to move through the blender and approach the blender's exit. Second, a right skewness was observed in most curves. This skewness was identified by a long tail. These results came in agreement with previous studies (69,162). Using the PDF values, the RTD metrics were computed using the mathematical equations in 5.2. The mean residence time (MRT), mean centered variance (MCV), and skewness for all the experiments are showed in Table 5-1 and Table 5-2. All distribution presented positive values for skewness. This means that all distributions had a right skewness i.e. "long trailing tails". Also, the results showed that increasing the rotation speed of the blender resulted in reducing the MRT (using the same carrier) in most cases. This indicates that increasing the RPM, for the same carrier, leads to an increase the speed of this carrier inside the unit and results in different MRT. Also, NEU and FUJ showed different RTD metrics at the same experimental conditions. This means that the tracer needed different times to travel through the blender when using carriers with different bulk properties, which travel at different speeds inside the whole line.

5.3.1.1 RTD metrics using NEU as a carrier

The following section focuses on the effect of tracer amount and rotation speed on the RTD measurements using NEU as a carrier.

Figure 5-5 (a & b) shows the effect of tracer volume and rotation speed on the residence time distribution using NEU as a carrier at 3kg/h. All the cases presented a long tail and a delay time. As the tracer amount increases from 25 ml to 90 ml, using the same rotation speeds, the PDF curve stay almost consistent with no change in the behavior. However, increasing the speed rotation leads to a clear change in the PDF profile, where at high rotation speed, the sharpness of the peak increases. This indicates that the rotation

speed has a distinctive effect on the RTD curve and its metrics, while the volume of tracer did not show any clear effect at the same rotation speed. This is exactly what is desirable and demonstrates that the tracer does not affect the RTD. Figures 5-6 (a, b and c) elaborates the effect of rotation speed on RTD metrics. Figure 5-6 (a) illustrates the effect of tracer amount and rotation speed on MRT. The MRT of 25 ml, 60 ml, and 90 ml tracer at 150 rpm were 6 .06 min, 6.12 min, and 6.29 min, respectively. While MRT of 25 ml, 60 ml, and 90 ml tracer at 300 rpm were 3.57 min, 3.78 min, and 3.41 min, respectively. These results showed that increasing the volume of tracer, at the same rotation speed, did not influence on MRT. However, increasing the rotation speed does lead to a significant reduction in the MRT. As the rotation speed increases from 150 rpm to 300 rpm, the MRT decreases to about the half. The result is intuitive, as the blades move faster, the powder is pushed through the system faster, and therefore resides within the blender for a short period of time. These results were in agreement with previous work performed in a continuous blender (56). The MCV and skewness for all cases ranged between 0.147 to 0.20 and 0.06 to 0.133, respectively. The change in MCV values by increasing the rotation speed followed a different pattern than the MRT. The MCV values (as shown in Figure 5.6 (b)**)** were found to stay consistent with increasing impeller rotation rate, except in case of 90 ml tracer, where the MCV slightly increases with increasing the impeller speed. All curves had positive values for skewness, as seen from the results in Figure 5-6 (c**)**, which means that all RTDs have right skewness. The right skewness of all RTD curves demonstrates what previously mentioned in section 4.1 that all RTD curves have trailing tails. These results agreed with previous work (69).

5.3.1.2 RTD metrics using FUJ as a carrier

Figures 5-7 (a & b) show the effect of tracer volume and rotation speed on the residence time distribution using FUJ as a carrier at 3kg/hour. All the cases showed a tail longer than that observed for NEU, as well a longer delay time. As the tracer amount increases from 25 ml to 90 ml using the same rotation speeds, the PDF curve showed inconsistency in its behavior. Figure 5-8 (a) showed that increasing the tracer amount led to increase the MRT for both 150 rpm and 300 rpm. As for NEU, increasing the rotation speed of the blender led to a reduction in the MRT. This demonstrates that both the rotation speed and the amount of the tracer have an influence on the RTD curve, and its metrics. For all cases, the MCV and skewness ranged between 0.147 to 0.207 and 0.06 to 0.133, respectively. The change in MCV values, by increasing the rotation speed and the tracer amount, followed same pattern as what we have seen in the MRT study. All curves had positive values for skewness, as shown in Figure 5-8 (c), which demonstrates that all RTDs have right skewness, indicating the curves have trailing tails. Next the FUJ experiments were repeated at 6 kg/h. Figures 5-9 (a and b) and Figures 5-10 (a, b, and c) presented RTD and its metrics using FUJ as a carrier at 6 kg/hr. Generally, increasing the speed of rotation reduced MRT, MCV and skewness. This means that the rotation speed has a clear effect on these metrics. In general, the RTD tracer data of using FUJ at 6 kg/h were better than using FUJ at 3 kg/h. The better RTD tracer data with the higher throughput indicated that at 3kg/h the carrier did not occupy enough volume within the blender, and with the increase in throughput, more material resided within the blender, allowing for the liquid to be dispensed at an improved rate. This also decreased the trailing tail indicating that the tail was possibly due to solution sticking to the surface of the blender prior to reaching the bed.

5.3.2 Comparison between NIR-MRT and Hold up (Mass)-MRT

Figures 5-11 (a, b, and c) illustrated the comparisons between the calculated MRT using NIR (NIR-MRT) and measured MRT using the mass hold up (Hold-up MRT) at the same experimental conditions. Figure 5-11(a) compared between the NIR-MRT and Hold-up MRT using NEU as a carrier. The results showed that NIR-MRTs are close to Hold-up MRT in most cases. However, when FUJ was used as a carrier at 3 kg/h, there is a big difference between NIR-MRT and Hold-up MRT (see Figure 5-11(b)). In all cases, NIR-MRT was much higher than Hold up-MRT. This might be due to the fill level of the powder in the blender. The volume fill of powder was not high enough, so the powder does not come in contact with the nozzle and liquid. That is why it took longer time for the liquid to come out and that is why NIR-MRT was greater than the Hold-up MRT. To increase the volume fill of powder inside the blender, the feeding rate of FUJ was increased from 3 kg/h to 6 kg/h. The results showed that NIR-MRTs were comparable to Hold-up MRTs in most cases. Moreover, BET surface area of NEU is more than 300 m^2/g (163) while the BET surface area of FUJ is less than 40 m^2/g (164). Therefore, the absorption capacity of NEU to tracer liquid is much higher than FUJ. The addition of tracer liquid into FUJ at 3 kg/h could result in formation of a relatively wet mass at high tracer volume. So, the flow properties of FUJ might be changed and leading to a delay in the tracer coming out of the blender

5.3.3 Tank-in-Series

Tab 5-5 presents the regression results of the tank-in-series equation using NEU as a carrier at 3 kg/h feeding rate. The system presented a good level of dispersion. The average number of tanks (n-value) for all impregnated products using NEU as a carrier was

2.17. Two tanks-in-series has been confirmed as a relatively good fit by several previous studies (159,160,165–167). This value (n=2) also points out that the material disperses as a bulk through the blender's length; then it undergoes back-mixing with the incoming material. Table 5-5 presented that the average **τ** delay (delay time in min) for all experiments using NEU as a carrier was 1.93 min. These results also indicate that n-value slightly increases by increasing the tracer volume at the same speed rate. However, as the rotation speed increases, the n value decreases, with the same tracer volume.

Table 5-6 shows the regression results of the tank-in-series equation using FUJ as a carrier at 3 kg/h and 6 kg/h. At 3kg/h feeding rate the average n- value was approximately 1.5, which means one tank and half in series. Also, the average τ delay was 2.685, which is higher than other studied cases. The bulk density of FUJ was measured using FT4 device and it was 0.52 g/ml. Therefore, when the feeding rate of FUJ was 3kg/h, the powder filling level was low (as discussed in the previous section). This means that the droplet of IBU liquid needs more time to reach the powder and mix with it. Also, because the volume of liquid added to the carrier exceeds the absorption capacity (specifically at 90 ml tracer volume), the mixing process was inefficient. According to this, the feeding rate of FUJ was increased from 3kg/h to 6 kg/h. As shown in Tab 5-6, the average n-series value was 2, which means two tanks in series.

This value showed better level of dispersion than using 3 kg/h. As mentioned early in this section, two tanks-in-series has been reported as a relatively good fit model. Also, Tab 5-6 showed that the average **τ** delay (delay time in min) FUJ as a carrier at 6 kg/h feeding rate was 1.4 min, which is lower than the average τ delay using FUJ as a carrier at 3 kg/h. Increasing the feeding rate results in an increasing of the powder fill level (mass

hold-up) in the blender, so that a droplet of IBU solution does not need a long time to touch the powder surface and mix with it.

5.3.4 Blend homogeneity (%RSD)

The previous sections demonstrated the characterization of GCG-70 blender on the macroscale level using the RTD and its metrics. Therefore, the next step of the characterization of the GCG-70 would be to understand performance over time. Therefore, experiments were conducted to monitor content homogeneity of carrier exiting the continuous blender. To measure the blend homogeneity of the products coming out of the blender, four impregnation experiments were run using NEU and FUJ as host materials, and at 150 and 300 rpm. In these experiments, the pumping rate was 25 ml/min and the feeding rate was 3 kg/hr. At the beginning, the host materials (NEU or FUJ) were fed until reaching the steady state by monitoring weight versus time exiting the blender. Then, the IBU solution was pumped for a while to reach the steady state. After that, 100 NIR spectra were collected for each experiment.

After analyzing these spectra to predict the IBU amount at the steady state (see Figure 5-12 & Figure 5-13), the relative standard deviation was calculated. When the RSD value was low, concentrations of IBU in all the acquired spectra were close to the mean concentration. On the other hand, when the RSD value was high, concentrations of IBU in all the acquired spectra were far from the mean concentration. Tab 5-7 demonstrates the RSD values of IBU using both NEU and FUJ. In all cases the RSD% values were very low (equal or less than 2.5%), which indicates that the impregnated products showed very good homogeneity. These results confirmed our hypothesis that impregnation of API in a porous carrier will result in highly homogenous products (53,100,146).

5.4 Conclusions

The work done in this chapter has demonstrated the feasibility of using a Glatt GCG-70 continuous horizontal tubular blender as a device to implement continuous impregnation. Using a continuous blender allows the impregnation process to occur much quicker with more control than when using a batch fluidized bed device. In order to understand the dynamics of impregnation in a continuous blender, certain characterization development was carried out.

The results showed that all tracer curves had two major characteristics: a delay time and long trailing tail. Also, it was observed that increasing the RPM, in all cases, led to reduce MRT. NEU has better flow properties and liquid absorption capacity than FUJ. In addition, since NEU had a lower bulk density, it was able to fill more of the blender tube to a higher level than FUJ, at the same feeding rate of 3 kg/h. Therefore, NEU showed better RTD tracer data than FUJ. Once the feeding rate of FUJ was increased to 6 kg/h, the RTD tracer data significantly improved. In addition, content uniformity results obtained over a longer period of time were comparable to those obtained from batch impregnation.

5.5 Figures

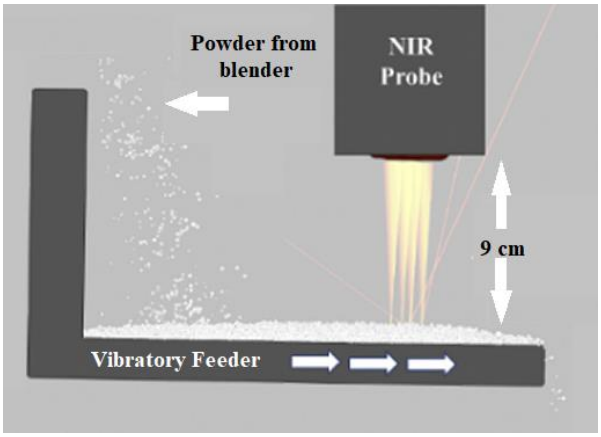

Figure 5-1 Near Infrared (NIR) sampling for RTD experiments

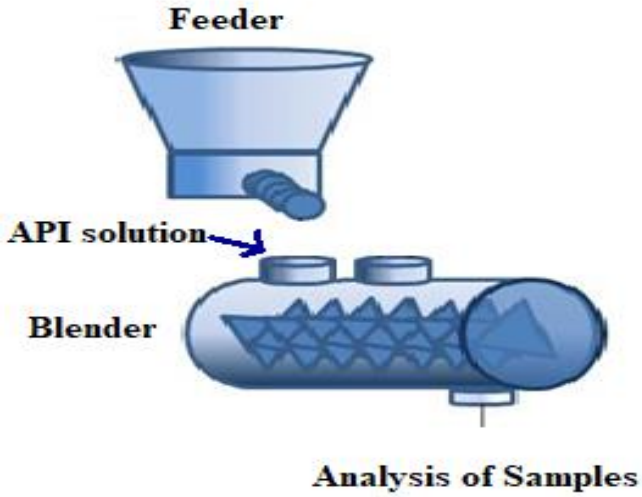

Figure 5-2 Schematic Diagram Experimental Set up

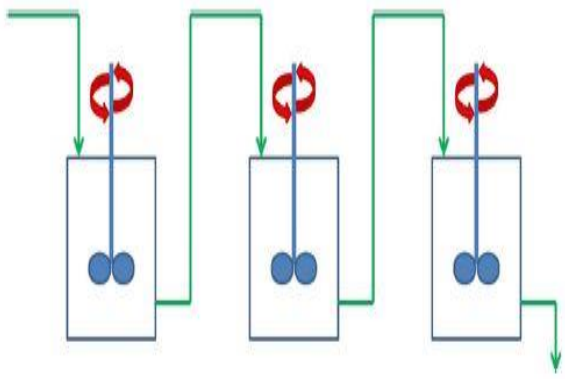

Figure 5-3 Depiction of the tanks-in series model where n=3 (54)

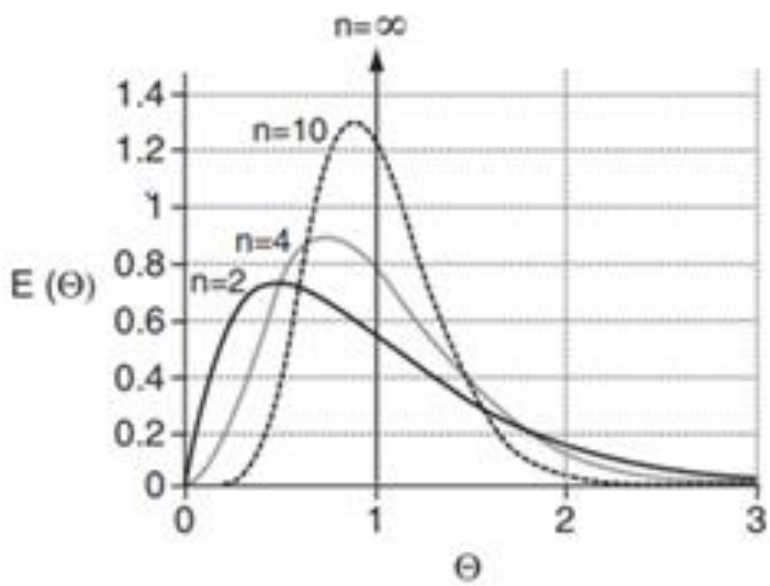

Figure 5-4 Tank in series response at various n (168)

(a)

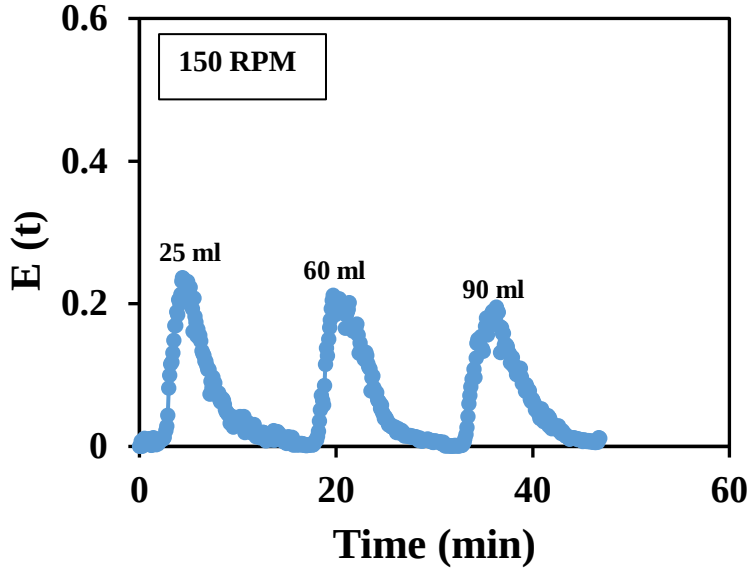

(b)

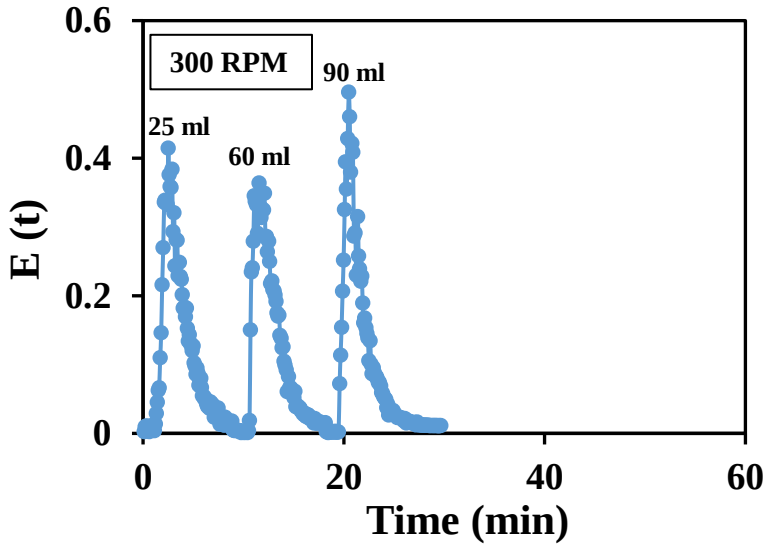

Figure 5-5 Effect of rotation rate on RTD using IBU solution as a liquid tracer (a) 150 rpm (b) 300 rpm. Other parameters: Flow rate — 3kg/h, and NEU as a carrier

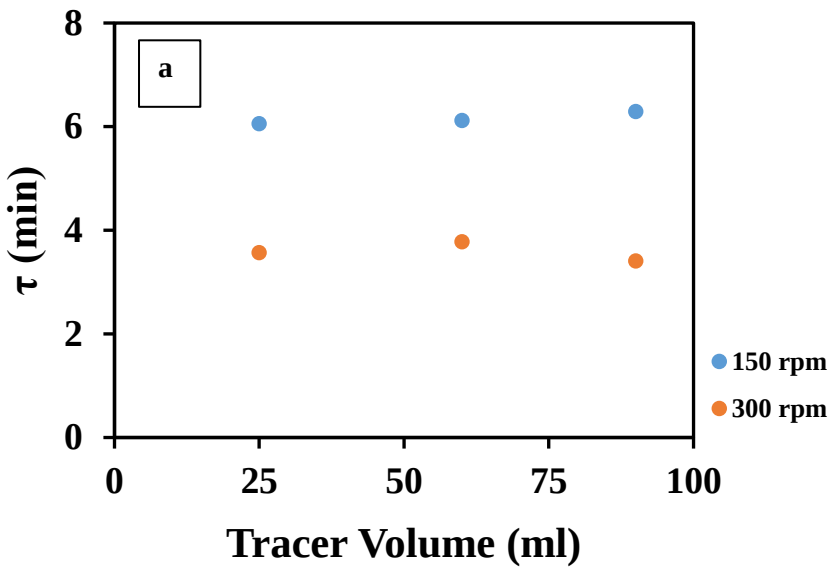
a
8
6
4
2
0
τ (min)
0
25
50
75
100
Tracer Volume (ml)
150 rpm
300 rpm

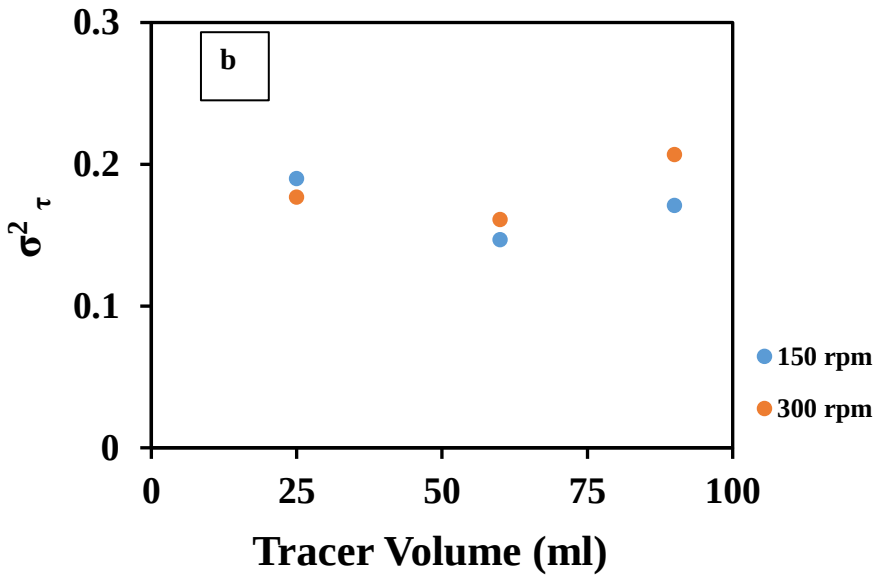
b
0.3
0.2
0.1
0
σ²τ
0
25
50
75
100
Tracer Volume (ml)
150 rpm
300 rpm

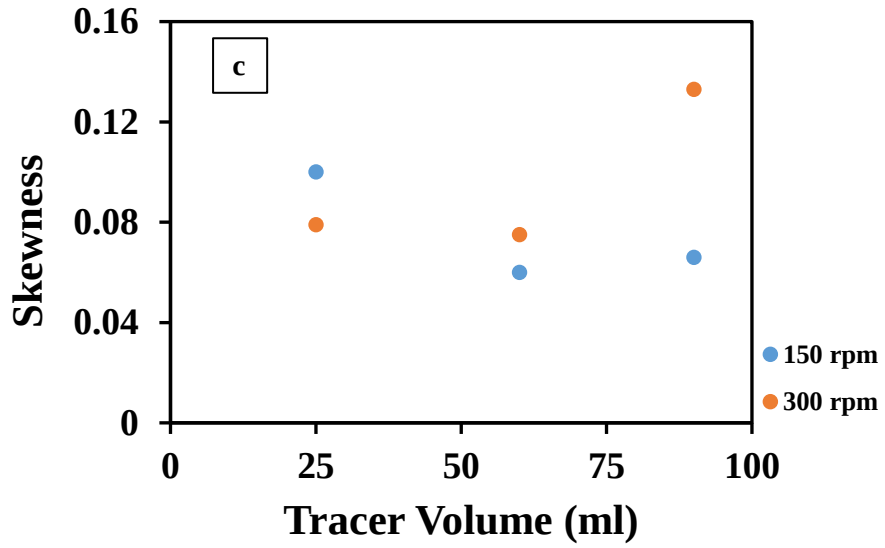

Figure 5-6 Effect of tracer volume and rotation rate on (a) mean residence time (b) mean centered variance (c) curve skewness. Other parameters: Flow rate — 3kg/h, and NEU as a carrier

(a)

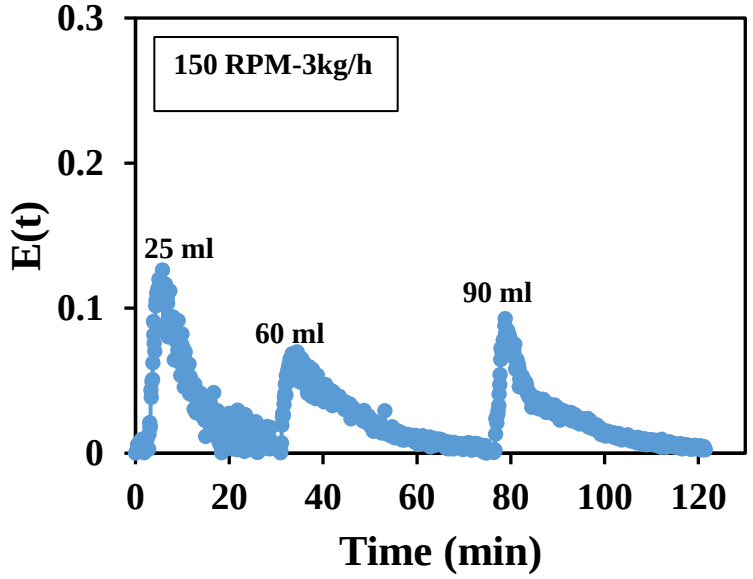

(b)

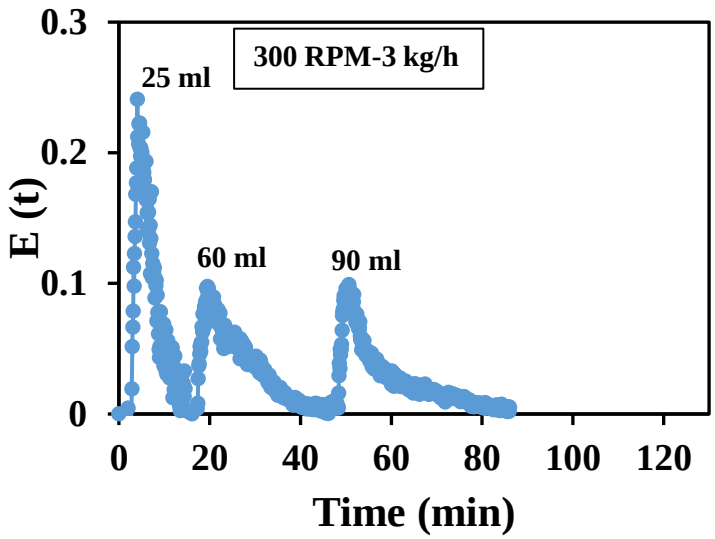

Figure 5-7 Effect of rotation rate on RTD using IBU solution as a liquid tracer (a) 150 rpm (b) 300 rpm. Other parameters: Flow rate — 3kg/h, and FUJ as a carrier

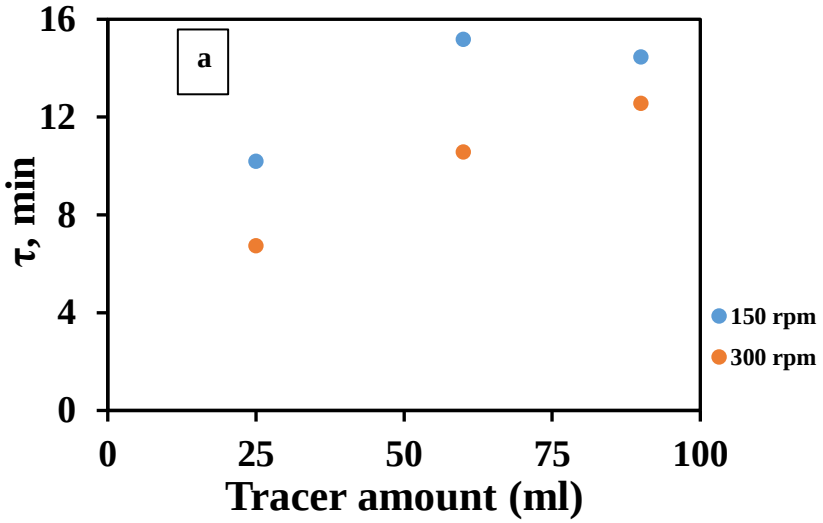

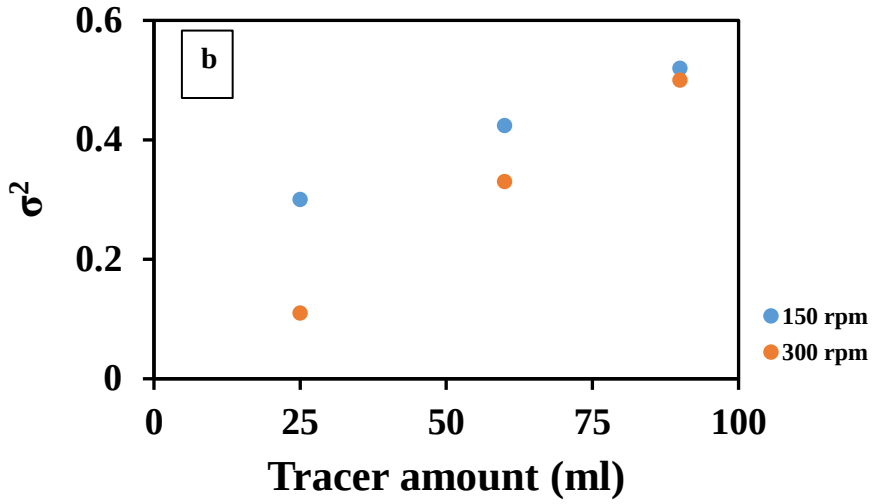

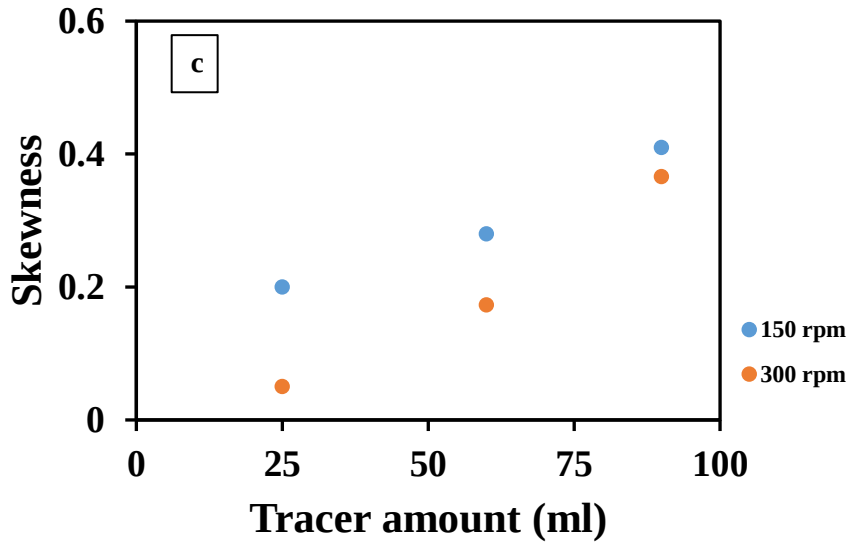

Figure 5-8 Effect of tracer volume and rotation rate on (a) mean residence time (b) mean centered variance (c) curve skewness. Other parameters: Flow rate — 3kg/h, and FUJ as a carrier

(a)

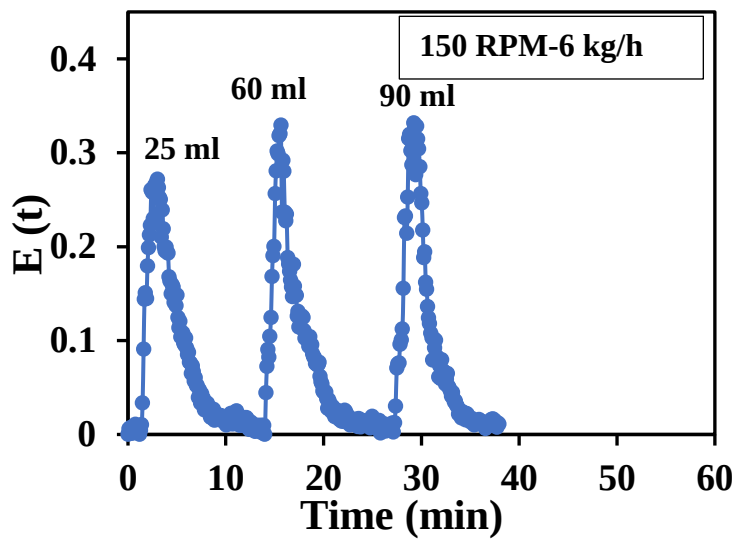

(b)

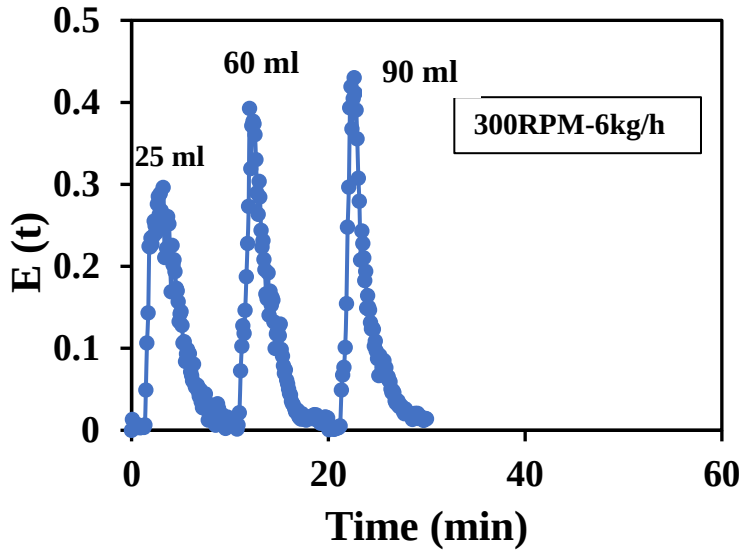

Figure 5-9 Effect of rotation rate on RTD using IBU solution as a liquid tracer (a) 150 rpm (b) 300 rpm. Other parameters: Flow rate — 6kg/h, and FUJ as a carrier

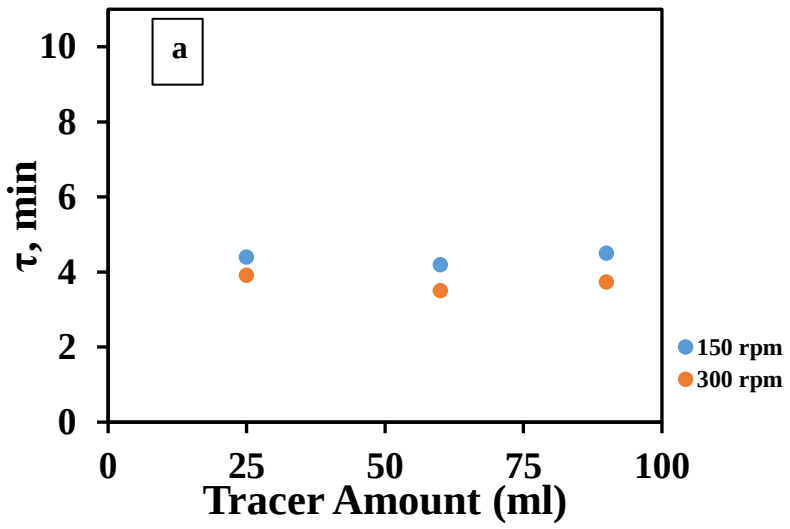
a
10
8
6
4
2
0
τ, min
0
25
50
75
100
Tracer Amount (ml)
150 rpm
300 rpm

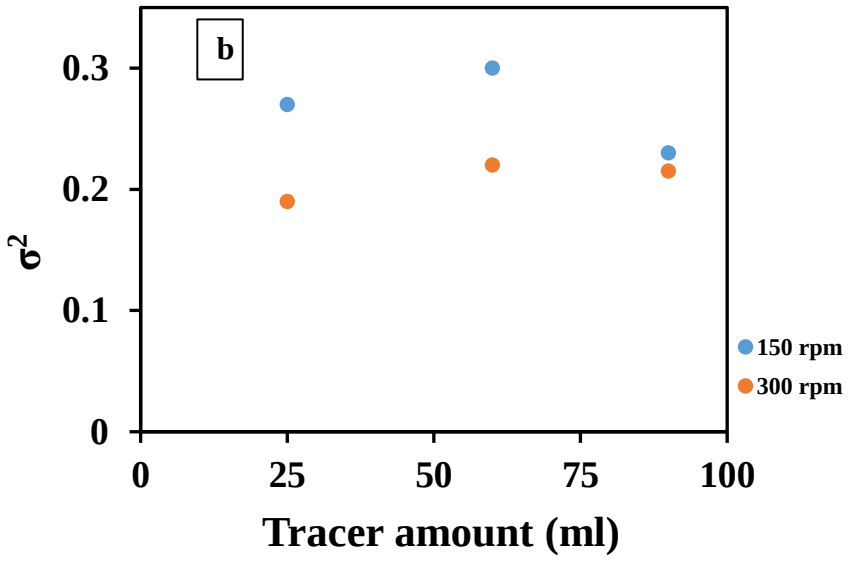
b
0.3
0.2
0.1
0
σ2
0
25
50
75
100
Tracer amount (ml)
150 rpm
300 rpm

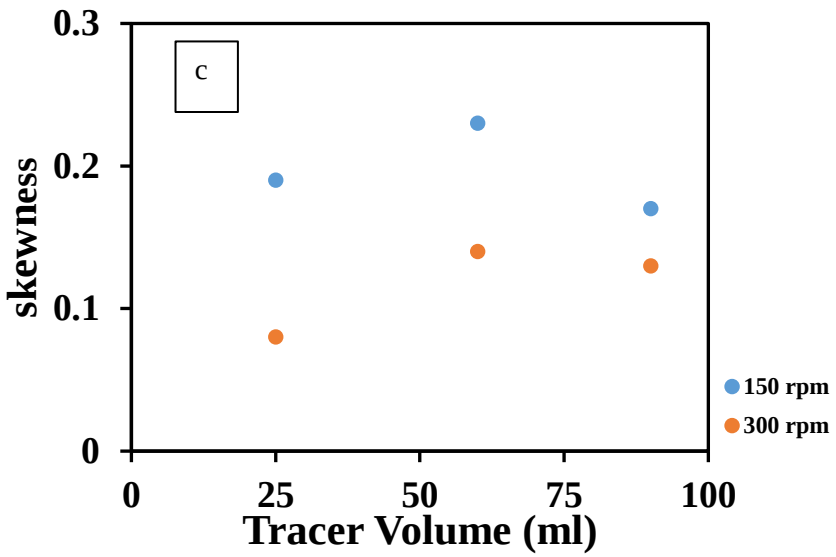

Figure 5-10 Effect of tracer volume and rotation rate on (a) mean residence time (b) mean centered variance (c) curve skewness. Other parameters: Flow rate — 6kg/h, and FUJ as a carrier

(a)

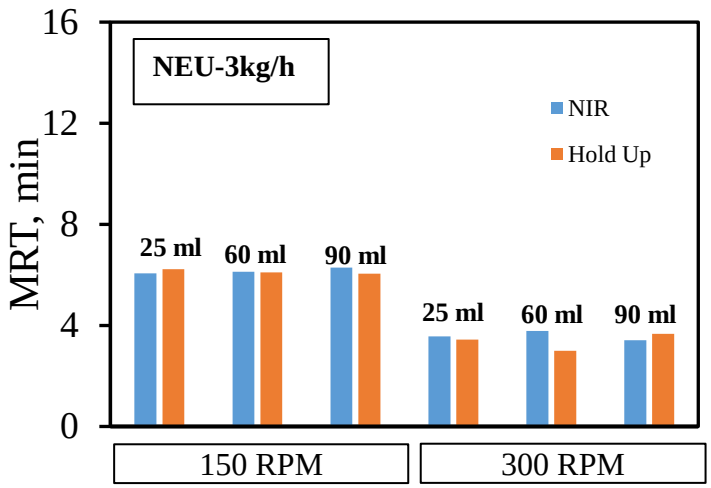

(b)

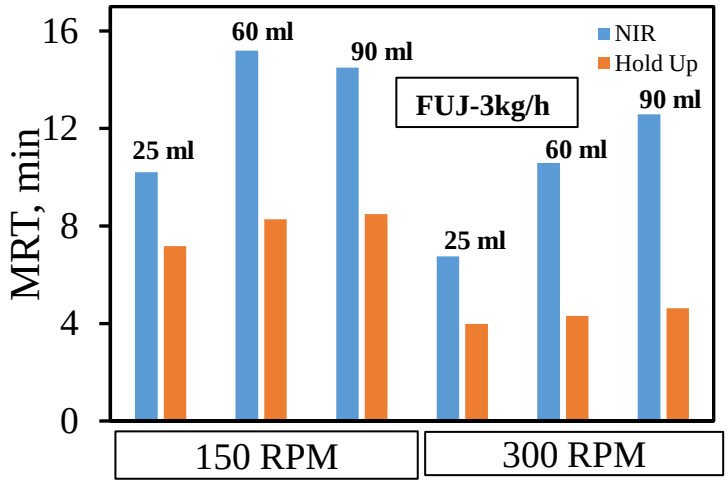

(c)

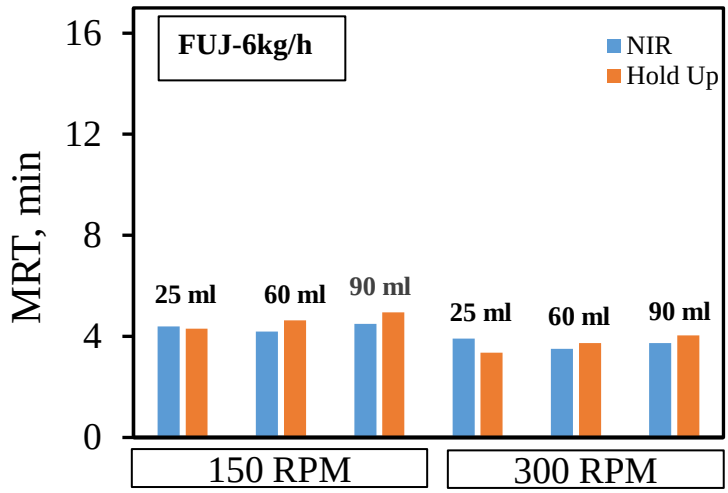

Figure 5-11 Comparison between Hold up MRT (Mss) and NIR-MRT using: a-NEU as a carrier at 3kg/h , b- FUJ as a carrier at 3kg/h and c- FUJ as a carrier at 6kg/h

(a)

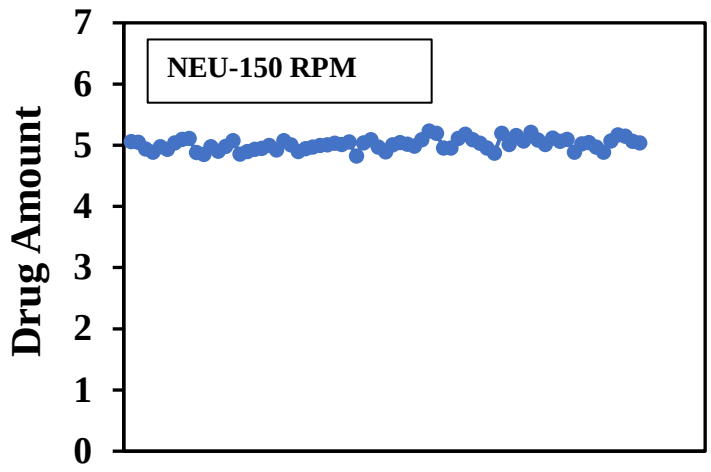

(b)

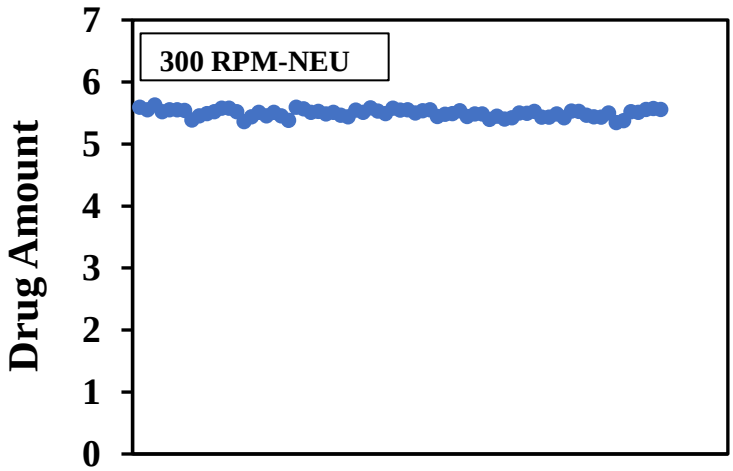

Figure 5-12 Measuring %RSD of impregnated products using NEU as a (a) 150 rpm (b) 300 rpm

(a)

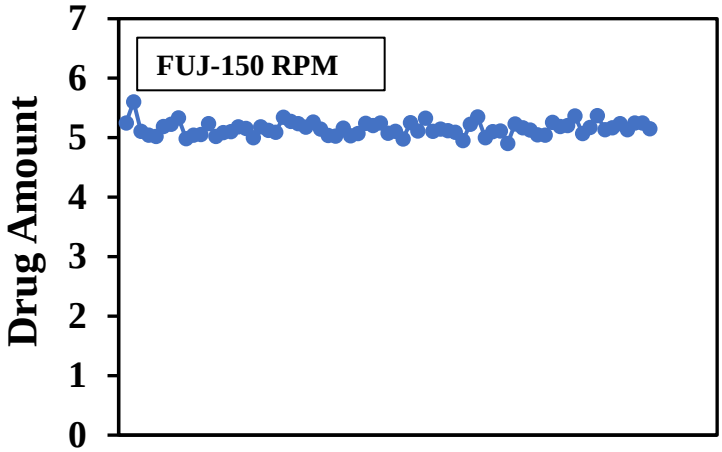

(b)

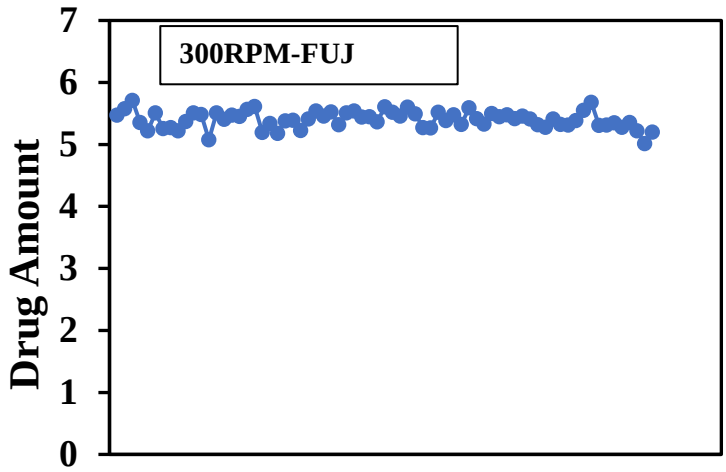

Figure 5-13 Measuring %RSD of impregnated products using FUJ as a (a) 150 rpm (b) 300 rpm.

5.6 Tables

Carrier	RPM	Tracer rate (ml/min)	MRT (min)	MCV	Skewness
NEU	150	25	6.06	0.19	0.1
		60	6.12	0.147	0.06
		90	6.29	0.173	0.066
	300	25	3.57	0.177	0.08
		60	3.78	0.16	0.08
		90	3.41	0.20	0.133

Tab 5-1 RTD metrics using NEU as a carrier at 3Kg/h feeding rate

Carrier	Feeding rate (kg/h)	RPM	Tracer rate (ml/min)	MRT	MCV	Skewness
FUJ	3	150	25	10.21	0.30	0.20
			60	15.19	0.43	0.286
			90	14.46	0.52	0.41
		300	25	6.74	0.11	0.054
			60	10.58	0.34	0.173
			90	12.56	0.518	0.366
	6	150	25	4.4	0.27	0.20
			60	4.19	0.23	0.23
			90	4.5	0.31	0.106
		300	25	3.91	0.194	0.14
			60	3.5	0.22	0.14
			90	3.73	0.21	0.135

Tab 5-2 RTD metrics using FUJ as a carrier

Carrier	RPM	Pump Rate (g/min)	Flow Rate (kg/h)	Bulk Density (g/ml)	MRT (min) Hold Up	No of blades
NEU	150	25	3	0.238	6.22	933
		60		0.332	6.1	963
		90		0.348	6.04	906
	300	25		0.228	3.44	1032
		60		0.198	3	900
		90		0.326	3.67	1200

Tab 5-3 Calculated MRT of NEU using Hold Up. Other experiment conditions Methanol was sprayed at 25, 60, and 90 ml/min in all experiment

Carrier	RPM	Pump Rate (g/min)	Flow Rate (kg/h)	Bulk Density (gm/min)	MRT (min) Hold Up	No of blades
FUJ	150	25	3	0.588	7.17	1075
		60		0.688	8.27	1240
		90		0.713	8.48	1272
	300	25		0.584	3.22	966
		60		0.698	4.78	1434
		90		0.718	5.65	1695
	150	25	6	0.590	3.98	597
		60		0.672	4.31	646
		90		0.715	4.62	693
	300	25		0.556	3.03	909
		60		0.671	3.41	1023
		90		0.724	3.71	1113

Tab 5-4 Calculated MRT of FUJ using Hold Up. Other experiment conditions Methanol was sprayed at 25, 60, and 90 ml/min in all experiment

Carrier	RPM	Pump Rate (g/min)	Flow Rate (kg/h)	ntank	tauDelay
NEU	150	25	3	2.02	2.61
		60		2.88	2.23
		90		2.77	1.84
	300	25		1.54	1.75
		60		1.7	1.75
		90		2.11	1.39

Tab 5-5 Tank in series values of NEU impregnated products

Carrier	RPM	Pump Rate (g/min)	Flow Rate (kg/h)	ntank	tauDelay
FUJ	150	25	3	1.5	3.21
		60		1.3	2.6
		90		1.1	2.9
	300	25		2.1	2.7
		60		1.5	2.1
		90		1.1	2.6
	150	25	6	1.8	1.45
		60		2.1	1.2
		90		1.51	1.6
	300	25		2.1	1.33
		60		2.6	1.1
		90		1.4	1.9

Tab 5-6 Tank in series values of FUJ impregnated products

Carrier	RPM	Actual Loading*	%RSD
NEU	**150**	**5.01**	**1.89**
	300	**5.59**	**1.11**
FUJ	**150**	**5.15**	**2.28**
	300	**5.4**	**2.51**

Tab 5-7 Actual loading and RSD values of NEU and impregnated products. Other experimental conditions: Feeding rate: 3Kg/h and 25 gm/ml pumping rate.

* gm of IBU in 50 gm carrier

Chapter 6 Conclusions and recommendations

The work presented in this dissertation focused on the impregnation of APIs into porous excipients as a strategy for improving physicochemical properties of the APIs. In this work, two novel loading methods were presented including the use of a Fluidized Bed Dryer and a continuous Glatt-70 Blender as impregnation devices. Depending on several case studies presented in this dissertation, the feasibility of using these two methods to impregnate APIs was confirmed. Also, the benefits of these two methods over other conventional formulations techniques were presented. A set of analytical methods was developed to characterize the impregnated products. It was shown that both fluidized bed impregnation and continuous impregnation can successfully impregnate different APIs into different porous carriers. This chapter sums up all presented aims in the dissertation and proposes some recommendations for future work.

6.1 Conclusions

The first specific aim focused on achieving a successful impregnation of API into a porous carrier using a fluidized bed dryer. The use of this instrument to impregnate API into porous carriers eliminates many unit operations in both drug and dosage form development as shown in Figure 6-1. Application of fluidized bed impregnation in pharmaceutical manufacturing is a promising tool to decrease both downstream and upstream development efforts, which are necessary to adjust the properties of both drugs and dosage forms. In this aim, a complete case of FB impregnation using a highly porous carrier (NEU) and Acetaminophen (APAP) as a model drug was conducted. The methodology for a successful FB impregnation was elaborated in Chapter 2. The resulting products were fully characterized, and the results demonstrated that these products have

properties, that are suitable for manufacturing of solid dosage forms. The results of this study suggested several important claims about impregnating APIs (APAP) into porous carriers (NEU) using a fluidized bed dryer:

- Successful proof of impregnation concept
- The blend uniformity of the impregnated products was high and independent of the drug loading or solvent type.
- The impregnated products preserve the same flow properties and particle size distribution compared to those of the pure carrier (NEU).
- The different evaporation profiles of the solvents do not influence the morphology or loading efficiency of APAP in NEU.
- APAP inside the pores of the carrier is mainly in its amorphous form. APAP is placed inside very fine pores (about 5 nm), which confined its dimensional growth, and prevented its recrystallization. This could improve API dissolution behavior in media where crystalline API presents poor solubility.

The second specific aim figured out the generality and robustness of using the fluidized bed process to impregnate different active pharmaceutical ingredients into different porous carriers. In this study, three different porous carriers were successfully impregnated with Indomethacin using a fluidized bed dryer. The impregnated products were entirely evaluated, and the results confirmed the following observations:

- The FB device is able to impregnate successfully different APIs in different porous carriers, demonstrating that the approach is robust. The resulting products generally showed favorable characteristics for manufacturing of solid dosage forms.

- Capability of the FB impregnation process to show a high blend uniformity. The blend uniformity was independent of drug loading or carrier type. However, NEU and AER impregnated products showed better flow properties than FUJ impregnated products.
- Amorphization of API inside the pores of the porous carriers.
- Improvement of the dissolution rate of all the impregnated products as compared to pure crystals of IMN. However, IMN-NEU and IMN-AER impregnated products presented faster dissolution rate than IMN-FUJ impregnated products.
- The differences in pore size of these porous carriers has an influence on the properties of the impregnated products. NEU and AER have smaller pore size and larger surface area than FUJ.

The third research aim focused on the characterization of continuous impregnation process using the Glatt GCG-70 blender. The study measured the RTDs using a liquid tracer. The important RTD measurements such as mean residence time, curve skewness and mean centered variance were compared. The RTD can be used as an effective tool to understand the impregnation process and enhance process control. Also, the RTD can be considered as an indicator to trace the materials and isolate them when any problem occurs during the process. RTDs were measured for two host materials (FUJ, NEU) using IBU solution as a liquid tracer as a function of process parameters (impeller speed, flow rate). Also, the space time (Mass MRT) from the hold-up was measured for all cases and compared to NIR-MRT. A tank in series model was used to model all the cases and the number of tanks was calculated. The results of this study showed that:

- The MRT decreases with an increase in impeller rotation speed

- For FUJ, increase the feed rate reduces the residence time
- In case of NEU, the NIR-MRTs matched the Mass-MRT for all cases while in the case of FUJ, the NIR-MRTs did not match the Mass-MRT at a 3 kg/h feed rate. However, for a 6 kg/h feed rate the NIR-MRTs were matching the Mass-MRT.
- The results further pointed out that NEU and FUJ showed different RTDs behavior because these materials have different properties such as flow properties, solvent absorption capacity and bulk density. Therefore, these material travel at different speeds inside the GCG-70 blender.
- All tracer curves measured in this study have two major characteristics: a delay time & a long tail
- All tracer curves presented in this study could be modeled by approximately 2 tanks in series

6.2 Recommendations for future work

The work presented in this dissertation discussed two viable methods for loading of APIs into porous carriers, demonstrated suitable experimental conditions to obtain a successful loading, and clarified the advantages of these two methods. Nevertheless, there are several substantial areas for future studies and recommendations to improve these two methods. Recommendations for future work can be discussed in two main directions. The first direction could be improving and developing the batch FB impregnation process. This could include expanding the applicability of using the FB to include different APIs, porous carriers, and solvents. Also, this direction could encompass studying the effect of different process parameters on the impregnation process in more details. The second direction of future work could be further developing the continuous impregnation process. This also

can be done by loading a set of APIs with different properties into different porous carriers. Also, this direction could include developing a continuous impregnation process using other devices such as a continuous fluidized bed dryer. A few examples are elaborated below.

6.2.1 Loading of peptide/protein into porous carrier using FB impregnation

Over the past few decades, many peptides/proteins with therapeutic effects have been explored. Unfortunately, the main obstacle in delivering these medicines are short half-life and stability problems. Huge efforts were considered to formulate these medicines in stable, effective, and acceptable dosage forms. Being porous carriers has many distinctive properties such as high stability and high loading capacity, the use of these carriers to load peptides/proteins could be considered as an effective technique to solve their formulating problems (169,170). Work in Chapter 3 highlighted that different solvents (transport media) can be used in FB impregnation with no major change in the properties of the impregnated products. This flexibility in changing the solvent could allow FB dryers to be used in loading of peptides/proteins without the need to include a strong solvent. In addition, the operating temperature can be easily adjusted to the room temperature using a FB dryer. All these properties could make the use of FB dryer as an ideal device to load peptides/proteins.

6.2.2 Expand FB co-impregnation of two drugs

In Chapter 3, the conclusions of this chapter were based on one carrier and one drug substance and further work should be carried out to investigate the generality of our results. However, additional work must be performed to study the effect of process parameters of the fluid bed operation on the properties of impregnated products. In addition, future work

should investigate the feasibility of impregnation of different active ingredients and different porous carriers. Moreover, a distinctive property of FB was mentioned in Chapter 2, where co-impregnation of Chlorpheinramine (CPM) and Ibuprofen (IBU) resulted in a complete amorphization of these two drugs with highly homogenous products (low %RSD). The co-loading of two drugs into one carrier using FB dryer offer many benefits for drug delivery. Also, this step can improve the properties of the loading drugs. Co-loading of two or more APIs could be done by in FBs. These APIs could be dissolved in one solvent and spray this solution into a porous carrier, or each drug could be dissolved separately in a solvent. Then spray the first drug solution and sequentially followed by the second one. It is of interest to study the effect of different spraying methods on the properties of impregnated products, in specific amorphization of both drugs and blend uniformity. Ensuring complete amorphization of both drugs is necessary to confirm the successful impregnation of these drugs. The loading percent and addition step of API solution could influence on the amorphization of loaded drugs. For example, if a sequential addition method is used to load two drugs into one porous carrier and the load percent of the first sprayed drug was very high, this might result in a saturation of the carrier's pores. In this case, there is no enough pores to load the second drug and this may lead to a failure in impregnation of the second drug. The un-impregnated drug in this case will stay as a crystal powder within the impregnated products or as a sprayed coat layer on the surface of the porous carrier. Accordingly, this failure mode will influence on other properties of impregnated products such as content uniformity, particle size distribution, flow properties, etc.

6.2.3 Continuous impregnation

Our results in Chapter 2 demonstrated the ability of loading the drug continuously into a porous carrier using GCG-70 blender. These results encouraged us to expand this study. Therefore, Chapter 5 included an elaborated study on a continuous impregnation process. At this point, it was very important to study the factors affecting the RTD to test the performance of continuous blender as an impregnation device. In this chapter, one type of solvent was used as a transport medium for API. In future work, different solvents should be used in continuous impregnation to help developing a criterion for selecting the best solvent that fits the industrial requirements of a given process. For examples the use of water as a transport medium instead of organic solvents is more suitable for pharmaceutical manufacturing. Water is safe, available and cheap. However, in this case, it is necessary to study the effects of different properties of water to avoid any failure mode of impregnation. For instance, it is important to check the required liquid/solid ratio to avoid any possible agglomeration of porous carrier as a wet mass. Moreover, it is of interest to check the solubility of the drug in water. Perhaps, it is better to start additional studies with a drug that has a good solubility in water. This drug can be considered as a model drug to test the ability of using water as a transport medium in impregnation. Then, other drugs with different water solubilities can be used.

Moreover, from our results in this dissertation, different factors affecting the RTD still need to be studied. This will result in expanding the applicability of using GCG-70 as an effective impregnating tool. For instance, the effect of different carriers with different properties on RTD are recommended to be studied. Also, it is of interest to mix two carriers with different bulk densities and various absorption capacities. Then, the distribution of

API between the carriers can be studied. This study can address the following question: Does the API distribute equally, or it will be concentrated in one carrier more than the other? Will the distribution be affected by density, porosity, and wetting properties? It is likely that the API will be concentrated more in a carrier with low bulk density and high absorption capacity. During the mixing process, the carrier with low density will be at the surface of the powder bed and close to the walls of the blender more often while porous carrier with high bulk density will be concentrated in the center of the powder bed. Therefore, the low-density carrier will contact API droplet faster and more often than the other carrier and if it has high absorption capacity, it will preferentially absorb the drug. Consequently, the drug will be concentrated in low density carrier with a higher absorption capacity. This idea emerged from some previous work, which applied on wet granulation (3).

6.2.4 Continuous Impregnation using other continuous devices

As mentioned previously, substantial work has shown the importance of the application of continuous processes in pharmaceutical manufacturing. There is a high competition among different companies to develop new manufacturing and analytical equipment for continuous processes. In this section, we hope to shed light on two equipments that could be suitable devices for continuous impregnation: hot melt extruder and continuous fluidized bed.

Hot melt extruder has built-in continuous process ability. In this device, the API can be melted by adjusting the temperature to be a little bit above the melting point of the drug. As it is known that most silica porous carriers have very high melting point. This property will allow them to stay intact at typical HME temperatures and melting only the

drug. Therefore, the melted drug will deeply penetrate the pores of the porous carriers. This step ensures that the drug will be placed in the pores of the porous carriers. The drug will be changed to amorphous and stay in a physical stable form inside the pores. According to this, we expect that some properties of API will be improved such as the dissolution rate.

Our results in Chapter 3 and Chapter 4 and some preliminary data in Chapter 2 were based on batch fluidized bed (Miniglatt). Therefore, it is of interest to expand these results in continuous fluidized impregnation. As we mentioned previously, API successfully impregnated into porous carrier using a Miniglatt. Thus, using a continuous fluidized bed dryer (see Figure 6-2) will combine the advantages of a fluidized bed dryer and with the benefits of a continuous system. Depending on the results presented in this study, some further research can be suggested regarding the use of this device, including:

- Examine the bottom-spray instead of top-spray. This method enhances the spray of API and avoids the effect of high air pressure on the nozzle performance. Moreover, in the continuous process, it is better to start running the device as a batch system for a while, and then switch to the continuous mode. This step will ensure the setup of the correct experimental conditions and enhance the control of these conditions during the process. Therefore, before starting the continuous process, 1-2 kg of a porous carrier will be placed inside the insert of the fluidized bed and run it as a batch. This mass needs high pressure to be fluidized. If top-spray nozzles are used in this experiment, it will be difficult to ensure that the nozzle position is within the fluidization of the porous carrier. This requirement was mentioned in Chapter 2. Immersing the nozzle within the fluidizing bed of the porous carrier reduces the drying time and prevent any spray coating. In impregnation, three important

parameters should be considered, which are drying time, spray time, and impregnation time. Using bottom-spray method makes the control of these parameters easier.

- Using bottom spray allows to include more than one nozzle in continuous fluidized bed. In continuous fluidized bed, it is better to divide the insert into four sections. Three of these sections are for spray and the remaining section is for drying see Figure 6-3. The presence of three nozzles is necessary to ensure the success of the impregnation process. As mentioned in Chapter 2, it is better to pump the API solution at slow rate. This will enhance the drying at relatively low temperature. Also, it ensures enough time for impregnation process. The loading percent of API can be adjusted at high or low level easily with no need to increase the pumping rate or drug concentration in the solution. We just need to use three nozzles for high load and one nozzle for low load with no change in other parameters. Also, the three nozzles can be used for low loading, but at very slow pumping rate and at relatively low temperature for drying. However, for high loading, the three nozzles run on medium to high speed of pumping rate with relatively medium to high drying temperature.

In addition, it is better to use low or medium air flow in continuous fluidized bed. All the materials to be used in continuous impregnation should have low bulk density and good fluidization characteristics, requiring low to medium air flow. Increasing the air flow to the high-level leads to accumulation of the used carrier in the air filter, which results in losing fraction of the porous carrier and reducing the target loading carriers.

6.3 Figures

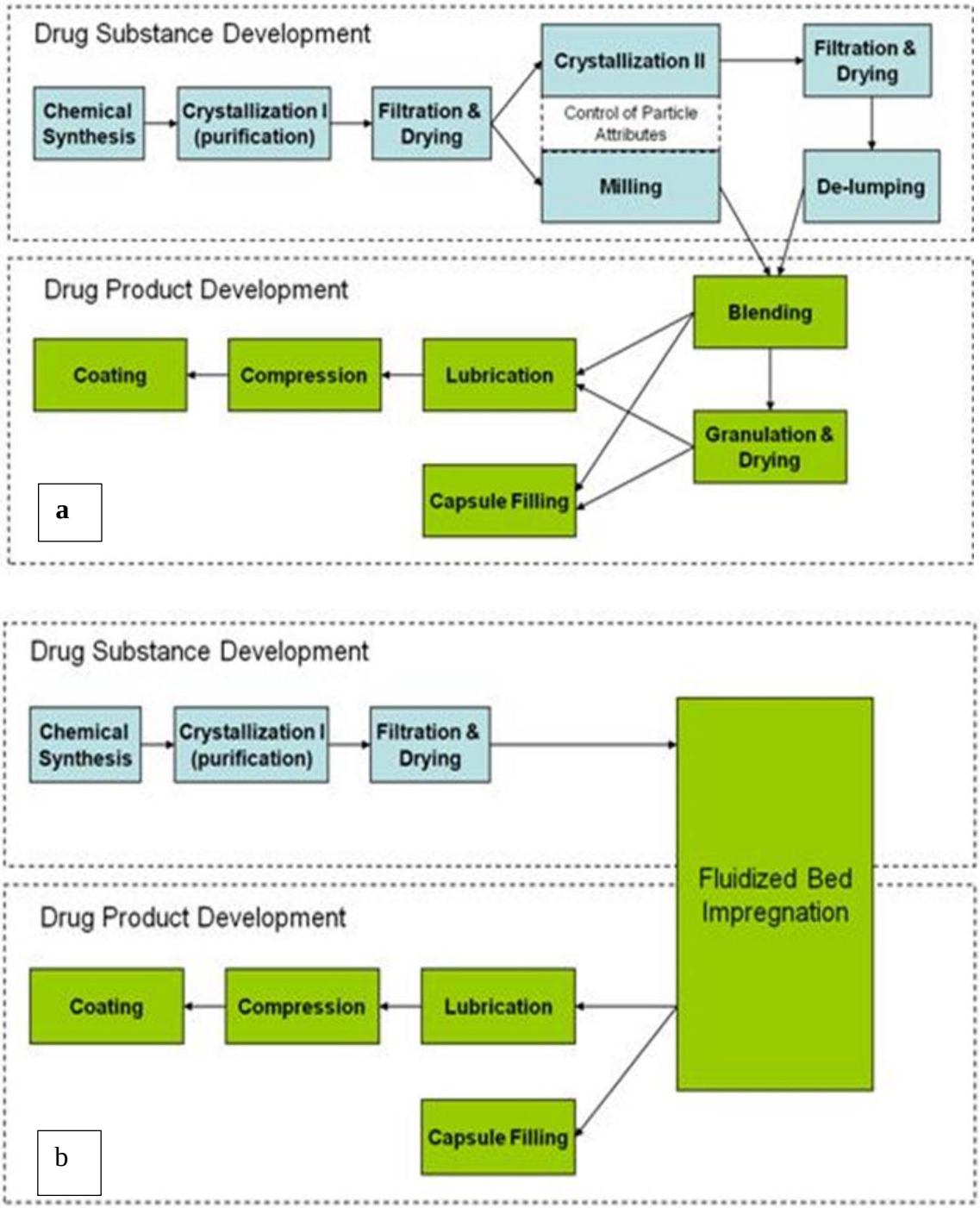

Figure 6-1 Required unit operations to manufacture of solid dosage forms by: a- Conventional Methods & b- Fluidized Bed Impregnation (53)

Figure 6-2 Continuous Fluidized Bed (GCG-2)

Figure 6-3 Insert of Continuous Fluidized Bed (GCG-2) with four sections

Chapter 7 Appendices

Appendix A

7.1A Predictive Models

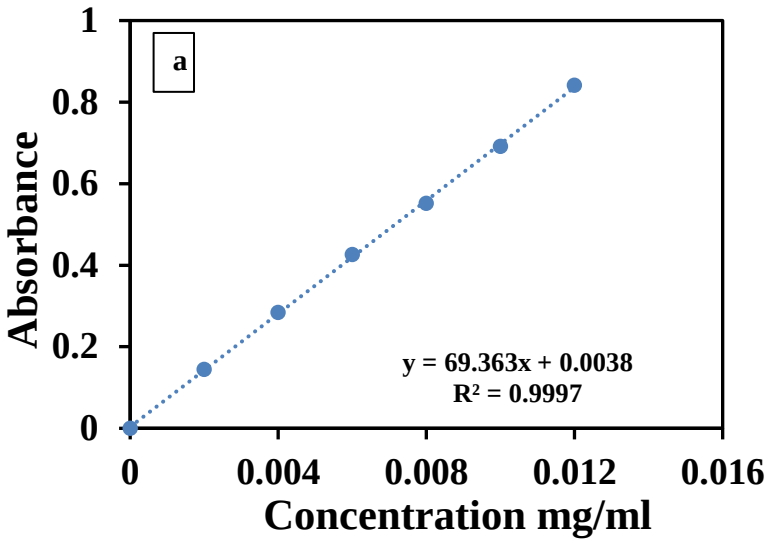

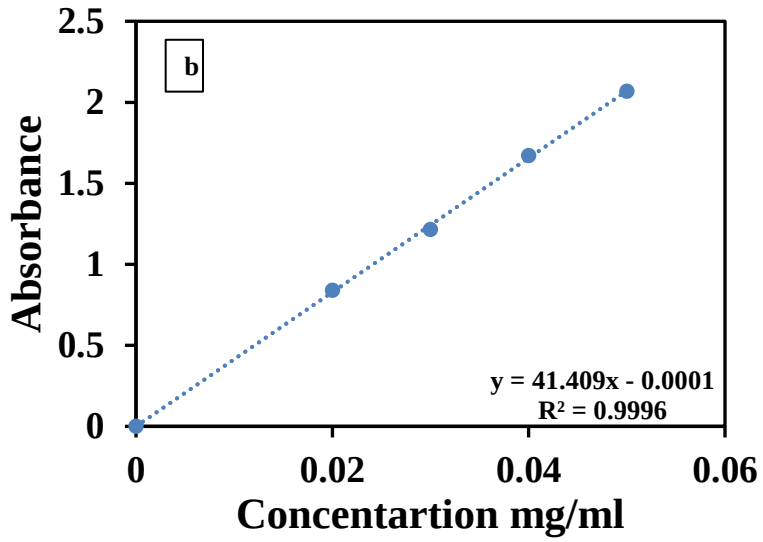

Figure 7-1A UV prediction models: a- Griseofulvin in Sodium Lauryl Sulphate (SLS)+ DI water; b-Ibuprofen in DI water+2% (SLS)

7.2A RTD study

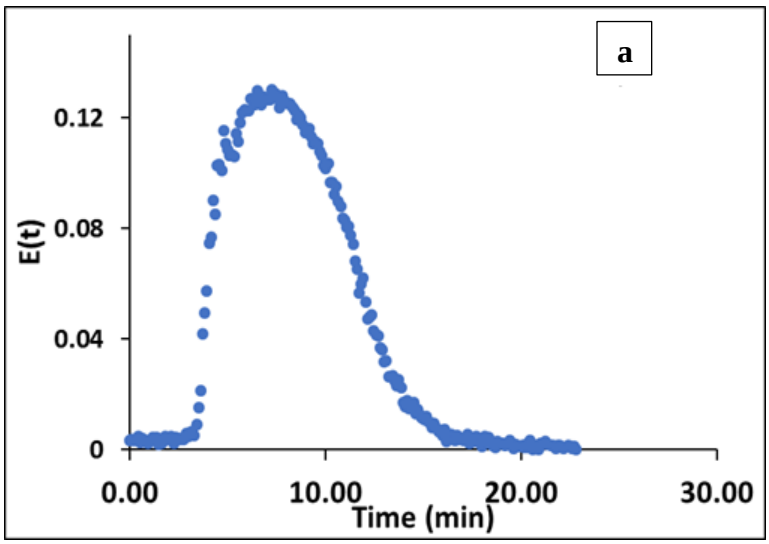

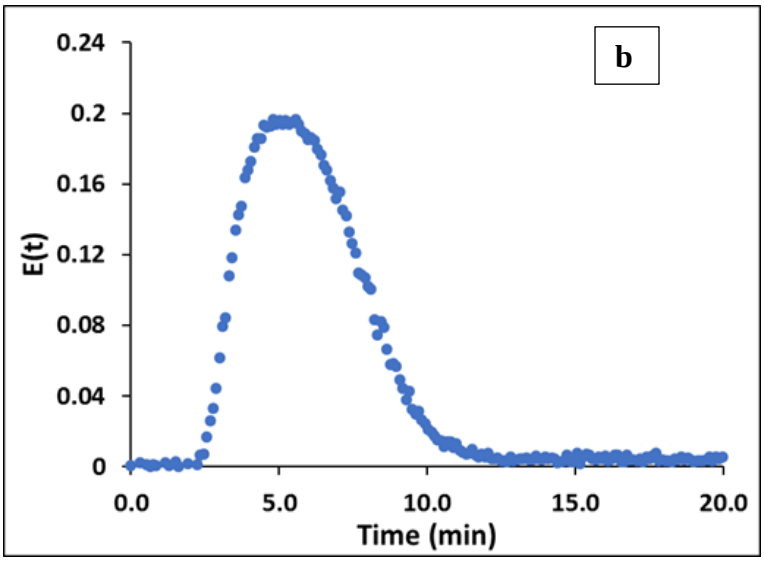

Figure 7-2A RTD study using Compap as a dry tracer (a) 100 rpm (b) 300 rpm. Other parameters: Flow rate — 3kg/h, NEU as a carrier, and Rotating Shaft: Granulating Shaft

Amount of tracer (gram)	RPM	MRT min	n
120	**100**	**8.37**	**4.562**
120	**300**	**6.35**	**4.425**

Tab 7-1A MRT, n-tank in series study using Compap as a dry tracer (a) 100 rpm (b) 300 rpm. Other parameters: Flow rate — 3kg/h, NEU as a carrier, and Rotating Shaft: Granulation Shaft

Appendix B

7.1B Prediction Models

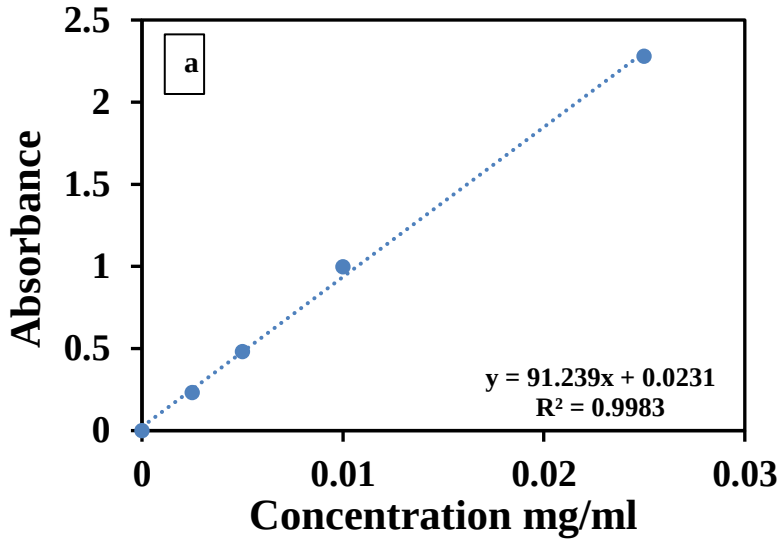

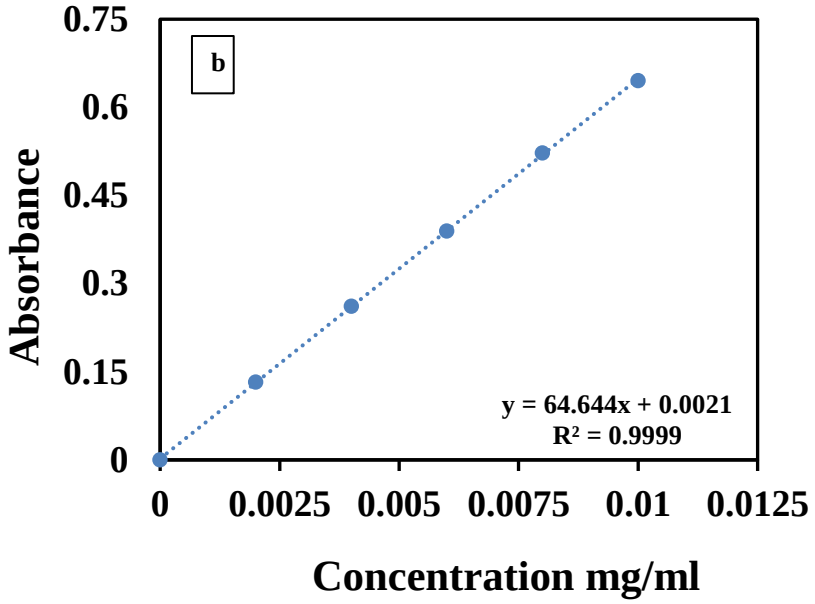

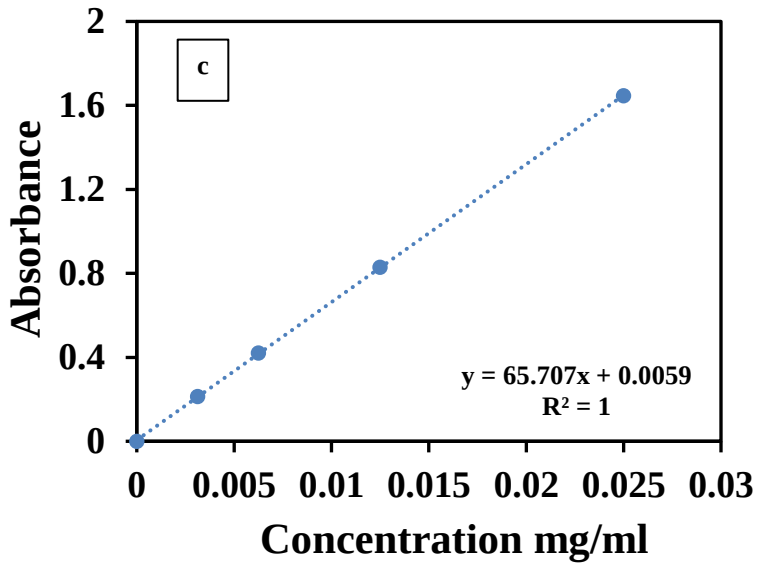

Figure 7-3B UV prediction models: a- APAP in Methanol; b-APAP in DI water; c-APAP in 0.1 N HCl

Appendix C

7.1C Prediction Models

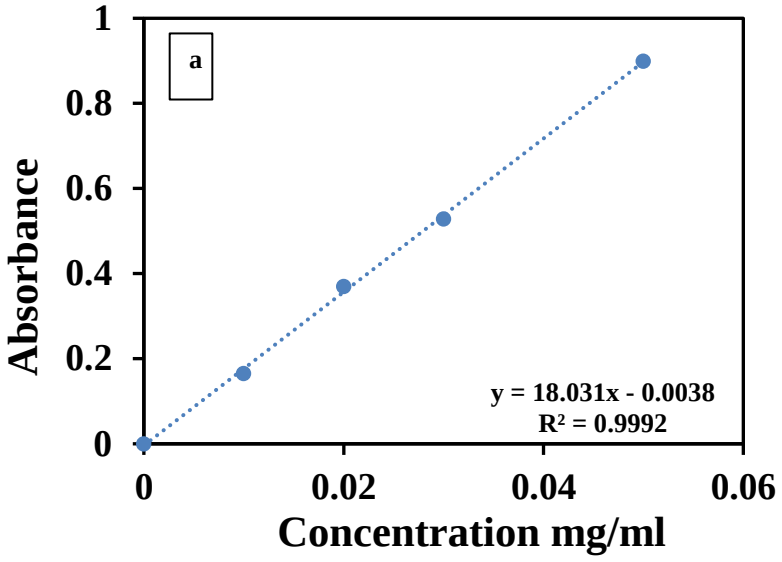

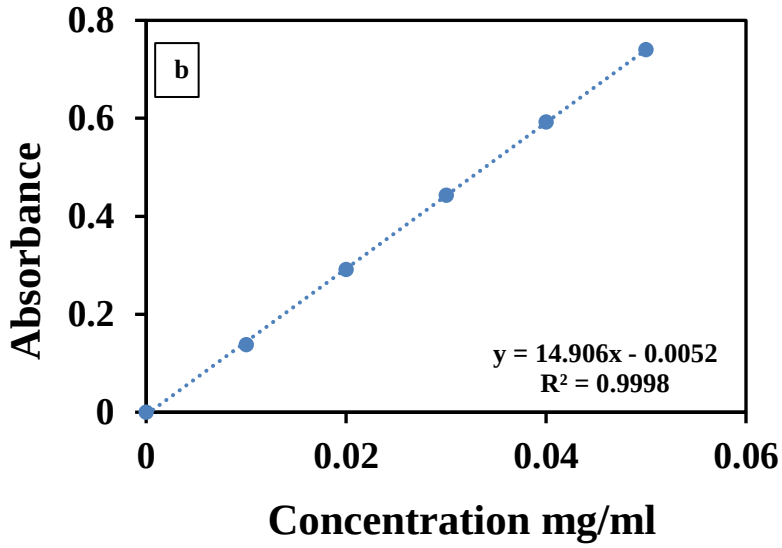

Figure 7-4C UV prediction models: a- Indomethacin in Methanol, b- Indomethacin in Phosphate Buffer pH 7.2

Appendix D

7.1D Bulk Density

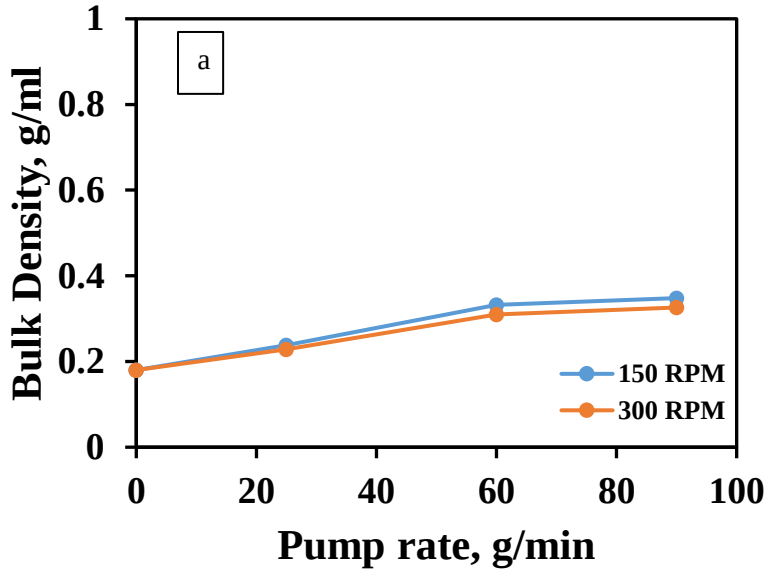

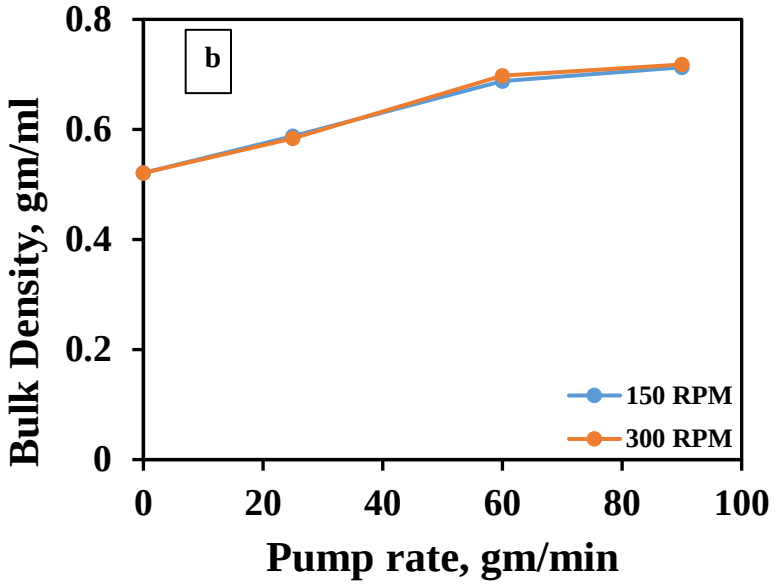

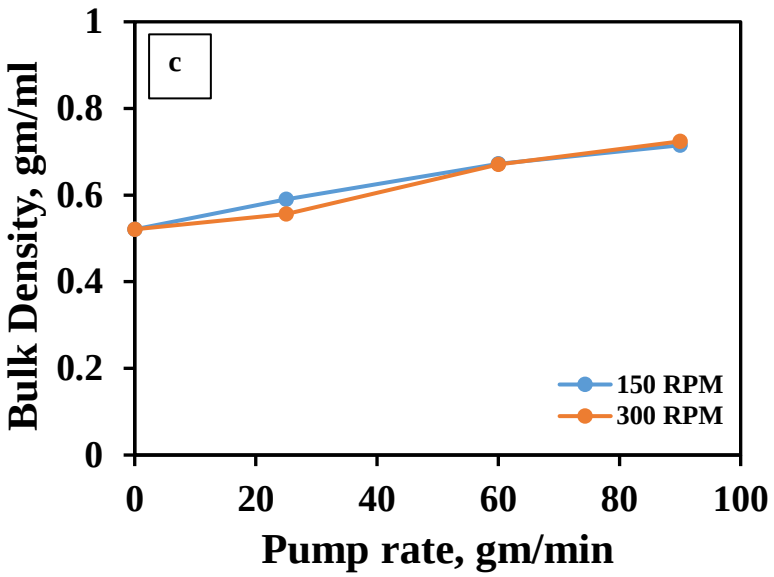

Figure 7-5C Effect of pumping rate on the bulk density of the impregnated product (a) Using NEU as a carrier at 3kg/h flow rate (b) Using FUJ as a carrier at 3kg/h flow rate (c) Using FUJ as a carrier at 6kg/h flow rate

References

1. Nickerson B. Sample Preparation of Pharmaceutical Dosage Forms: Challenges and Strategies for Sample Preparation and Extraction. Am Assoc Pharm Sci. 2011;145.
2. Oka S, Sahay A, Meng W, Muzzio F. Diminished segregation in continuous powder mixing. Powder Technol [Internet]. 2017;309:79–88. Available from: http://dx.doi.org/10.1016/j.powtec.2016.11.038
3. Oka S, Smrčka D, Kataria A, Emady H, Muzzio F, Štěpánek F, et al. Analysis of the origins of content non-uniformity in high-shear wet granulation. Int J Pharm. 2017;528(1–2):578–85.
4. Zheng J. Formulation and Analytical Development for Low-Dose Oral Drug ProductsTitle. Hoboken: John Wiley & Sons, Inc.; 2009.
5. Moës LHC& AJ. Effect of Drug Agglomerates Upon the Kinetics of Mixing of Low Dosage Cohesive Powder Mixtures. Drug Dev Ind Pharm. 1989;15(12):1911–31.
6. Prescott, J. K. Garcia TP. A solid dosage and blend content uniformity troubleshooting diagram. Pharm Technol. 2001;25(3):68–88.
7. Sahay N, Ierapetritou M. Nihar SCM. IFAC Proc Vol. 2009;7(PART 1):405–10.
8. Huang CY, Sherry Ku M. Prediction of drug particle size and content uniformity in low-dose solid dosage forms. Int J Pharm. 2010;383(1–2):70–80.
9. Saffari M, Ebrahimi A, Langrish T. A novel formulation for solubility and content uniformity enhancement of poorly water-soluble drugs using highly-porous mannitol. Eur J Pharm Sci [Internet]. 2016;83:52–61. Available from:

http://dx.doi.org/10.1016/j.ejps.2015.12.016

10. FDA. Guidance for Industry: Powder Blends and Finished Dosage Units - Stratified In-Process Dosage Unit Sampling and Assessment. 2003;
11. Amidon, Gordon L.; Lennernäs, Hans; Shah, Vinod P.; Crison JR. A Theoretical Basis for a Biopharmaceutic Drug Classification: The Correlation of in Vitro Drug Product Dissolution and in Vivo Bioavailability. Pharm Res. 1995;12(3):413–20.
12. Rodriguez Aller MR, Guillarme D, Veuthey J-L, Gurny R. Strategies for formulating and delivering poorly water-soluble drugs. J Drug Deliv Sci Technol. 2015;30:342–51.
13. Li Di, Edward H. Kerns GTC. Drug-Like Property Concepts in Pharmaceutical Design. Curr Pharm Des. 2009;15(19):2184–94.
14. Takagi T, Ramachandran C, Bermejo M, Yamashita S, Yu LX, Amidon GL. A provisional biopharmaceutical classification of the top 200 oral drug products in the United States, Great Britain, Spain, and Japan. Mol Pharm. 2006;3(6):631–43.
15. Mallick S, Pattnaik S, Swain K, De PK. Formation of physically stable amorphous phase of ibuprofen by solid state milling with kaolin. 2008;68:346–51.
16. Michiel VanSpeybroeck, ValéryBarillaro, Thao DoThi, RandyMellaerts, JohanMartens, Jan VanHumbeeck, JanVermant, PieterAnnaert , Guy VanDen Mooter PA. Ordered Mesoporous Silica Material SBA-15: A Broad-Spectrum Formulation Platform for Poorly Soluble Drugs. J Pharm Sci. 2009;98(8):2648–58.
17. Bahl D, Hudak J, Bogner RH. Comparison of the ability of various pharmaceutical silicates to amorphize and enhance dissolution of indomethacin upon co-grinding. Pharm Dev Technol. 2008;13(3):255–69.

18. Mellaerts R, Mols R, Jammaer JAG, Aerts CA, Annaert P, Van Humbeeck J, et al. Increasing the oral bioavailability of the poorly water soluble drug itraconazole with ordered mesoporous silica. Eur J Pharm Biopharm. 2008;69(1):223–30.

19. Meer T, Fule R, Khanna D, Amin P. Solubility modulation of bicalutamide using porous silica. J Pharm Investig. 2013;43(4):279–85.

20. Maniruzzaman M, Ross SA, Islam MT, Scoutaris N, Nair A, Douroumis D. Increased dissolution rates of tranilast solid dispersions extruded with inorganic excipients. Drug Dev Ind Pharm. 2017;43(6):947–57.

21. Pardhi V, Chavan RB, Thipparaboina R, Thatikonda S, Naidu VGM, Shastri NR. Preparation, characterization, and cytotoxicity studies of niclosamide loaded mesoporous drug delivery systems. Int J Pharm [Internet]. 2017;528(1–2):202–14. Available from: http://dx.doi.org/10.1016/j.ijpharm.2017.06.007

22. Pawar JN, Desai HR, Moravkar KK, Khanna DK, Amin PD. Exploring the potential of porous silicas as a carrier system for dissolution rate enhancement of artemether. Asian J Pharm Sci [Internet]. 2016;11(6):760–70. Available from: http://dx.doi.org/10.1016/j.ajps.2016.06.002

23. El-Badry M, Fathy M. Enhancement of the dissolution and permeation rates of meloxicam by formation of its freeze-dried solid dispersions in polyvinylpyrrolidone K-30. Drug Dev Ind Pharm. 2006;32(2):141–50.

24. Chen H, Augustijns P, Humbeeck J Van, Martens JA, Mellaerts R, Jammaer JAG, et al. Physical State of Poorly Water Soluble Therapeutic Molecules Loaded into SBA-15 Ordered Mesoporous Silica Carriers: A Case Study with Itraconazole and Ibuprofen. Langmuir. 2008;24(16):8651–9.

25. Qu F, Zhu G, Huang S, Li S, Sun J, Zhang D, et al. Controlled release of Captopril by regulating the pore size and morphology of ordered mesoporous silica. Microporous Mesoporous Mater. 2006;92(1–3):1–9.

26. Verraedt E, Pendela M, Adams E, Hoogmartens J, Martens JA. Controlled release of chlorhexidine from amorphous microporous silica. J Control Release [Internet]. 2010;142(1):47–52. Available from: http://dx.doi.org/10.1016/j.jconrel.2009.09.022

27. Bahl D, Bogner RH. Amorphization of Indomethacin by Co-Grinding with Neusilin US2 : Amorphization Kinetics , Physical Stability and Mechanism. 2006;23(10).

28. Laitinen R, Löbmann K, Strachan CJ, Grohganz H, Rades T. Emerging trends in the stabilization of amorphous drugs. Int J Pharm [Internet]. 2013;453(1):65–79. Available from: http://dx.doi.org/10.1016/j.ijpharm.2012.04.066

29. Krupa A, Majda D, Jachowicz R, Mozgawa W. Thermochimica Acta Solid-state interaction of ibuprofen and Neusilin US2. Thermochim Acta [Internet]. 2010;509(1–2):12–7. Available from: http://dx.doi.org/10.1016/j.tca.2010.05.009

30. Wei Q, Keck CM, Müller RH. European Journal of Pharmaceutics and Biopharmaceutics Preparation and tableting of long-term stable amorphous rutin using porous silica. Eur J Pharm Biopharm [Internet]. 2017;113:97–107. Available from: http://dx.doi.org/10.1016/j.ejpb.2016.11.009

31. Li X, Peng H, Tian B, Gou J, Yao Q, Tao X, et al. Preparation and characterization of azithromycin – Aerosil 200 solid dispersions with enhanced physical stability. Int J Pharm [Internet]. 2015;486(1–2):175–84. Available from:

http://dx.doi.org/10.1016/j.ijpharm.2015.03.029

32. Gupta MK, Goldman D, Bogner RH, Tseng Y, Gupta MK, Goldman D, et al. Enhanced Drug Dissolution and Bulk Properties of Solid Dispersions Granulated with a Surface Adsorbent Enhanced Drug Dissolution and Bulk Properties of Solid Dispersions Granulated with a Surface Adsorbent. 2002;7450.

33. Shah A, Serajuddin ATM. Conversion of solid dispersion prepared by acid – base interaction into free- fl owing and tabletable powder by using Neusilin 1 US2. Int J Pharm [Internet]. 2015;484(1–2):172–80. Available from: http://dx.doi.org/10.1016/j.ijpharm.2015.02.060

34. Gumaste SG, Dalrymple DM, Serajuddin ATM. Development of Solid SEDDS , V : Compaction and Drug Release Properties of Tablets Prepared by Adsorbing Lipid-Based Formulations into Neusilin ® US2. 2013;3186–99.

35. Schlack H, Schubert R, Becker D, Schlack H, Schubert R. Properties of Fujicalin ® , a New Modified Anhydrous Dibasic Calcium Phosphate for Direct Compression : Comparison with Dicalcium Phosphate Dihydrate Properties of Fujicalin Õ , a New Modified Anhydrous Dibasic Calcium Phosphate for Direct Compression : C. 2001;9045.

36. Tourne C, Nicole L, Lerner DA, Devoisselle JM, Charnay C, Be S. Inclusion of ibuprofen in mesoporous templated silica : drug loading and release property. 2004;57:533–40.

37. Barillaro RY, Thi TDO, Mellaerts R, Martens J, Speybroeck MVAN, Humbeeck JANVAN, et al. Ordered Mesoporous Silica Material SBA-15 : A Broad-Spectrum Formulation Platform for Poorly Soluble Drugs. 2009;98(8):2648–58.

38. Kinnari P, Mäkilä E, Heikkilä T, Salonen J, Hirvonen J, Santos HA. Comparison of mesoporous silicon and non-ordered mesoporous silica materials as drug carriers for itraconazole. 2011;414:148–56.

39. Hentzschel CM, Alnaief M, Smirnova I, Sakmann A, Leopold CS, Alnaief M, et al. Tableting properties of silica aerogel and other silicates Tableting properties of silica aerogel and other silicates. 2012;9045.

40. Llusa M, Levin M, Snee RD, Muzzio FJ. Measuring the hydrophobicity of lubricated blends of pharmaceutical excipients. Powder Technol [Internet]. 2010;198(1):101–7. Available from: http://dx.doi.org/10.1016/j.powtec.2009.10.021

41. Knapik J, Wojnarowska Z, Grzybowska K, Hawelek L, Sawicki W, Wlodarski K, et al. Physical Stability of the Amorphous Anticholesterol Agent (Ezetimibe): The Role of Molecular Mobility. 2014;

42. Wojnarowska Z, Grzybowska K, Dulski M, Knapik J, Jurkiewicz K, Smolka W, et al. Toward a Better Understanding of the Physical Stability of Amorphous Anti-In fl ammatory Agents: The Roles of Molecular Mobility and Molecular Interaction Patterns. 2015;(August).

43. Mcnamara D, Yin S, Pan D, Crull G, Timmins P, Vig B. Characterization of Phase Separation Propensity for Amorphous Spray Dried Dispersions. 2017;

44. Patel S, Kou X, Hou HH, Huang YB, Strong JC, Zhang GGZ, et al. Mechanical Properties and Tableting Behavior of Amorphous Solid Dispersions. J Pharm Sci [Internet]. 2017;106(1):217–23. Available from: http://dx.doi.org/10.1016/j.xphs.2016.08.021

45. Barthe L, Desportes S, Steinmetz D, Hemati M. Chemical Engineering Research and Design Metallic salt deposition on porous particles by dry impregnation in fluidized bed : Effect of drying conditions on metallic nanoparticles distribution. 2008;7(February):915–22.

46. Desportes S, Steinmetz D, He M. Production of supported asymmetric catalysts in a fluidised bed. 2005;157:12–9.

47. Chevalier E, Viana M, Cazalbou S, Makein L, Dubois J, Chulia D. Acta Biomaterialia Ibuprofen-loaded calcium phosphate granules : Combination of innovative characterization methods to relate mechanical strength to drug location. Acta Biomater [Internet]. 2010;6(1):266–74. Available from: http://dx.doi.org/10.1016/j.actbio.2009.07.040

48. Mellaerts R, Jammaer JAG, Speybroeck M Van, Chen H, Humbeeck J Van, Augustijns P, et al. Physical State of Poorly Water Soluble Therapeutic Molecules Loaded into SBA-15 Ordered Mesoporous Silica Carriers : A Case Study with Itraconazole and Ibuprofen. 2008;(11):8651–9.

49. Maclean J, Medina C, Daurio D, Alvarez-nunez F, Jona J, Munson E, et al. Manufacture and Performance Evaluation of a Stable Amorphous Complex of an Acidic Drug Molecule and Neusilin. 2011;100(8):3332–44.

50. Grobelny P, Kazakevich I, Zhang D, Bogner R. Amorphization of itraconazole by inorganic pharmaceutical excipients : comparison of excipients and processing methods Amorphization of itraconazole by inorganic pharmaceutical excipients : comparison of excipients and processing methods. 2015;7450.

51. Maniruzzaman M, Nair A, Scoutaris N, Bradley MSA, Snowden MJ, Douroumis

D. One-step continuous extrusion process for the manufacturing of solid dispersions. Int J Pharm [Internet]. 2015;496(1):42–51. Available from: http://dx.doi.org/10.1016/j.ijpharm.2015.09.048

52. Bouledjouidja A, Masmoudi Y, Van Speybroeck M, Schueller L, Badens E. Impregnation of Fenofibrate on mesoporous silica using supercritical carbon dioxide. Int J Pharm [Internet]. 2016;499(1–2):1–9. Available from: http://dx.doi.org/10.1016/j.ijpharm.2015.12.049

53. Plamen I. Grigorov, Benjamin J. Glasser and FJM. Formulation and Manufacture of Pharmaceuticals by Fluidized-Bed Impregnation of Active Pharmaceutical Ingredients into Porous Carriers. AIChE J. 2013;59(12):4538–52.

54. Engisch W, Muzzio F. Using Residence Time Distributions (RTDs) to Address the Traceability of Raw Materials in Continuous Pharmaceutical Manufacturing. 2016;64–81.

55. Abboud L and SHSR of TWSJ. New Prescription For Drug Makers: Update the Plants. Wall St J. 2003;

56. Vanarase AU, Muzzio FJ. Effect of operating conditions and design parameters in a continuous powder mixer. Powder Technol [Internet]. 2011;208(1):26–36. Available from: http://dx.doi.org/10.1016/j.powtec.2010.11.038

57. Poechlauer P, Manley J, Broxterman R, Ridemark M. Continuous Processing in the Manufacture of Active Pharmaceutical Ingredients and Finished Dosage Forms: An Industry Perspective. 2012;

58. Ingredients T, Stages TM. Changing the Mind Set. 2005;(June):730–8.

59. Leuenberger H. New trends in the production of pharmaceutical granules : batch

versus continuous processing. 2001;52:289–96.

60. Betz G, Junker-bürgin P, Leuenberger H, Leuenberger H, Betz G, Junker-bu P. Batch And Continuous Processing In The Production Of Pharmaceutical Granules. 2003;7450.

61. M. W. Continuous processing in secondary production. Chem Eng Pharm Ind RD Manuf. 2011;837–851.

62. Ramachandran R, Arjunan J. Model-Based Control-Loop Performance of a Continuous Direct Compaction Process. 2011;249–63.

63. Boukouvala F, Niotis V, Ramachandran R, Muzzio FJ, Ierapetritou MG. An integrated approach for dynamic flowsheet modeling and sensitivity analysis of a continuous tablet manufacturing process. Comput Chem Eng [Internet]. 2012;42:30–47. Available from: http://dx.doi.org/10.1016/j.compchemeng.2012.02.015

64. S. C. Perspective on Continuous Manufacturing. Present IFPAC Annu Meet Balt MD,. 2012;

65. Yu LX, Kopcha M. The future of pharmaceutical quality and the path to get there. Int J Pharm [Internet]. 2017;528(1–2):354–9. Available from: http://dx.doi.org/10.1016/j.ijpharm.2017.06.039

66. Lee SL, Connor TFO, Yang X, Cruz CN, Yu LX, Woodcock J. Modernizing Pharmaceutical Manufacturing : from Batch to Continuous Production. 2015;191–9.

67. Allison G, Cain YTAN, Cooney C, Garcia TOM, Bizjak TG, Holte O, et al. Regulatory and Quality Considerations for Continuous Manufacturing May 20 –

21 , 2014 Continuous Manufacturing Symposium. J Pharm Sci [Internet]. 2015;104(3):803–12. Available from: http://dx.doi.org/10.1002/jps.24324

68. T. O'Connor, S. Lee, in: Y. Chen, G.G.Z. Zhang, L. Yu RVM. Chapter37 - Emerging Technology for Modernizing Pharmaceutical Production: Continuous Manufacturing A2 - Qiu, Yihong. Developing Solid Oral Dosage Forms,. 2nd ed. Boston: Academic Press; 2017. 1031–1046 p.

69. Escotet-espinoza MS, Moghtadernejad S, Oka S, Wang Y, Roman-ospino A, Schäfer E, et al. Effect of tracer material properties on the residence time distribution (RTD) of continuous powder blending operations . Part I of II : Experimental evaluation. Powder Technol [Internet]. 2019;342:744–63. Available from: https://doi.org/10.1016/j.powtec.2018.10.040

70. Fisher AC, Lee SL, Harris DP, Buhse L, Kozlowski S, Yu L, et al. Advancing pharmaceutical quality : An overview of science and research in the U . S . FDA ' s Of fi ce of Pharmaceutical Quality. Int J Pharm [Internet]. 2016;515(1–2):390–402. Available from: http://dx.doi.org/10.1016/j.ijpharm.2016.10.038

71. Gors A. Part I : Single-Purpose Equipment.

72. Meng W, Oka S, Liu X, Omer T, Ramachandran R. Effects of Process and Design Parameters on Granule Size Distribution in a Continuous High Shear Granulation Process. 2017;283–95.

73. Meng W, Kotamarthy L, Panikar S, Sen M, Pradhan S, Marc M, et al. Statistical analysis and comparison of a continuous high shear granulator with a twin screw granulator : Effect of process parameters on critical granule attributes and granulation mechanisms. Int J Pharm [Internet]. 2016;513(1–2):357–75. Available

from: http://dx.doi.org/10.1016/j.ijpharm.2016.09.041

74. Järvinen MA, Paavola M, Poutiainen S, Itkonen P, Pasanen V, Uljas K, et al. Comparison of a continuous ring layer wet granulation process with batch high shear and fl uidized bed granulation processes. Powder Technol [Internet]. 2015;275:113–20. Available from: http://dx.doi.org/10.1016/j.powtec.2015.01.071

75. PAT G for I. A Framework for Innovative Pharmaceutical Development. Manuf Qual Assur FDA. 2004;

76. Q8(R2) G for I. Pharmaceutical Development. FDA. 2009;

77. Llusa M, Mohr S, Baumgartner R, Paudel A, Koscher G, Khinast J. Continuous low-dose feeding of highly active pharmaceutical ingredients in hot-melt extrusion. Drug Dev Ind Pharm. 2016;42(8):1360–4.

78. RV Tiwari, H Patil MR. Contribution of hot-melt extrusion technology to advance drug delivery in the 21st century. Expert Opin Drug Deliv. 2016;13(3):451–64.

79. P. V. DANCKWERTS. Continuous flow systems Distribution of Residence Times. Chem Eng Sci. 1953;2(8).

80. Muzzio F. Mixing mechanics. 2017;3373(September):55120.

81. Gao Y, Vanarase A, Muzzio F, Ierapetritou M. Characterizing continuous powder mixing using residence time distribution. Chem Eng Sci [Internet]. 2011;66(3):417–25. Available from: http://dx.doi.org/10.1016/j.ces.2010.10.045

82. Fernando J.Muzzio and Sarang Oka. Mixing Mechanics: Using residence time distribution to understand contiuous blending. Powder Bulk Eng. 2017;16–21.

83. Augsburger LL and SWH. Pharmaceutical Dosage Forms: Tablets.Vol.1,2,3. New York: Informa Healthcare USA; 2008.

84. Gibson M. Pharmaceutical preformulation and formulation: a practical guide from candidate drug selection to commercial dosage form. New York: Informa Healthcare USA; 2009.

85. Rengarajan GT, Enke D, Steinhart M, Beiner M. Stabilization of the amorphous state of pharmaceuticals in nanopores. J Mater Chem. 2008;18(22):2537–9.

86. Geldart D. Types of Fluidization. Powder Technol [Internet]. 1973;7(5):285–92. Available from: http://dns2.asia.edu.tw/~ysho/YSHO-English/1000 CE/PDF/Pow Tec7, 285.pdf

87. Brunauer S, Emmett PH, Teller E. Adsorption of Gases in Multimolecular Layers. J Am Chem Soc. 1938;60(2):309–19.

88. Carson JW, Wilms H. Development of an international standard for shear testing. Powder Technol. 2006;167(1):1–9.

89. Freeman R. Measuring the flow properties of consolidated, conditioned and aerated powders - A comparative study using a powder rheometer and a rotational shear cell. Powder Technol. 2007;174(1–2):25–33.

90. Pharmacopea US. 711 DISSOLUTION. In.

91. K.H. Esbensen PP-M. Process sampling: theory of sampling – the missing link in process analytical technologies (PAT), Process Analytical Technology. John Wiley & Sons, Ltd; 2010. 37–80 p.

92. Sekulic SS, Ward HW, Brannegan DR, Stanley ED, Evans CL, Sciavolino ST, et al. On-line monitoring of powder blend homogeneity by near-infrared spectroscopy. Anal Chem. 1996;68(3):509–13.

93. Shi Z, Cogdill RP, Short SM, Anderson CA. Process characterization of powder

blending by near-infrared spectroscopy: Blend end-points and beyond. J Pharm Biomed Anal. 2008;47(4–5):738–45.

94. Popo M, Romero-Torres S, Conde C, Romañach RJ. Blend uniformity analysis using stream sampling and near infrared spectroscopy. AAPS PharmSciTech. 2002;3(3):1–11.

95. Rantanen J, Wikström H, Turner R, Taylor LS. Use of in-line near-infrared spectroscopy in combination with chemometrics for improved understanding of pharmaceutical processes. Anal Chem. 2005;77(2):556–63.

96. Song SW, Hidajat K, Kawi S. Functionalized SBA-15 materials as carriers for controlled drug delivery: Influence of surface properties on matrix-drug interactions. Langmuir. 2005;21(21):9568–75.

97. Mura P, Valleri M, Cirri M, Mennini N. New solid self-microemulsifying systems to enhance dissolution rate of poorly water soluble drugs. Pharm Dev Technol. 2012;17(3):277–84.

98. Kutza C, Metz H, Kutza J, Syrowatka F, Mäder K. Toward a detailed characterization of oil adsorbates as “solid liquids.” Eur J Pharm Biopharm. 2013;84(1):172–82.

99. Gupta MK, Vanwert A, Bogner RH. Formation of physically stable amorphous drugs by milling with neusilin. J Pharm Sci. 2003;92(3):536–51.

100. Plamen I. Grigorov, Benjamin J. Glasser and FJM. Improving Dissolution Kinetics of Pharmaceuticals by Fluidized Bed Impregnation of Active Pharmaceutical Ingredients. AIChE J. 2016;62(12):4201–14.

101. Wong WS, Lee CS, Er HM, Lim WH. Preparation and Evaluation of Palm Oil-

Based Polyesteramide Solid Dispersion for Obtaining Improved and Targeted Dissolution of Mefenamic Acid. J Pharm Innov. 2017;12(1):76–89.

102. Lemsi M, Galai H, Louhaichi MR, Fessi H, Kalfat R. Amorphization of Atorvastatin Calcium by Mechanical Process: Characterization and Stabilization Within Polymeric Matrix. J Pharm Innov. 2017;12(3):216–25.

103. Ambrogi V, Latterini L, Marmottini F, Tiralti MC, Ricci M. Oxybenzone entrapped in mesoporous silicate MCM-41. J Pharm Innov. 2013;8(4):212–7.

104. KEN K. QIAN RHB. Application of Mesoporous Silicon Dioxide and Silicate in Oral Amorphous Drug Delivery Systems. J Pharm Sci. 2012;101(2).

105. Allgeier MC, Piper JL, Hinds J, Yates MH, Kolodsick KJ, Meury R, et al. Isolation and Physical Property Optimization of an Amorphous Drug Substance Utilizing a High Surface Area Magnesium Aluminometasilicate (Neusilin ® US2). J Pharm Sci [Internet]. 2016;105(10):3105–14. Available from: http://dx.doi.org/10.1016/j.xphs.2016.06.019

106. Kinoshita M, Baba K, Nagayasu A, Yamabe K, Shimooka T, Takeichi Y, et al. Improvement of solubility and oral bioavailability of a poorly water-soluble drug, TAS-301, by its melt-adsorption on a porous calcium silicate. J Pharm Sci. 2002;91(2):362–70.

107. Konno T, K.K. KK. Physical and chemical changes of medicinals in mixtures with adsorbents in the solid state. I. Effect of vapor pressure of the medicinals on changes in crystalline properties. Chem Pharm Bull. 1985;34(1):301– 307.

108. Qian KK, Wurster DE, Bogner RH. Spontaneous crystalline-to-Amorphous phase transformation of organic or medicinal compounds in the presence of porous

media, part 3: Effect of moisture. Pharm Res. 2012;29(10):2698–709.

109. SHOU-CANG SHEN, WAI KIONG NG, LEONARD CHIA, YUAN-CAI DONG, REGINALD B.H. TAN. Stabilized Amorphous State of Ibuprofen by Co-Spray Drying With Mesoporous SBA-15 to Enhance Dissolution Properties. J Pharm Sci. 2010;99(4):1997–2007.

110. Dhall M, Nanda S, Madan AK. Studies on flash evaporation for preparation of porous solid dispersions using piroxicam as a model drug. J Pharm Innov. 2011;6(4):232–40.

111. Speybroeck M Van, Barillaro V, Thi T Do, Mellaerts R, Martens J, Humbeeck J Van, et al. Ordered Mesoporous Silica Material SBA-15: A Broad-Spectrum Formulation Platform for Poorly Soluble Drugs. J Pharm Sci [Internet]. 2009 Aug 1 [cited 2019 May 13];98(8):2648–58. Available from: https://www.sciencedirect.com/science/article/pii/S0022354916330283?via%3Dihub

112. Gao Y, Ierapetritou MG, Muzzio FJ. Determination of the confidence interval of the relative standard deviation using convolution. J Pharm Innov. 2013;8(2):72–82.

113. K.S.W. GSJ a. S. Adsorption, Surface Area and Porosity. AP; 1982.

114. Dollish FR, Fateley WG BF. Characteristic Raman Frequencies of Organic Compounds. Appendix O. NY,USA: Wiley: New York, NY, USA; 1974.

115. Hernández B, Pflüger F, Kruglik SG, Ghomi M. Characteristic Raman lines of phenylalanine analyzed by a multiconformational approach. J Raman Spectrosc. 2013;44(6):827–33.

116. Diniz JEM, Borges RS, Alves CN. A DFT study for paracetamol and 3,5-

disubstituted analogues. J Mol Struct THEOCHEM. 2004;673(1–3):93–7.

117. Mellaerts R, Aerts CA, Humbeeck J Van, Augustijns P, Den Mooter G Van, Martens JA. Enhanced release of itraconazole from ordered mesoporous SBA-15 silica materials. Chem Commun. 2007;d(13):1375–7.

118. Shaw LR, Irwin WJ, Grattan TJ, Conway BR. The effect of selected water-soluble excipients on the dissolution of paracetamol and ibuprofen. Drug Dev Ind Pharm. 2005;31(6):515–25.

119. Bahl D, Bogner RH. Amorphization Alone Does Not Account for the Enhancement of Solubility of Drug Co-ground with Silicate: The Case of Indomethacin. AAPS PharmSciTech. 2008;9(1):146–53.

120. Christian Leuner JD. Improving drug solubility for oral delivery using solid dispersions. Eur J Pharm Biopharm. 2000;50:47±60.

121. Maniruzzaman M, Boateng JS, Snowden MJ, Douroumis D. A Review of Hot-Melt Extrusion: Process Technology to Pharmaceutical Products. ISRN Pharm. 2012;2012:1–9.

122. Jang DJ, Sim T, Oh E. Formulation and optimization of spray-dried amlodipine solid dispersion for enhanced oral absorption. Drug Dev Ind Pharm. 2013;39(7):1133–41.

123. Fei Y, Kostewicz ES, Sheu MT, Dressman JB. Analysis of the enhanced oral bioavailability of fenofibrate lipid formulations in fasted humans using an in vitro-in silico-in vivo approach. Eur J Pharm Biopharm [Internet]. 2013;85(3 PART B):1274–84. Available from: http://dx.doi.org/10.1016/j.ejpb.2013.03.001

124. Maniruzzaman M, Rana MM, Boateng JS, Mitchell JC, Douroumis D. Dissolution

enhancement of poorly water-soluble APIs processed by hot-melt extrusion using hydrophilic polymers. Drug Dev Ind Pharm. 2013;39(2):218–27.

125. Ahern RJ, Hanrahan JP, Tobin JM, Ryan KB, Crean AM. Comparison of fenofibrate-mesoporous silica drug-loading processes for enhanced drug delivery. Eur J Pharm Sci [Internet]. 2013;50(3–4):400–9. Available from: http://dx.doi.org/10.1016/j.ejps.2013.08.026

126. Bora Pk. A review on solid dispersion. Indian Res J Pharm Sci. 2012;1(12):1–9.

127. Savjani KT, Gajjar AK, Savjani JK. Drug Solubility: Importance and Enhancement Techniques. ISRN Pharm [Internet]. 2012;2012(100 mL):1–10. Available from: https://www.hindawi.com/archive/2012/195727/

128. Joshi JT. A Review on Micronization Techniques. J Pharm Sci Technol [Internet]. 2011;3(7):651–81. Available from: https://www.yumpu.com/en/document/view/12266567/a-review-on-micronization-techniques-journal-of-pharmaceutical-

129. Vallet-Regi M, Rámila A, Del Real RP, Pérez-Pariente J. A new property of MCM-41: Drug delivery system. Chem Mater. 2001;13(2):308–11.

130. Schiffter HA, Lee G. Single-droplet evaporation kinetics and particle formation in an acoustic levitator. Part 2: Drying kinetics and particle formation from microdroplets of aqueous mannitol, trehalose, or catalase. J Pharm Sci. 2007;96(9):2284–95.

131. Jia L. Nanoparticle Formulation Increases Oral Bioavailability of Poorly Soluble Drugs: Approaches, Experimental Evidences and Theory. Curr Nanosci. 2005;1(3):237–43.

132. Vallet-Regi, M., F. Balas and DA. Mesoporous materials for drug delivery. Angew Chem Int Ed Engl. 2007;46(40):7548–58.

133. Torchilin VP. Recent advances with liposomes as pharmaceutical carriers. Nat Rev Drug Discov [Internet]. 2005;4(2):145–60. Available from: http://www.ncbi.nlm.nih.gov/pubmed/15688077

134. Nunes CD, Vaz PD, Fernandes AC, Ferreira P, Romão CC, Calhorda MJ. Loading and delivery of sertraline using inorganic micro and mesoporous materials. Eur J Pharm Biopharm. 2007;66(3):357–65.

135. Semete B, Booysen L, Lemmer Y, Kalombo L, Katata L, Verschoor J, et al. In vivo evaluation of the biodistribution and safety of PLGA nanoparticles as drug delivery systems. Nanomedicine Nanotechnology, Biol Med [Internet]. 2010;6(5):662–71. Available from: http://dx.doi.org/10.1016/j.nano.2010.02.002

136. Wang Y, Zhao Q, Han N, Bai L, Li J, Liu J, et al. Mesoporous silica nanoparticles in drug delivery and biomedical applications. Nanomedicine Nanotechnology, Biol Med [Internet]. 2015;11(2):313–27. Available from: http://dx.doi.org/10.1016/j.nano.2014.09.014

137. Rouquerol, J.A., D.; Fairbridge, C. W.; Everett, D. H.; Haynes, J. M.; Pernicone, N.; Ramsay, J. D. F.; Sing, K. S. W.; Unger KK. Recommendations for the characterization of porous solids (Technical Report). Pure Appl Chem. 1994;66(8).

138. Klafter, J.D. JM. Molecular dynamics in restricted geometries. 1st ed. New York City, NY; 1989.

139. Jackson CL, McKenna GB. Vitrification and crystallization of organic liquids confined to nanoscale pores. Chem Mater. 1996;8(8):2128–37.

140. Wojnarowska Z, Mazgalski J, Bieg T, Dulski M, Wrzalik R, Sawicki W, et al. Study of the Amorphous Glibenclamide Drug: Analysis of the Molecular Dynamics of Quenched and Cryomilled Material. Mol Pharm. 2010;7(5):1692–707.

141. Gupta MK, Tseng YC, Goldman D, Bogner RH. Hydrogen bonding with adsorbent during storage governs drug dissolution from solid-dispersion granules. Pharm Res. 2002;19(11):1663–72.

142. Zhang Y, Zhi Z, Jiang T, Zhang J, Wang Z, Wang S. Spherical mesoporous silica nanoparticles for loading and release of the poorly water-soluble drug telmisartan. J Control Release [Internet]. 2010;145(3):257–63. Available from: http://dx.doi.org/10.1016/j.jconrel.2010.04.029

143. Izquierdo-Barba I, Martinez Á, Doadrio AL, Pérez-Pariente J, Vallet-Regí M. Release evaluation of drugs from ordered three-dimensional silica structures. Eur J Pharm Sci. 2005;26(5):365–73.

144. Xu W, Riikonen J, Lehto VP. Mesoporous systems for poorly soluble drugs. Int J Pharm [Internet]. 2013;453(1):181–97. Available from: http://dx.doi.org/10.1016/j.ijpharm.2012.09.008

145. Kinnari P, Mäkilä E, Heikkilä T, Salonen J, Hirvonen J, Santos HA. Comparison of mesoporous silicon and non-ordered mesoporous silica materials as drug carriers for itraconazole. Int J Pharm. 2011;414(1–2):148–56.

146. Omar TA, Oka S, Muzzio FJ, Glasser BJ. Manufacturing of Pharmaceuticals by Impregnation of an Active Pharmaceutical Ingredient into a Mesoporous Carrier: Impact of Solvent and Loading. J Pharm Innov. 2018;

147. Liu Z, Wang Y, Muzzio FJ, Callegari G, Drazer G. Capillary Drop Penetration Method to Characterize the Liquid Wetting of Powders. Langmuir. 2017;33(1):56–65.

148. Oka S, Smrčka D, Kataria A, Emady H, Muzzio F, Štěpánek F, et al. Analysis of the origins of content non-uniformity in high-shear wet granulation. Int J Pharm. 2017;

149. Mathew O'Brien, James McCauley EC. Analytical Profiles of Drug substances. Florey K, editor. London, UK: Academic Press; 1984. 211–238 p.

150. Yoshioka M, Hancock BC, Zografi G. Crystallization of indomethacin from the amorphous state below and above its glass transition temperature. J Pharm Sci. 1994;83(12):1700–5.

151. Mateo-Ortiz D, Méndez R. Relationship between residence time distribution and forces applied by paddles on powder attrition during the die filling process. Powder Technol [Internet]. 2015;278:111–7. Available from: http://dx.doi.org/10.1016/j.powtec.2015.03.015

152. Mangal H, Kleinebudde P. Experimental determination of residence time distribution in continuous dry granulation. Int J Pharm [Internet]. 2017;524(1–2):91–100. Available from: http://dx.doi.org/10.1016/j.ijpharm.2017.03.085

153. Boukouvala F, Niotis V, Ramachandran R, Muzzio FJ, Ierapetritou MG. An integrated approach for dynamic flowsheet modeling and sensitivity analysis of a continuous tablet manufacturing process. Comput Chem Eng [Internet]. 2012;42:30–47. Available from: http://dx.doi.org/10.1016/j.compchemeng.2012.02.015

154. Boukouvala F, Dubey A, Vanarase A, Ramachandran R, Muzzio FJ, Ierapetritou M. Computational approaches for studying the granular dynamics of continuous blending processes, 2 - Population balance and data-based methods. Macromol Mater Eng. 2012;297(1):9–19.

155. Gao Y, Muzzio FJ, Ierapetritou MG. A review of the Residence Time Distribution (RTD) applications in solid unit operations. Powder Technol [Internet]. 2012;228:416–23. Available from: http://dx.doi.org/10.1016/j.powtec.2012.05.060

156. Moghtadernejad S, Escotet-Espinoza MS, Oka S, Singh R, Liu Z, Román-Ospino AD, et al. A Training on: Continuous Manufacturing (Direct Compaction) of Solid Dose Pharmaceutical Products. J Pharm Innov. 2018;13(2):155–87.

157. M. Ierapetritou, M.S. Escotet-Espinoza RS. Process simulation and control for continuous pharmaceutical manufacturing of solid drug product. In: Rantanen PKJKJ, editor. Continuous Manufacturing of Pharmaceuticals. John Wiley & Sons Ltd; 2017. p. 33–105.

158. Van Snick B, Holman J, Cunningham C, Kumar A, Vercruysse J, De Beer T, et al. Continuous direct compression as manufacturing platform for sustained release tablets. Int J Pharm [Internet]. 2017;519(1–2):390–407. Available from: http://dx.doi.org/10.1016/j.ijpharm.2017.01.010

159. Rehrl J, Karttunen AP, Nicolaï N, Hörmann T, Horn M, Korhonen O, et al. Control of three different continuous pharmaceutical manufacturing processes: Use of soft sensors. Int J Pharm. 2018;543(1–2):60–72.

160. S.C. Galbraith et al. Modeling and simulation of continuous powder blending applied to a continuous direct compression process. Pharm Dev Technol. 2018;1–

11.

161. Toson P, Siegmann E, Trogrlic M, Kureck H, Khinast J, Jajcevic D, et al. Detailed modeling and process design of an advanced continuous powder mixer. Int J Pharm [Internet]. 2018;552(1–2):288–300. Available from: https://doi.org/10.1016/j.ijpharm.2018.09.032

162. Portillo PM, Vanarase AU, Ingram A, Seville JK, Ierapetritou MG, Muzzio FJ. Investigation of the effect of impeller rotation rate, powder flow rate, and cohesion on powder flow behavior in a continuous blender using PEPT. Chem Eng Sci [Internet]. 2010;65(21):5658–68. Available from: http://dx.doi.org/10.1016/j.ces.2010.06.036

163. FUJI Chemical Industry Co. LTD. No Title. Tech Newsl. 2007;(October).

164. FUJI Chemical Industry Co. LTD. No Title. Tech Newsl. 2007;(December).

165. Escotet-Espinoza MS, Moghtadernejad S, Oka S, Wang Z, Wang Y, Roman-Ospino A, et al. Effect of material properties on the residence time distribution (RTD) characterization of powder blending unit operations. Part II of II: Application of models. Powder Technol [Internet]. 2019;344:525–44. Available from: https://doi.org/10.1016/j.powtec.2018.12.051

166. Tian G, Lee SL, Yang X, Hong MS, Gu Z, Li S, et al. A dimensionless analysis of residence time distributions for continuous powder mixing. Powder Technol [Internet]. 2017;315:332–8. Available from: http://dx.doi.org/10.1016/j.powtec.2017.04.007

167. Kruisz J, Rehrl J, Sacher S, Aigner I, Horn M, Khinast JG. RTD modeling of a continuous dry granulation process for process control and materials diversion. Int

J Pharm [Internet]. 2017;528(1–2):334–44. Available from: http://dx.doi.org/10.1016/j.ijpharm.2017.06.001

168. Fogler HS. Elements of chemical reaction engineering. Upper Saddle River, N.J.: Prentice Hall PTR; 1999. 951 p.

169. Zhou Z, Taylor RNK, Kullmann S, Bao H, Hartmann M. Mesoporous organosilicas with large cage-like pores for high efficiency immobilization of enzymes. Adv Mater. 2011;23(22–23):2627–32.

170. Kovalainen M, Mönkäre J, Mäkilä E, Salonen J, Lehto VP, Herzig KH, et al. Mesoporous silicon (PSi) for sustained peptide delivery: Effect of PSi microparticle surface chemistry on peptide YY3-36 release. Pharm Res. 2012;29(3):837–46.